SAND2017-3179R

Consensus on Intermediate Scale Salt Field Test Design

Spent Fuel and Waste Disposition

Prepared for
US Department of Energy
Spent Fuel and Waste
Science and Technology

Kristopher L. Kuhlman,
Melissa M. Mills & Edward N. Matteo
Sandia National Laboratories

March 28, 2017
SFWD-SFWST-2017-000099

DISCLAIMER

This information was prepared as an account of work sponsored by an agency of the U.S. Government. Neither the U.S. Government nor any agency thereof, nor any of their employees, makes any warranty, expressed or implied, or assumes any legal liability or responsibility for the accuracy, completeness, or usefulness, of any information, apparatus, product, or process disclosed, or represents that its use would not infringe privately owned rights. References herein to any specific commercial product, process, or service by trade name, trade mark, manufacturer, or otherwise, does not necessarily constitute or imply its endorsement, recommendation, or favoring by the U.S. Government or any agency thereof. The views and opinions of authors expressed herein do not necessarily state or reflect those of the U.S. Government or any agency thereof.

Sandia National Laboratories is a multi-mission laboratory managed and operated by Sandia Corporation, a wholly owned subsidiary of Lockheed Martin Corporation, for the U.S. Department of Energy's National Nuclear Security Administration under contract DE-AC04-94AL85000.

SUMMARY

This report summarizes the first stage in a collaborative effort by Sandia, Los Alamos, and Lawrence Berkeley National Laboratories to design a small-diameter borehole heater test in salt at the Waste Isolation Pilot Plant (WIPP) for the US Department of Energy Office of Nuclear Energy (DOE-NE). The intention is to complete test design during the remainder of fiscal year 2017 (FY17), and the implementation of the test will begin in FY18. This document is the result of regular meetings between the three national labs and the DOE-NE, and is intended to represent a consensus of these meetings and discussions.

The suite of tests is essentially modular, each test consisting of a central test borehole with water vapor collection and liquid brine sampling equipment, surrounded by satellite observation and instrumentation boreholes. Observation boreholes will be associated with temperature, electrical resistivity, and acoustic emission (AE) measurements. The first test of this modular design will be isothermal (no heating), and the second stage will be heated to a maximum borehole temperature of approximately 120°C. Later tests will be designed using information gathered from the first two boreholes, will be conducted at other temperatures, and may include other measurement types and test designs.

The suite of field tests is focused on the objectives of quantifying brine availability, brine migration, and brine chemistry under heat-generating-waste relevant conditions in bedded salt. To accomplish the first two objectives, we will quantify the mass flowrate of water and conservative tracer into the borehole while circulating out humidity inside the central test borehole. Brine chemistry will be monitored through brine and gas sampling during the experiment. To interpret water inflow data, we will use thermal-hydrologic (TH), thermal-hydrologic-chemical (THC), and thermal-hydrologic-mechanical (THM) modeling to estimate formation properties, given the applied boundary conditions and observed inflow data. To interpret observed chemistry data, we will use thermal-chemical (TC) and THC models to interpret observed changes in the chemistry of inflowing brine, from observations of precipitating minerals and samples of brine composition while constantly removing water vapor from the borehole.

Appendix A presents key components from historic heater tests in both bedded and domal salt. One motivation for this test is to "get back underground" and rebuild capabilities that have been lost with retiring staff since the bulk of *in situ* testing in salt was conducted in the 1980s. That being the case, this report presents key references and figures from previous tests as a first step in the design and implementation of the current suite of tests.

ACKNOWLEDGEMENTS

The SNL authors want to thank LANL and LBNL staff who actively participated in the development of the test design from the early stages, including Phil Stauffer, Hakim Boukhalfa, Doug Weaver, Brian Dozier, Shawn Otto, Jonny Rutqvist, and Yuxin Wu. We would like to thank those who reviewed and commented on aspects of the proposed experiment design and this report, including Pat Brady, Bob MacKinnon, Bill Spezialetti, Prasad Nair, Carlos Jové Colón, and Paul Domski. Special thanks to Michael Schuhen and Wes Deyonge for insightful comments and helpful advice on test design, to Paul Domski for providing WIPP brine chemistry data, and to Charles Bryan and Carlos Jové Colón for review and material related to brine chemistry and acid gas generation. Thanks to Ernie Hardin for technical and editorial review of the entire report; his suggestions improved the report and aspects of test design.

CONTENTS

LIST OF FIGURES

LIST OF TABLES

ACRONYMS

AE	acoustic emissions
BPC	borehole pressure cell
CBFO	DOE-EM Carlsbad Field Office
CMH	chilled-mirror hygrometer
CRDS	cavity ring-down spectroscopy
D_2O	deuterated water
DOE	US Department of Energy
DOE-EM	DOE Office of Environmental Management
DOE-NE	DOE Office of Nuclear Energy
DRZ	disturbed rock zone
EDS	energy dispersive X-ray spectography
ERT	electrical resistivity tomography
FCRD	DOE-NE Fuel Cycle Research and Development
FIB-SEM	focused ion beam-scanning electron microscopy
FY	fiscal year
LANL	Los Alamos National Laboratory
LBNL	Lawrence Berkeley National Laboratory
LVDT	linear variable differential transformer
MCC	Mississippi Chemical Company potash mine (in Salado Formation above WIPP)
MB139	Salado marker bed 139 (1.5 m below WIPP repository horizon)
MIIT	WIPP Materials Interface Interactions Test (1980s)
MU-0	WIPP Salado map unit zero
RH	relative humidity
RTD	resistance temperature device
SANS	small-angle neutron scattering
SCCM	standard cm^3/min
SDDI	CBFO Salt Defense Disposal Investigations (2013)
SDI	CBFO Salt Disposal Investigations (2011)
SEM	scanning electron microscopy
SNL	Sandia National Laboratories
STEM	scanning transmission electron microscopy
TGA	thermogravimetric analysis
THMC	thermal, hydrological, mechanical, and chemical processes (also other subsets TC, TH, THM & THC)
TSI	WIPP Thermal/Structural Interactions tests (1980s)
US	United States of America
WIPP	DOE-EM Waste Isolation Pilot Plant
XRD	X-ray diffraction

CONSENSUS ON INTERMEDIATE-SCALE SALT FIELD TEST DESIGN

1. INTRODUCTION

The US desire to dispose of radioactive waste in geologic salt originated with Hess et al. (1957), and has motivated the development of our current extensive technical basis for waste disposal in salt. Salt has a low permeability to brine transport and a high thermal conductivity compared to other potential disposal media like clay or granite. This makes its thermal and hydraulic diffusivities the same order of magnitude (McTigue 1985; Cosenza & Ghoreychi 1993). Since these two diffusivities in salt are approximately equal, interplay between coupled thermal, mechanical, and hydrological processes is especially important. We can design salt repositories for heat-generating waste while understanding these coupled processes, taking advantage of salt's favorable thermal conductivity and permeability. Despite these favorable properties, geologic salt is a complex medium for which to quantitatively predict reconsolidation, room closure, brine migration, and solution chemistry because it creeps, is highly soluble, and contains saturated brines.

1.1 Field Test Goals

The long-range goals of the DOE-NE field-testing campaign for salt are related to the long-term isolation safety case for disposal of heat generating waste in salt. This intermediate-scale borehole heater test is one component of the field-testing campaign, focused on the quantification of brine inflow and composition. The transient evolution of brine inflow and the brine composition after excavating a drift or borehole can be thought of as initial conditions in the long-term performance assessment modeling of a salt repository system over long time scales. The high-level goals of this intermediate-scale field test (as opposed to the other parts of the overall testing campaign, such as small-scale laboratory tests or drift-scale emplacement demonstrations) are to:

1) improve understanding of brine availability and brine chemistry in bedded salt;
2) collect datasets for validating numerical models, populating constitutive models, and improving process model understanding;
3) collect field data to improve understanding of acid gas generation mechanisms; and
4) revitalize in-house expertise at participating national laboratories in implementing *in situ* experiments in salt at WIPP (Figure 1).

The proposed borehole heater test will be relatively low cost and performed at a small spatial scale. The test will be used to develop instrumentation and methods for further *in situ* testing, demonstrations, and characterization activities. A single-heater borehole test will be used to assess changes in physical-chemical properties associated with brine and vapor liberation and migration at elevated temperature. A follow-on to these borehole tests might include international collaborations for model prediction and validation (Hansen et al. 2016b).

The test is primarily focused on brine availability to a small-diameter (10 to 15 cm [4" to 6"]) horizontal borehole. This report provides a conceptual design of the borehole heater experiment, further specifying the recommendations of Hansen et al. (2016b). Brine availability quantifies how much natural brine flows into an excavation (borehole or room), and is thereby available to enhance waste package corrosion, limit the closure of brine-filled cavities, or to facilitate radionuclide transport. Understanding the amount of brine available to flow into a borehole or excavation in salt primarily involves understanding the mechanism of brine migration and the distribution of the disturbed rock zone (DRZ). As a secondary goal, the test will collect unique data on brine composition, which could change during the experiment due to transport of multiple types of water present in a bedded salt formation. Although the current disposal concept for heat-generating radioactive waste in salt does not necessarily include emplacing waste in

horizontal boreholes, this test is being designed as a horizontal borehole test to quantify relevant THMC processes in salt, which could be upscaled to the drift scale. The test will avoid mapped clay or anhydrite inter-layers. Data collected in response to the imposed constant-humidity and low-pressure conditions at the central borehole will hopefully allow more ready validation of numerical models, than data collected from a disposal demonstration that has less controlled conditions.

In addition to the two primary goals of brine availability and brine chemistry, we have identified lower-level goals that we will investigate in observation boreholes (if they do not interfere with the primary goals) or in later tests:

- Vapor flow in a partially saturated DRZ;
- Evolution of an unsaturated DRZ surrounding drifts and boreholes;
- Porosity and permeability changes in the DRZ surrounding boreholes;
- Acoustic emissions (AE) and other micro-mechanical processes during heating and cooling;
- Geophysical changes (e.g., electrical resistivity or ultrasonic wave propagation) in response to temperature changes, deformation, and brine transport;
- Tight coupling between mechanical, hydrological, and thermal processes in salt;
- Release of brine in response to sudden changes in borehole temperature (both increases and decreases);
- Long-term brine availability over multiple years (stability of steady-state inflow);
- Corrosion and degradation of materials (e.g., steel and cement).

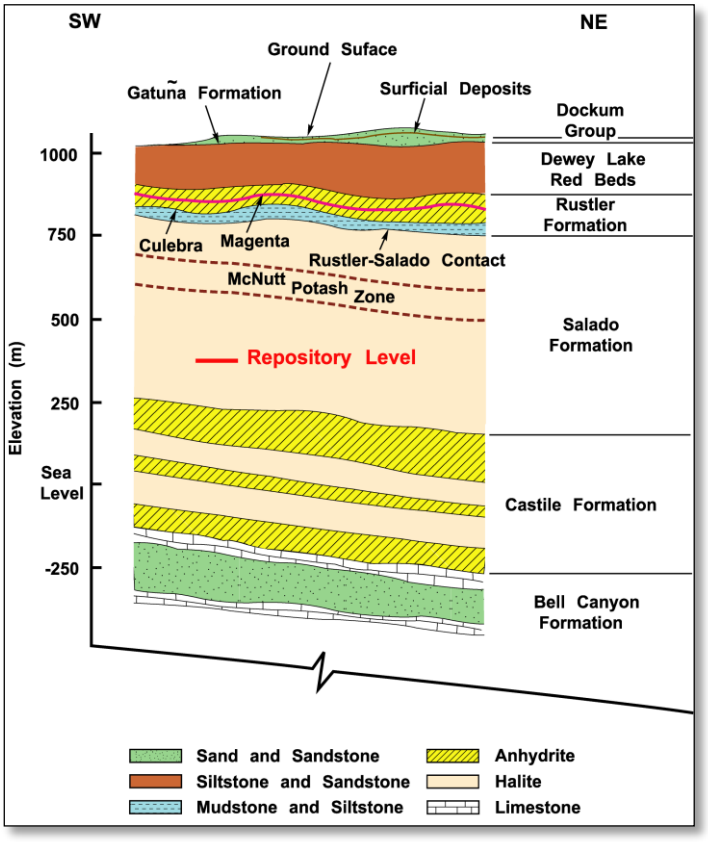

Figure 1. Generalized Waste Isolation Pilot Plant (WIPP) stratigraphy.

The data we plan to collect will require several analytical and numerical models to interpret. Some semi-analytical solutions may be used to assist in interpreting heat conduction (Carslaw & Jaeger 1953) and brine inflow (McTigue 1985, 1993), but there are few analytical solutions available to predict coupled THMC systems. Non-linear numerical solutions are needed when considering brine density and viscosity changes with temperature and composition, free thermal convection of brine and gas in a porous medium, brine chemistry at high ionic strength, salt dissolution and precipitation, or significant mechanical or chemical coupling. One of our goals is to collect data that may ultimately require a non-linear coupled numerical model to interpret, to provide a validation dataset for these numerical models.

The proposed suite of intermediate-scale borehole heater tests is modular and several arrangements of central test and satellite observation boreholes are planned at multiple maximum borehole wall temperatures, including ambient (unheated, ~30 °C), 50 °C, 120 °C, 160 °C, and 200 °C. The first two tests (ambient and 120 °C) are described in this report in more detail than the other three. The design of subsequent borehole tests will be revisited based on lessons learned executing the first two tests. In the first two tests, the central borehole will be the collection point for the brine inflow system, which builds upon a design used in several successful borehole heater tests in bedded and domal salt (see Appendices A-3, A-4, A-5, A-6, and A-7).

1.2 Relevant History

There have been several well-documented drift-scale borehole heater tests in bedded and domal salt that observed brine inflow including: Project Salt Vault (1965-1967), Avery Island (1978-1983), Carlsbad potash mines (1981-1983), WIPP Rooms A and B (1984-1990), and Asse (1983-1985). Heated borehole brine inflow tests have shown significantly less brine flows into boreholes completed in domal salt (Krause 1983; Rothfuchs et al. 1988) compared to bedded salt (10 to 100 times less). Heater tests in bedded salt have shown less brine inflow into boreholes that do not intersect clay or anhydrite layers (Bradshaw & McClain 1971; Nowak & McTigue 1987). These non-salt units have higher permeability than halite, often have higher brine-filled porosity, have markedly different mechanical responses compared to salt (e.g., salt creeps and heals, anhydrite is brittle, and clay allows shearing of sedimentary layers), and involve more hydrated mineral phases (e.g., clays, polyhalite, or gypsum that evolve water during heating) than halite.

Previous heated borehole tests at WIPP focused on thermal-structural interactions (i.e., WIPP TSI Rooms A and B – Tyler et al. 1988). These heated rooms included brine inflow observations in large-diameter vertical boreholes. These vertical boreholes at WIPP were at least 76 cm [30”] in diameter, and intersected Clay F below the floor of Rooms A and B. Non-salt layers encountered in these vertical boreholes contributed significantly to observed brine inflow, especially at temperatures above 100 °C (Figure 2). Borehole B042 in WIPP Room B operated at 130 °C and collected 35 liters of condensed water vapor over 600 days (Nowak & McTigue 1987). Deal et al. (1993) consolidated clays collected from the WIPP disposal horizon in oedometers at 13.8 MPa [2,000 psi]. They found them to have 25 to 29% brine content volumetrically (~12 wt-%), not including inter-layer or bound water that will be released during heating.

While a large number of previous salt heater tests exist, motivation for this proposed suite of borehole heater tests stems from a renewed US interest to conduct heater tests in salt related to disposal of heat-generating waste. Historic tests in salt are discussed in more detail in recent historical surveys: Kuhlman et al. (2012), Kuhlman & Malama (2013), and Kuhlman & Sevougian (2013). Sevougian et al. (2013) presented a summary of a workshop convened to discuss and prioritize research concepts related to heat-generating waste in salt. The US/German workshop on salt repository research has fostered and documented collaboration between salt researchers in the US, Germany, and the Netherlands (e.g., Hansen et al. 2016a; 2017). Recent DOE-NE funded laboratory and numerical modeling efforts at Sandia, Los Alamos, and Lawrence Berkeley National Laboratories have been summarized in Kuhlman (2014) and Stauffer et al. (2015).

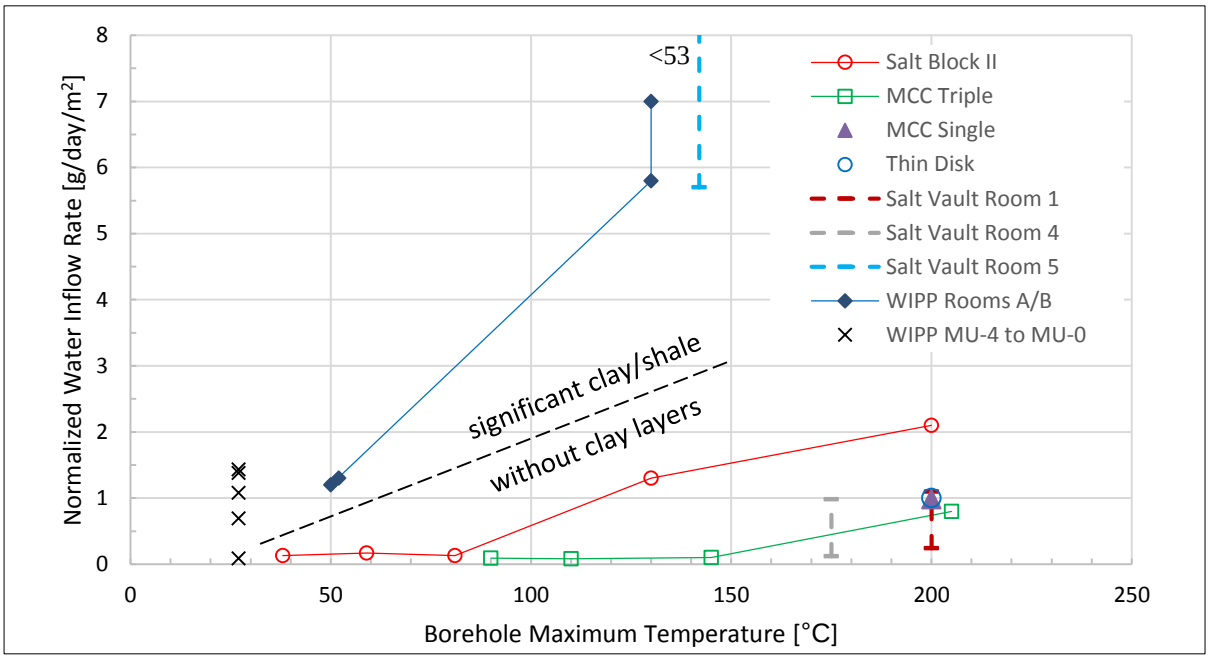

Figure 2. Normalized water production rate in bedded salt (data modified from Shefelbine 1982; Appendix A-10).

At WIPP, the US Department of Energy Office of Environmental Management (DOE-EM) Carlsbad Field Office (CBFO) began planning two large-scale heated disposal demonstrations: Salt Disposal Investigations (SDI; DOE CBFO 2011) and Salt Defense Disposal Investigations (SDDI; DOE CBFO 2013). The "SDI Area" at WIPP (Figure 3) was partially mined to accommodate these possible future tests. Stauffer et al. (2015) summarized modeling and instrumentation development carried out in planning for SDDI at WIPP. This report builds upon this recent background work (see Appendix A for discussion of relevant points from historic salt heater tests), and presents an initial consensus regarding a DOE-NE funded plan to begin field testing in salt related to heat-generating waste.

1.3 Proposed Field Test in Context of Performance Assessment

The main focus of these intermediate scale borehole heater tests is brine availability, since brine availability determines how much natural brine flows into an excavation (borehole or room), and is thereby available to potentially cause waste package corrosion, limit closure of brine-filled cavities, or to facilitate radionuclide transport. In a salt repository for "hot" radioactive waste (i.e., above brine boiling temperature at the waste package) moisture will be driven away from the waste packages. Salts will precipitate out of brine near the waste package, and thermally enhanced creep closure will reconsolidate any backfill and close any gaps or voids to create a dry low-permeability zone surrounding the waste packages. After tens to hundreds of years, depending on waste type, the waste radioactive decay heating rate will eventually decrease allowing temperatures to drop below the brine boiling temperature, and allowing liquid to migrate back toward the waste packages. However, low-permeability reconsolidated salt backfill and precipitated salt on the heater will minimize the amount of brine that contacts the packages.

In all salt disposal systems, the far-field ultra-low permeability of the salt formation and its proven stability over geologic time provides the primary natural barrier that contains radioactive waste over performance assessment relevant time scales (10^4 to 10^6 years). Salt creep closes open excavations, and closes fractures or other voids in the near field that could serve as transport pathways from the repository. While this intermediate-scale borehole heater test is focused on the quantification of inflow and

composition of brine, this is essentially the development of an initial condition in the long-term performance of a salt repository system, for which we have great confidence in its ability to provide isolation from the shallow geosphere.

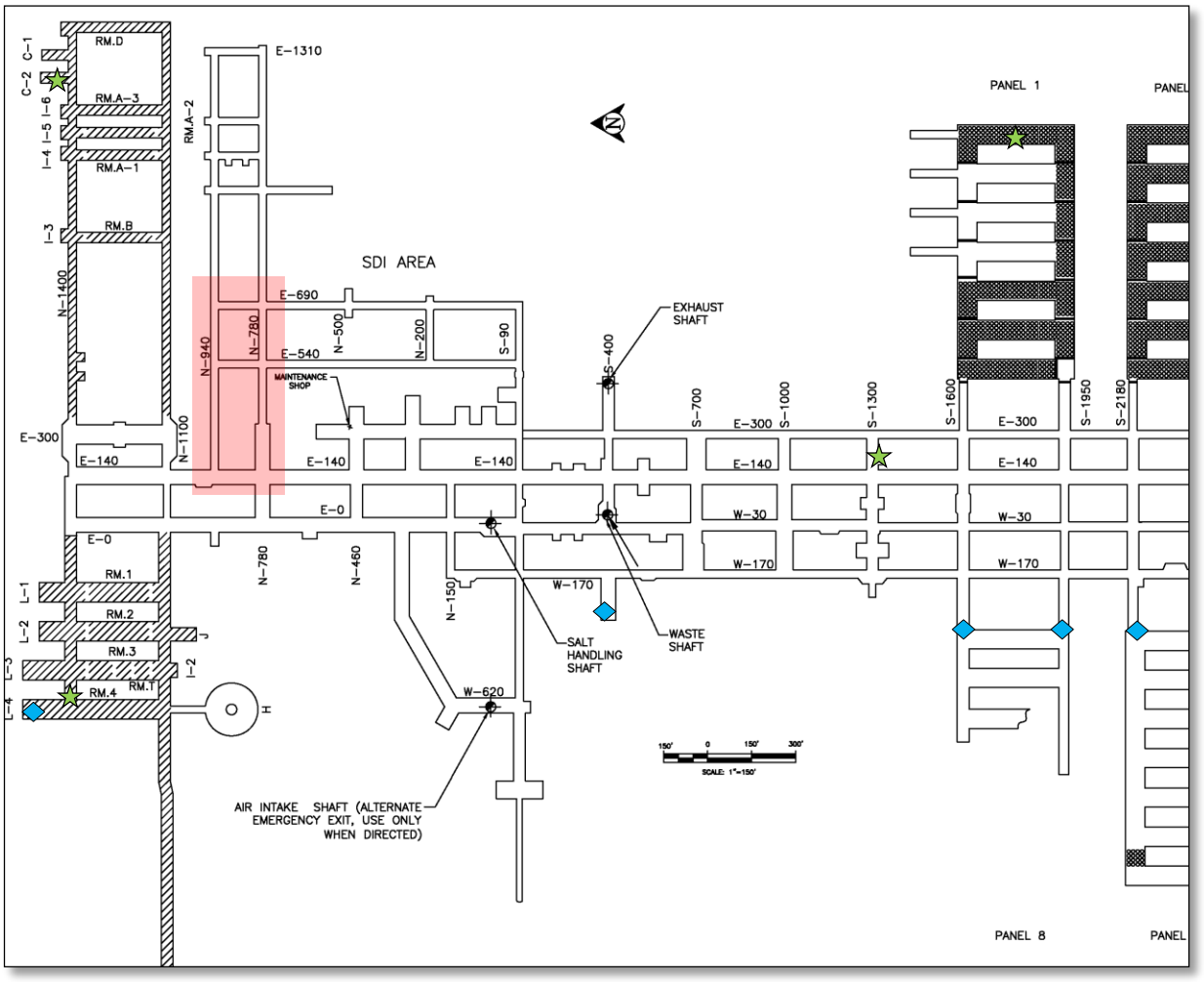

Figure 3. WIPP underground layout. Possible test location shaded red. MU-0 lithologic data locations marked with stars; MU-0 brine inflow observations marked with diamonds.

2. FIELD EXPERIMENTAL PROCESS DESCRIPTION

2.1 Location and Design Strategy

The field test will be conducted in a portion of the SDI Area of WIPP (e.g., the red shaded area in Figure 3). The precise location of the boreholes will be chosen to be at least two drift diameters away from a drift corner or intersection, to minimize edge effects and stress concentrations near tested intervals. Location will consider the dimensions of the access drift (smaller cross-section drifts being more favorable than larger, since they will have a smaller DRZ) and the time lag between drift excavation and deployment of the tests. We assume new drifts will not be available for testing in FY18, but if they were available for future tests, a test room should be constructed for multiple tests, with adequate room to limit end effects and test interference. From a purely geomechanical viewpoint, all the holes for multiple tests would be drilled and instrumented immediately upon mining a new test drift, and tests would be run in parallel.

This approach would capture more of the early-time room deformation, but would not allow performing tests sequentially and learning or improving methodologies from one test to another. This approach will not be taken with the first two boreholes, but may be possible for later borehole tests.

For the initial two tests, boreholes will be drilled immediately before the planned beginning of the test (as soon as is feasible), based on coordination with underground operations personnel. We will attempt to minimize accumulated pre-test borehole damage, and unmeasured early brine inflow (when brine inflow is expected to be largest). Both phenomena are associated with boreholes being open for extended periods before tests begin. Testing and instrumentation installation will begin immediately after borehole construction, to minimize the uncertainty associated with unmeasured early boreholes conditions. Drilling the boreholes immediately before the tests and running the tests serially, rather than in parallel, may lead to higher costs associated with drilling boreholes. Both this cost and any possible impacts to the data should be considered when coordinating test interval construction and instrumentation. Running tests in parallel will require multiple sets of packers, heaters, and instrumentation to be installed simultaneously and would preclude re-using equipment across tests.

The central borehole of each test will be cored or drilled sub-horizontally at 10.2 cm [4”] or 15.2 cm [6”] diameter and 6.1 m [20’] in length, at a horizontal level 60 to 90 cm [2’ to 3’] from the floor in a typical room on the WIPP disposal horizon. This orientation places the test elevation sufficiently far from mapped clay or anhydrite layers, targeting Map Unit 0 (MU-0); see Figure 5 and discussion of previous isothermal brine inflow boreholes in MU-0 in Appendix A-1.

2.1.1 Test Interval Location to Avoid Interbeds and DRZ

A sub-horizontal test borehole orientation (i.e., with a downward dip to accumulate brine for collection at end of the borehole) will minimize crossing major lithologic changes or interbeds (e.g., see mapped clay and anhydrite layers in Figure 4 and Figure 5). This orientation will keep test intervals within a single mapped unit. MU-0 is the target unit, and is an “argillaceous halite” with minor dispersed clay and polyhalite (Figure 5). The reasons for choosing this stratigraphic location and orientation include making the test results more transferrable to other bedded salt formations, ease of access from existing WIPP excavations, and controlling the influence of Clay F that contributed large amounts of brine in Rooms A and B (Figure 2). A horizontal borehole orientation was also chosen because there have been fewer historical heater tests focusing on brine production in bedded salt with a horizontal orientation (e.g., Bradshaw & McClain 1971, Ewing 1981b, Shefelbine 1982). Previous heater tests at WIPP were in vertical boreholes, except the 300 W horizontal borehole heater tests in Room T that did not monitor brine inflow (Molecke 1992). Figure 2 shows normalized brine production rate from boreholes in bedded salt, as a function of the borehole maximum temperature. Boreholes in WIPP Rooms A and B, and Project Salt Vault Room 5 intersected significant clay or shale layers. These boreholes produced much more brine than other bedded salt deposits at similar temperatures (The 1-m diameter Salt Block II sample came from the Mississippi Chemical Company (MCC) potash mine near WIPP). There are large uncertainties on results from Project Salt Vault, due to the way brine collection was performed and reported.

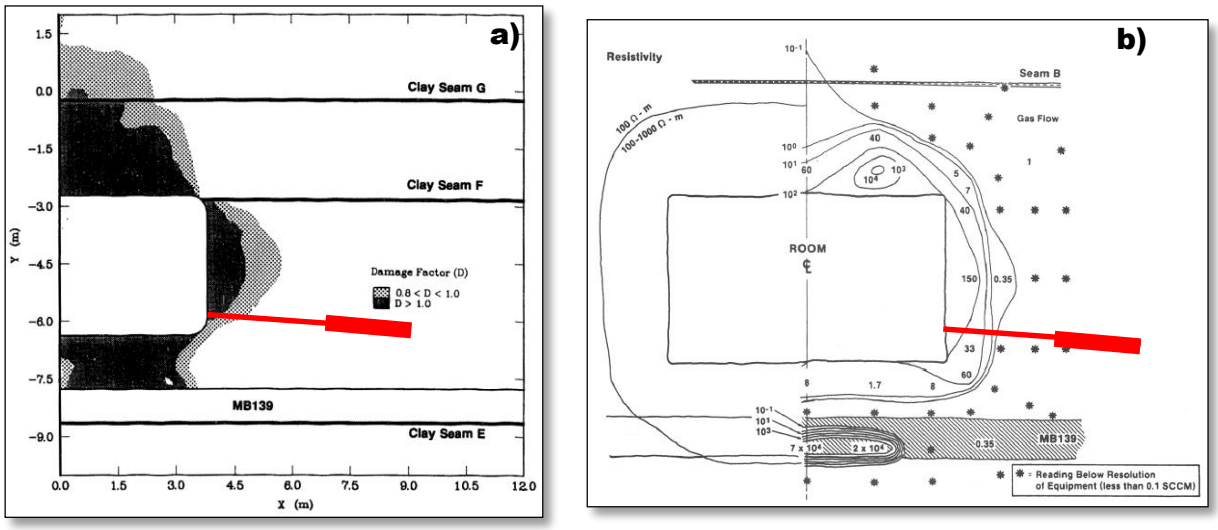

Figure 4. Model-predicted and observed DRZ at WIPP, with approximate borehole and test interval indicated (a: Figure 2-10 from Van Sambeek et al. 1993, b: Figure 5 of Stormont 1997b).

Each heated test interval will be located at the end of its borehole, and it will use a combination of plugs and packers for isolation between the access drift and the test portion of the borehole. The length of the borehole will be long enough to place the test interval beyond the access drift DRZ to the extent practical, but placing the test interval too deep will complicate the setup. See the 4.5 m borehole and test interval locations indicated on Figure 4. "Cartoon" representations of typical accumulation of damage surrounding drifts at Asse and WIPP are illustrated in Figure 6. The major DRZ with significant open fractures will likely be confined to the first 1.5 m [5'] of the borehole; see the $D > 1.0$ area in Figure 4a and gas flowrates > 1 standard cm^3/min (SCCM) in Figure 4b. Lesser damage may extend 3 m [10'] into the wall, based on geophysical and petrographic analysis of cores and boreholes (Holcomb et al. 2001; Hansen 2003). The testing interval should be at least 3 to 4.5 m [10' to 15'] away from the access drift wall, and 4.5 to 6.1 m [15' to 20'] if practical.

Low-pressure gas flowrate testing will be conducted in the boreholes after drilling (Figure 4b; Section 2.4.6), before installing brine collection equipment, to identify the extent of the damage zone using an approach similar to that of Stormont et al. (1987). Borehole packers or seals will be installed deep enough to get beyond most of the observed damage, but not too deep to complicate borehole equipment installation and monitoring.

2.1.1 Expected MU-0 Lithology

Appendix D of Finley et al. 1992 (see Appendix A-1.2 this document) shows the types of insoluble residues found in Room L4 borehole samples from MU-0. The insoluble hydrous minerals from these samples include smectite, gypsum, and polyhalite (see Figure 17 in Appendix A-1). Soluble hydrous minerals (e.g., magnesium chloride salts) are not believed to exist in large quantities in MU-0.

Powers (2017) described the non-halite components in WIPP argillaceous halite:

> "…appear to average ~1% but are higher in coarser halite. The clay proportion dominates in the coarser halite intervals, and sulfate dominates in the fine halite intervals. Clay is not uniformly distributed. Some occurs as irregular blebs between crystals, but clay also forms thin (e.g., 2-3 mm; 0.08-0.12 inch), irregular curved discontinuous stringers."

Saulnier et al. (1991) described MU-0, encountered in vertical boreholes C2H01-A, B, and C drilled from Room C2 (see Figure 3 for borehole locations), as "Medium to coarse argillaceous halite, clay decreases downsection, polyhalite increases downsection." They described MU-0 in vertical borehole N4P50 drilled from SPDV Room 4, as "coarse, colorless, trace polyhalite, argillaceous halite." They described MU-0 in vertical borehole S0P01-A (S1300 drift), as "Coarsely crystalline clear halite." They described MU-0 in vertical borehole, S1P71 drilled from Room 7 of Panel 1, as "Coarse, colorless halite, minor intercrystalline brown clay."

Deal et al. (1989) described MU-0 in their generalized stratigraphy (their Appendix H) as:

> "Clear to moderate reddish orange/brown, moderate brown and grayish brown. Medium to coarsely crystalline. <1 to 5% argillaceous material. Predominantly brown, some gray, intercrystalline argillaceous material and discontinuous breaks and partings. Upper 0.6 meters of unit is argillaceous halite decreasing in argillaceous material content downward. None to <1% polyhalite. Contact with lower unit is gradational based on polyhalite content."

Boreholes will be logged upon drilling by inspecting core. A remote video or photo inspection process to will be used look for discontinuous (i.e., unmapped) clay stringers which may significantly affect test results. If significant unanticipated discontinuous clay is encountered during drilling the central test borehole at a test site, a different location or horizon will be chosen.

Based solely on geological observations of MU-0 at WIPP, the packer-isolated portion of the borehole should be located away from the upper portion of MU-0, in the deeper (i.e., stratigraphically lower) portions of MU-0 if possible, to minimize clay content. This could be achieved by lowering the collar height of the borehole (i.e., starting at a lower elevation in the room), or by drilling the borehole at a slightly steeper angle down.

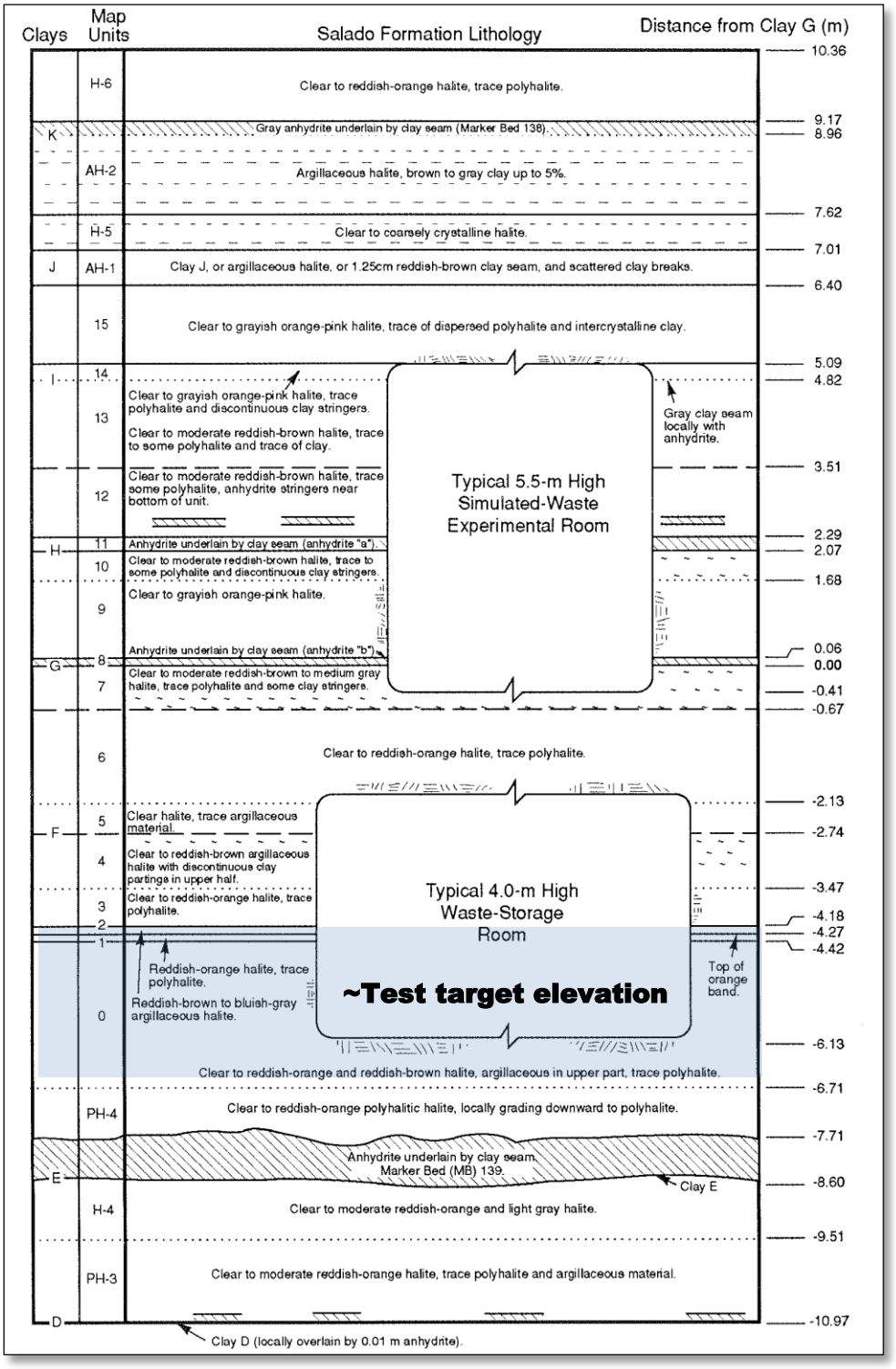

Figure 5. Generalized WIPP stratigraphy (Figure 2-3 of Roberts et al. 1999); MU-0 shaded blue.

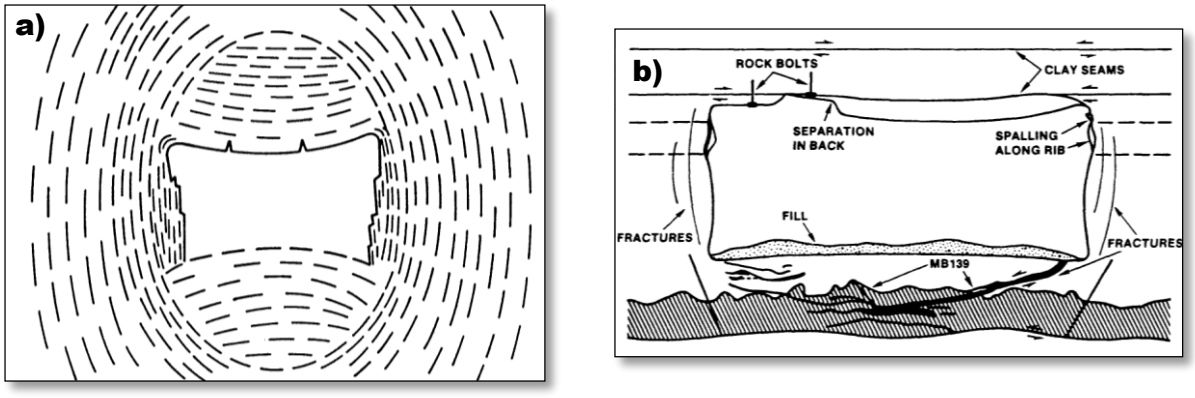

Figure 6. Fractures around mined openings at Asse (a) and WIPP (b) (Figures 3 and 11 of Borns & Stormont 1988).

2.2 Heated Borehole Backfill Considerations

For the first two tests, a central test borehole configuration without backfill is preferred to:

- Allow simpler implementation. It is difficult to fill a horizontal borehole completely with granular backfill, especially in an annular space around a heater. WIPP Room T involved partially backfilling canisters in horizontal remote-handled waste boreholes; the boreholes were not completely backfilled (Molecke 1992);
- Minimize material added to the test interval that may increase the complexity of the chemical and hydrological response. Run-of-mine backfill would contribute to the observed brine inflow and composition, and could have significant anhydrite or clay components, depending on its source;
- Allow straightforward sampling of gases and liquids from the borehole. Backfilled boreholes have included vapor sampling (Westinghouse 1987; Rothfuchs et al. 1988) and permeability estimation using gas flow tests (Bechthold et al. 1999; Rothfuchs et al. 1999), but backfill would make it more difficult to collect liquid brine chemistry samples;
- Allow easier removal of heaters, sampling equipment and monitoring devices after the completion of the test. This will allow possible re-use and will allow more straightforward collection of salt core from near the heater (i.e., coring would not require over-coring the entire heater in a single pass using a very large core barrel, core can instead be collected in pieces or just along one side of the borehole); and
- Allow possible use of radiative heaters and borehole-wall imaging of efflorescence development during the test (Shefelbine 1982).

The primary reason for considering backfilling the borehole is to minimize heat transfer complications from thermal radiation and free convection of air in the borehole. Free convection of hot air within the borehole would alter the applied distribution of temperature in the borehole, complicating simulation of proper boundary conditions using porous medium THMC models. This effect will be minimized by enclosing the heater element in a block of solid material, to provide a “thermal ballast” and displace low heat capacity air. This approach adds foreign material to the borehole, so the chemical stability of added materials in hot brine will be considered. A secondary reason to backfill the borehole is that disposal drifts would likely be backfilled in typical configurations.

The heater should be roughly centered in the borehole either by using centralizing arms or rings (e.g., Appendix A-7, Figure 40), or by simply filling all or most the borehole with the heater. The latter could be done by either making the heater borehole small diameter (same as the heater), or by making the heater or heater/block combination large diameter (same as the boreholes with centralizers or spacers attached to the heater block).

If there is only a small clearance between the heater and the borehole at the beginning of the test, the combination of salt creep and salt precipitation from brine inflow could make the heater removal very difficult (e.g., see WIPP Room B heater removal in Appendix A-2, Figure 21). A tight clearance may also preclude sampling of liquid brines from the borehole during the test. Conversely, borehole closure or rock pressure measurements could be made on the surface of the heater block, if it is made of rigid material and the clearance is tight.

Another heater/borehole configuration option is to place strip heaters along the surface of the borehole and backfill inside of them. While it would be easier to backfill a cylindrical cavity than an annular cavity, the top of the borehole would still be difficult to backfill completely. If heaters are placed against the intact salt, the inner backfill is not located in the primary path for the energy transfer between the heater and the far field, like it is when the heater is in the center of the borehole.

2.3 Test Interval and Observation Boreholes

Around the central test interval boreholes, several smaller-diameter satellite observation boreholes will be drilled and instrumented. The number and size of satellite boreholes depends on the needs of the test. Observation boreholes can be oriented and located in a variety of ways around the test borehole. One suggested layout is shown in Figure 7, with a 10.2 cm [4”] test borehole and multiple 5.1 cm [2”] observation boreholes. The observation holes are at different orientations and distances away from the test interval. The arrangements of boreholes in Avery Island tests, described in Appendix A-3 (Figure 27), suggest alternatives. The total number of observation holes could be reduced by sharing some observation holes between neighboring test locations, but drilling small-diameter observation boreholes is not difficult or expensive. For the first two boreholes, we foresee only executing one test from the test suite at a time, therefore only one test borehole and associated observation boreholes will be drilled to minimize any creep closure effects and missed observations of brine inflow or borehole closure in boreholes before the test begins. The importance of possible impacts due to leaving boreholes open before instrumenting tests should be weighed against the logistical and financial implications of drilling boreholes in multiple efforts, rather than drilling all boreholes in one mobilization of the drilling crew.

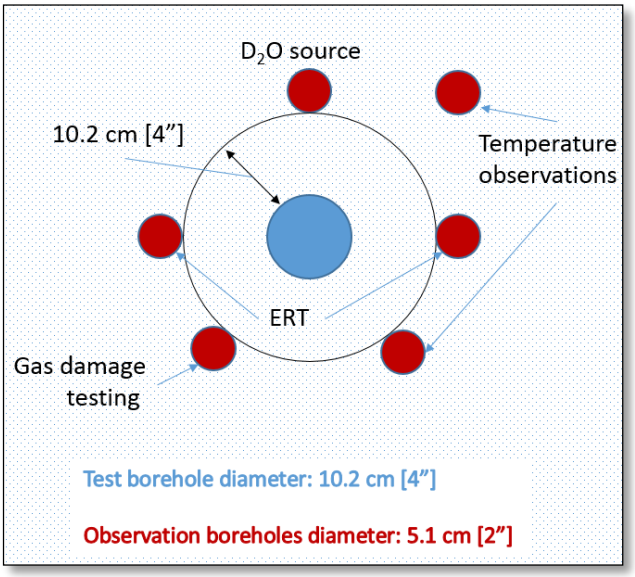

Figure 7. Possible configuration of test borehole and observation boreholes.

2.4 Test Conditions and Features

2.4.1 Test Matrix

Table 1 provides a proposed set of conditions for the suite of borehole tests. The overall intermediate-scale field-testing campaign will have at least five sets of boreholes as different components or stages of the experiment. Each set of central borehole and satellite observation boreholes will be associated with different maximum borehole wall temperatures. The isothermal test will take at least 200 days, based on observations from previous isothermal boreholes at WIPP (Appendix A-1, Figure 14). The exponential decay of borehole inflow rate is related to the permeability of the salt and the geometry of the borehole (McTigue 1993).

Table 1. Proposed test matrix.

		Test Target Temperature (°C)	Step Heating	Cement	Drift Closure Observations	Acoustic Emission Sensors	Duration (days)
Initial tests	1	Ambient (~30)	No	No	No	None	200
	2	120	No	No	No	1-2	100
Follow-on tests	3	50	No	Yes	Yes	1-2	100
	4	160	Yes	TBD	Yes	4-6	200
	5	200	No	TBD	Yes	4-6	100

Test target temperatures will be chosen to straddle different temperature thresholds associated with sources of water to the borehole (Table 2). Based on these estimated key dehydration and phase-change temperatures (and the estimated presence of these minerals in MU-0), the borehole heater tests should be conducted at the target maximum temperatures of 50 °C, 120 °C, 160 °C, and 200 °C. This should keep the maximum temperature well below the decrepitation temperature (where fluid inclusions will fracture the salt), and will straddle either side of the lowest gypsum and smectite (corrensite) clay dehydration temperatures (65 and 100 °C), and the lower (possibly “contaminated”) polyhalite and bischofite

dehydration temperatures (150-155 °C). Krumhansl et al. (1991b) indicate the range of temperatures required to dry out the borehole walls in WIPP Room B heaters was 120-130 °C.

Table 2. Expected MU-0 sources of brine sorted by minimum dehydration temperature (data from Powers et al. 1978 and Roedder & Bassett 1981)

Component	Formula	wt% water	Dehydration/release temp [°C]	wt% in MU-0
Smectite	$Al_2Si_4O_{10}(OH)_2 \cdot n(H_2O)$	5-18	65[#] & 100-400	≤ 2% [§]
Gypsum	$CaSO_4 \cdot 2(H_2O)$	21	75-175	≤ 2%
Polyhalite	$Ca_2K_2Mg(SO_4)_4 \cdot 2(H_2O)$	6	150-160[+] & 340-360	≤ 2% [¥]
Bischofite	$MgCl_2 \cdot 6(H_2O)$	53	155-220*	None[^]
Carnallite	$KMgCl_3 \cdot 6(H_2O)$	39	180-224*	None[^]
Fluid Inclusions	(Brine inclusion chemistry variable)	74[@]	240-250	0.1-0.75

+	Lower dehydration temperatures for polyhalite may be due to "contamination" (Roedder & Bassett 1981).
@	Weight % water in saturated NaCl brine.
#	Caporuscio et al. (2013) Figure 32, likely due to corrensite clay dehydration.
^	Little or no magnesium chloride salt is expected to exist before the test in the salt, but the brine is expected to evolve to a Mg-Cl brine and these salts will precipitate (see Krumhansl et al. (1991b) and figures in Appendix A-2).
§	Clay content in MU-0 is observed to increase going stratigraphically up in the interval.
¥	Polyhalite content in MU-0 is observed to increase going stratigraphically down in the interval.
*	Dehydration temperatures for hydrated Mg-Cl salts are such that lower RH → lower dehydration temperatures.

For the initial heated test (120 °C), it is expected ~1,000 Watts of power will be required to maintain the maximum wall temperature at an approximate steady-state in the middle of the 1.5 m [5'] heated test interval. For the planned radial test geometry, a true steady-state temperature distribution will not develop, but the rate of change in temperature with time is expected to stabilize. This estimate is based on analytical solutions to the heat conduction problem (McTigue 1985; Eqn. 83) and numerical TH solutions (e.g., FEHM or TOUGH2). The analytical solution has simplified geometry and only takes into account linear heat conduction in the intact salt. Analytical solutions do not take into account a cooling effect that may occur due to removal of heated air and evaporation of brine from the borehole into the dry N_2 circulating through the borehole. Heat will also be lost through the packer assembly and into the access drift.

Table 3 lists the planned tests, data measurements, and other observations and where they will be made.

Table 3. Borehole test components (all 5 tests).

	Packer/plug equipment	Internal equipment	External equipment	Data collected
Borehole Test Interval	Inflow/outflow gas lines		Dry N_2 gas Gas flowmeters Data collector and power Chilled-mirror hygrometer Two-ended sample container	RH Gas composition
	Pass-through	RTDs	Data collector and power	Temperature
	Brine sampling access tube		One-use samplers	Liquid brine samples
	Pass-through	Heater / heater block	Power	Power applied, T on heater block
	Pass-through	LVDTs on heater block	Data collector and power	Borehole closure
		Cement plug near borehole end	Over-core after test to retrieve samples	Cement/salt interface characteristics
Satellite Observation Borehole	Inflow/outflow gas lines		Gas source (w/ Ar & Xe tracers) Gas flowmeters Gas pressure & T Data collector and power	Characterization of DRZ extent and permeability of damaged regions
		RTDs	Data collector and power	Temperature
		Deuterated water tracer	In-drift sampling to assess leakage	Tracer breakthrough to test borehole and distribution
		AE sensors / sources	Data collector and power	Passive monitoring of AE events and damage mapping via active sources
		ERT electrodes	ERT controller	Salt resistivity in space and time

Instruments are described in Section 4, and a summary of testing chronology is given in Appendix B.

2.4.2 Access Drift Monitoring

Power applied to the heater through time will be monitored. The heater power controller will be set to a target temperature (rather than a target power level), using a temperature sensor on the outside of the heater block.

Access drift barometric pressure, air temperature, and relative humidity (RH) will be monitored at high frequency. These parameters are important to monitor because they are essentially the boundary conditions applied in the access drift DRZ. Air pressure, air temperature, and RH will be monitored with sensors sensitive enough to discern expected differences in these variables between the drift air and the borehole test interval.

Air in equilibrium with Na-Cl brine has a RH of 75%, but Mg-Cl brines have equilibrium RH of 40% or lower, depending on the precise composition (Appendix A-2.1, Figure 21). Mine ventilation at WIPP often contains more or less humidity than this, but the differences are moderated as ventilation air moves through the underground. The moderation effect may depend on the ventilation flowrate. RH of the air in the access drift will provide a measure of dis-equilibrium with respect to the salt formation, and the potential for moisture to exchange between ventilation air and the tested rock mass. Atmospheric data from the central WIPP "mine weather station" or other WIPP ventilation datasets, including the flowrate, will be monitored during the test for comparison with test location data.

To the extent possible, the ventilation in the access drift should be limited or controlled. Doors or bulkheads could be used to route ventilation around the active test area. Controlling and limiting the transients in the ventilation system will help simplify future modeling of the test results.

2.4.3 Salt Temperature Monitoring

Temperature will be monitored very close to, or in contact with, the heater surface, to determine the hottest point in the borehole (e.g., between the heater block and heater). Temperature will be measured along a line parallel to the borehole axis, and along one circumferential ring around the heater. Temperature will also be monitored through time in satellite boreholes at two different radii away from the heated borehole (Figure 7). Section 4.3 discusses temperature monitoring devices.

Heat conduction should be the primary heat transfer mechanism in the intact salt, as opposed to radiation and convection. It will be important to characterize the distribution of temperature in the heated borehole since this is the source of heat flux (i.e., the boundary condition) for the THMC problem. Observations of temperature in satellite boreholes will only require monitoring along the length of the boreholes. The observation hole diameter will be small compared to the heated borehole, and there should not be a significant temperature gradient across the diameter of the observation holes.

Spatial and temporal distribution of temperature data will be used with TH(MC) models to estimate thermal transport properties of the salt (thermal conductivity and heat capacity). The temperature distribution must be well characterized because it drives brine flow (i.e., thermal expansion of brine; McTigue 1985) and enhances creep closure.

2.4.4 Vapor Collection and Gas Sampling

Water vapor extraction will be monitored at high frequency. Data collection frequency will be approximately minutes or seconds between observations to resolve temporal fluctuations in brine inflow as a function of changes in temperature, access drift air pressure and humidity, and creep closure of the borehole and access drift (see high-frequency lab data in Figure 34 of Appendix A-4). The primary method for high-frequency monitoring of brine inflow will be monitoring water vapor production. Water vapor production will be determined by measuring the mass flowrate of gas circulation through the test interval, and estimating its absolute humidity. Periodic measurements of weight gain in downstream desiccant traps will be performed as a secondary lower-frequency method for estimating brine inflow. The traps will provide a cumulative estimate of moisture production, and help prevent re-cycling of

deuterated water (D_2O) tracer that would otherwise be release to the access drift air and potentially migrate back into the test interval.

The flowrate of gas (other than water) going into and out of the borehole will be measured to quantify the mass balance, and estimate the leakiness of the borehole system (i.e., packers, plug, and near-borehole DRZ).

Figure 8 illustrates the layout and connection of borehole equipment. The equipment will allow for multiple configurations:

1) gas flowrate damage testing (upstream constant pressure, downstream outflow closed, observe upstream pressure – Section 2.4.6);
2) water vapor inflow measurement (upstream constant flowrate, downstream open, measure upstream/downstream gas flowrate and downstream humidity);
3) gas sampling (upstream constant pressure, downstream sampler attached, outflow closed); and
4) liquid brine sampling (downstream closed, possibly applying upstream pressure to lift out brine samples).

For water vapor sampling, an inflow line will be connected to a dry nitrogen gas supply (with as little water content as practical) by a flowmeter valve that will measure a range of flowrates relevant to the flowrates controlled by the upstream valve on the N_2 tank. The end of the N_2 inlet tubing will be positioned near the back of the borehole. An outflow line will be branched to outputs such as a flowmeter valve (that must tolerate possibly hot, acidic moisture in the outflow stream) through a downstream set of desiccant canisters to the exhaust. The end of the N_2 outlet tubing will be near the packer, to encourage the gas to sweep through as much of the heated borehole interval as possible.

An inline chilled-mirror hygrometer (CMH), and a double-ended sample container will be connected downstream of the borehole. Since humidity measurements are important, the exhaust line will also have a redundant hygrometer gauge taking higher-frequency humidity readings throughout the test (e.g., a lower-cost resistive or capacitive hygrometer sensor). The CMH will take readings for more accurate estimates of RH (Section 4.8). Appendix B presents a bounding calculation illustrating a that typical a N_2 gas cylinder would last no longer than 53 days, removing the expected amount of brine flowing into an isothermal horizontal borehole at WIPP.

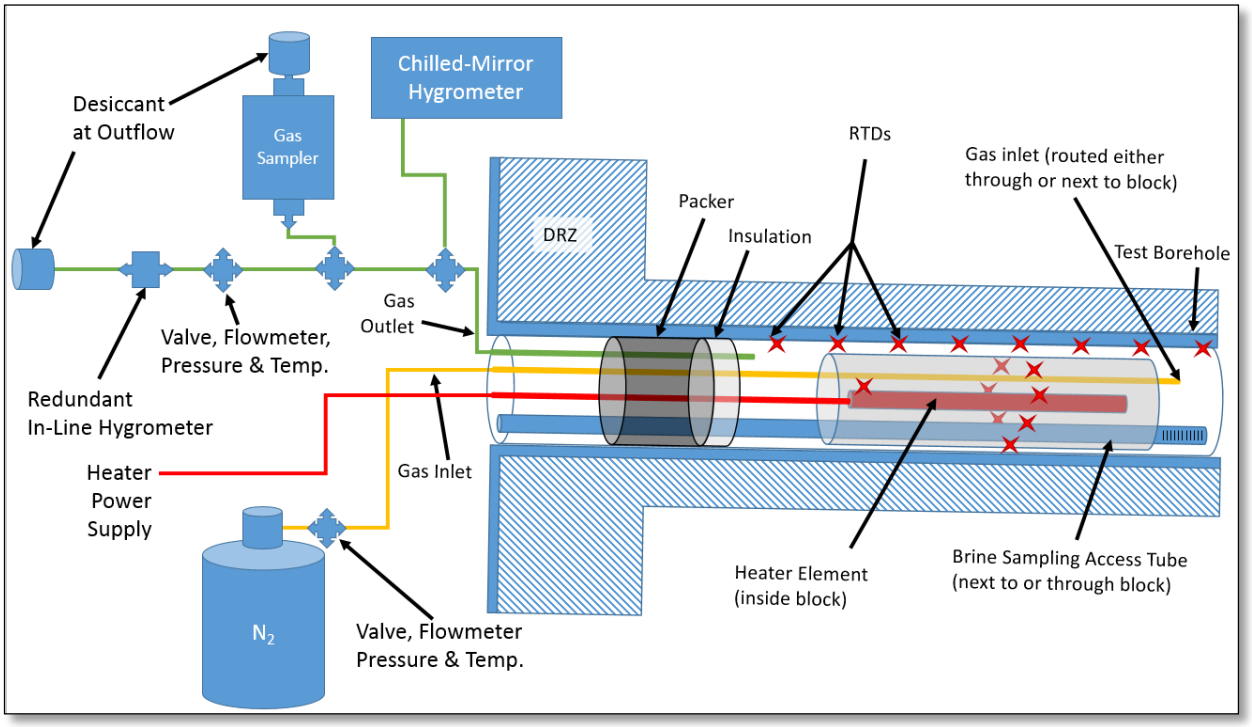

Figure 8. Schematic of test borehole equipment.

The water vapor sampling system will be operated at multiple N_2 flowrates to investigate the efficiency of the moisture removal from the borehole. This data should inform the choice of optimal rate for moisture removal in future tests, or may illustrate any effects of depressing the humidity in the borehole below its equilibrium value with the salt (i.e., a N_2 flowrate that is too high).

Gas samples will be collected using a double-ended sampling vessel attached to a sampling port in the downstream tubing. Humid borehole gas will first flush through the sample container (both valves open), then the downstream sample container valve will be closed, and finally the upstream sample container valve will be closed. A desiccant canister will be installed downstream of the sample outlet to minimize recycling of D_2O in the access drift. The gas sample composition will be tested using gas chromatography. The distribution of isotopes of water (e.g., deuterated water tracer – see Section 2.4.10) will be analyzed using a cavity ring-down spectrometer (CRDS).

The observed water inflow rate through time will be used with the applied constant-humidity boundary condition to estimate the flow and transport properties of the salt via parameter fitting TH(MC) models to the data (e.g., FEHM, PFLOTRAN, or TOUGH2). Gas and liquid samples will be used to monitor the breakthrough of deuterated water tracer from the observation borehole, which will provide a measure of transport velocity, related to the permeability, effective saturation, and effective porosity of the salt – although these parameters might not each be uniquely estimable. Interpretation of tracer data may require a THC model accounting for the fractionation of deuterated water during flow from the source to the evaporation in the central test borehole (heated or isothermal). Gas sample data would provide information on the transport of inert gas tracers (i.e., Ar and Xe) introduced in the observation boreholes, to the test borehole. Tracer transport may require a two-phase TH(MC) flow model to interpret, since the system could be mostly brine-saturated, although salt that is mostly gas-saturated could behave like a single-phase gas system (Stormont et al. 1987).

2.4.5 Brine Composition Sampling

The packer isolation system will also be equipped with a brine sampling access tube to collect liquid brine samples from the test borehole (Figure 8). The composition of the fluid in the borehole will evolve due to two competing processes. One is the possibly changing source of brine flowing into the borehole. Brine collected in the borehole would include components of intergranular brine, intragranular fluid inclusions, water vapor released from dehydration of minerals, and brine from condensation of steam that dissolves salt and then flows into the borehole. A second effect would be the evaporation and concentration brine in the borehole, due to constant removal of moisture (see Appendix A-2). The superposition of these two competing processes may make it difficult to discern the source of any observed changes in liquid brine chemistry during the test.

The design of the brine sampling tool is not complete, but it will include the ability to collect samples of liquid brine for laboratory compositional analysis. The tool should use a robust approach not subject to plugging (e.g., small-diameter tubing would likely become plugged between sampling events by crystallizing salt as the hot salt-saturated brine is cooled). Sampling would be done through a slotted or perforated access tube. This sampling access tube and its openings to the borehole should be large enough diameter so it does not become plugged after repeated sampling events. Possible approaches include:

- Use capillary tubes to wick up standing brine at the end/bottom of the sampling tube. These capillaries would each lift up a small amount of brine. This approach does not require pumping, but might not capture a large volume of brine, which could make some laboratory analyses difficult or less accurate.
- Samplers could comprise fiberglass wool or fine-sand material to wick up brine from the end/bottom of the sampling access tube. This would be analogous to using a giant “Q-tip” to wick up brine. This approach also would not require pumping, but may not acquire large enough sample volumes and samples would require additional processing steps (e.g., centrifugation or rinsing of samples from sampler).
- A small diameter tubing (larger than a capillary) could be used to pump brine up from the bottom of the borehole. Pumping requires either syphoning brine up or using applied gas pressure from the moisture extraction system, but could potentially acquire larger-volume samples.

Samples of liquid brine acquired during testing will be used in conjunction with post-test samples of precipitated salts for calibrating transient thermal-chemical models (e.g., EQ3/6 or PHREEQC). It may be possible to treat the borehole system as a beaker-type mixing experiment, with a stream of inflowing brine, outflowing moisture, and precipitation of solids through time. These models will be used to estimate any discernable changes in the temporal composition of brine flowing into the borehole from the observed changes in borehole brine chemistry.

2.4.6 Gas Flowrate Damage Testing

Gas flow in packed-off intervals can be used to estimate the damage in borehole intervals to assess the extent of the DRZ. An interval of a borehole is isolated (either between two packers or behind a single packer), and gas pressure is applied to the interval. In the constant-pressure test, a low pressure (e.g., 70 kPa [10 psi gauge]) is applied and the resulting gas flowrate is observed. The test runs until a steady state is achieved (which is on the order of a few seconds or minutes). In the falling-pressure test, a pressure is applied to the interval, and the interval is closed in, followed by monitoring the decay of pressure in the interval. Falling-pressure tests are typically more useful on lower-permeability intervals. The tests can be repeated in different intervals of the borehole to assess damage along the length of the borehole. These tests have been run at WIPP (Appendix A-9 and Figure 4b) and at Avery Island (Appendix A-3.2) with success. The tests performed at WIPP (Stormont et al. 1987; data from gas flowrate damage testing listed in their Appendix C) applied 70 kPa [10 psi gauge] across a 1-m section of

13 cm-diameter borehole and had a lower limit of 0.1 SCCM (standard cm^3/min), which corresponds to a gas permeability of approximately 3×10^{-6} darcy [3×10^{-18} m^2]. The configuration used at Avery Island (Appendix A-3.2, Figure 31) involved grouting the borehole above the mechanical packer and was able to interpret gas permeability down to 10^{-21} m^2 (~1 nanodarcy). The minimum interpretable permeability is related to the sealing ability of the packer system.

Since the moisture inflow system (Section 2.4.4) also uses gas flow, the N_2 flow system will be plumbed to allow the downstream outlet to be closed, while maintaining the upstream pressure and monitoring the flowrate. This will allow an estimation of the gas-accessible permeability of the borehole during the bine inflow test. This test could observe changes in the DRZ surrounding the access drift or boreholes, or change in the gas saturation in the test interval. Low pressure gas will likely not displace brine in a partially saturated DRZ during testing. It will be difficult to differentiate changes in total porosity (i.e., either damage or healing) from changes in gas saturation, due to the existence of two-phase brine and gas flow (i.e., brine flowing in to the DRZ surrounding boreholes, reducing the gas-accessible porosity).

The gas used to conduct the damage test should include different tracer gas in each borehole, which would be analyzed for in the gas samples collected from the test borehole. This would provide a measure of gas transport in the salt. The tracer gas should be inert, stable at elevated temperatures, and naturally rare in the testing environment (e.g., Ar and Xe at ≤10% concentrations in a N_2 carrier gas). Gas tracers will provide information regarding their earliest breakthrough (or lack or breakthrough) during a brine collection test. This could be related to an advective gas porosity of the salt, for a gas-only pathway. The magnitude of gas concentrations in the test borehole samples (especially under two-phase flow conditions) may not be uniquely interpretable. Therefore, this type of measurement is considered to be of secondary importance.

WIPP site pressure-safety regulations require a pressure-safety plan be prepared for any system involving high-pressure gas (i.e., connected to a N_2 cylinder). Strategies to meet these requirements and achieve test are being explored and addressed in FY17 laboratory and preliminary field testing.

Stormont et al. (1987) discuss gas tracer experiments using SF_6, conducted in vertical boreholes in drift N1420 at WIPP. These tracer tests showed there was significant gas-saturated porosity in the marker bed and in the DRZ of the access drifts. Any gas tracer experiments as part of this plan would not be in Marker Bed 139 (MB139), and would likely not have gas-saturated connected porosity between the boreholes.

2.4.7 Geomechanical Monitoring

Borehole closure will be monitored in the test borehole using multiple linear variable differential transformer (LVDT) gauges or possibly other less-accurate displacement monitoring devices. These will monitor closure of the borehole throughout the test due to creep. These may be mounted on the heater block, if it is manufactured from material with well-known mechanical properties (i.e., thermal expansion coefficient). Borehole closure observations will help constrain THM models and predict borehole closure effects during the test. There is a large amount of existing drift and borehole closure information for comparison, gathered from the TSI experiments in the WIPP North Experimental Area (Tyler et al. 1988; Munson et al. 1991, 1992a, 1992b, 1997a). Borehole strain was measured in brine inflow boreholes at WIPP in Rooms A and B (Nowak & McTigue 1987).

Extensometers could be installed in observation boreholes, with wires or rods used to monitor relative motion of an anchor point in the salt and the collar at the access drift (Section 4.4). Extensometers provide observations of relative displacement between two or more fixed points, which could also be used to constrain THM models that include creep closure and deformation of the access drift.

Borehole pressure cells (BPC) could be installed into a grouted observation borehole to measure changes in stress due to thermal effects and creep closure of the heated borehole (Section 4.5). They are typically installed in pairs, giving data about the changes in vertical and horizontal stress during the test.

Observations of stress or pressure in the salt are difficult to make reliably (Bechthold et al. 2008) but can be used to constrain THM models that include creep closure and deformation of the access drift.

Large-scale geomechanical observations of drift closure are not the primary goal of the first two tests, and will be deferred to later tests. Borehole closure observations may be included in the first two tests if they do not complicate the observations related to the primary goals of the test.

2.4.8 Cement Exposure Test

A short plug of Class G or H cement or variant concrete will be placed in the back of at least one borehole in a follow-on test. The point of the test is not to create a solid sealing plug of cement, so a small amount of cement can be emplaced to the end of the borehole with a long "pusher" rod. Cement and concrete are ubiquitous in construction and have been proposed as repository sealing materials. Although some studies have been conducted on the topic of cements in a salt repository (e.g., WIPP Plugging and Sealing Program; Tyler et al. 1988), it would be valuable to take exposed samples from the salt and cement interface, and to help understand how the interface between the cement, salt, and aggregate behaves in contact with a hot, acidic brine. This test may impact brine composition samples and even inflow rates of moisture to the vapor collection system, so cement exposure tests should be deferred to follow-on tests.

Samples of cement and the cement/brine interface would be recovered from the borehole after the end of the test. They would be examined quantitatively using scanning electron microscopy (SEM)/energy dispersive X-ray spectography (EDS) and X-ray diffraction (XRD) for elemental compositions, and porosimetry (multi-beam SEM, nitrogen adsorption) for pore-alteration. The aim would be to quantify the effects that heat, brine, and acid gas have on the chemical and structural properties of the cement.

2.4.9 Electrical Resistivity Surveys

Electrical resistivity surveys will be conducted within and between satellite boreholes on either side of the test borehole (Figure 7) to estimate the evolution of brine content in the salt surrounding the boreholes. Appendix A-8 shows some resistivity vs. brine content relationships used in previous salt work in electrical resistivity. Typically, the higher brine content in bedded salt (compared to domal salt), means the resistivity of the formation will be lower than in domal salt.

Salt resistivity is expected to change by orders of magnitude due to changes in brine content (see Appendix A-8), while changes in temperature should only result in changes in resistivity of only a few percent. Electrical resistivity tomography (ERT) is the process of estimating formation resistivity from multiple sets of applied current and measured voltage electrode pairs. It is not clear whether ERT could distinguish between difference in brine content due to changes in porosity (i.e., damage or healing) or equivalent changes in brine saturation, due to flow of brine into or out of gas-saturated salt. Distinguishing between these two interpretations may require jointly interpreting results from the ERT surveys and a seismic or active AE survey (Section 2.4.11).

Electrical geophysical methods often have problems with metal located in or near the test interval. WIPP drifts include extensive rockbolts and chain-link fencing, while the test borehole will include tubing, packers, and wires associated with the test (Figure 8). ERT may still produce usable results in the presence of these metal components, since it is the change of resistivity through time (i.e., between individual surveys) that is being interpreted.

2.4.10 Deuterated Water Tracer

A deuterated water (D_2O) tracer will be added to one of the observation boreholes above the test borehole. A small amount (e.g., 10 mL to 100 mL) of liquid D_2O will be added to an isolated section of one of the observation boreholes. Leakage of D_2O from the source borehole should be reduced by using multiple packers or plugs to isolate it from the access drift, and air samples should be taken during the test to assess the level of leakage directly from the source borehole into the access drift. Limiting the source to a short interval at the back of the borehole would make behave it more like a point source. Samples of

water vapor and liquid brine from the test borehole will be analyzed with CRDS to quantify hydrogen isotopes in the water. Quantifying the breakthrough of tracer from the D_2O source in an observation borehole to the test borehole will be used to estimate brine transport velocities, including the effective porosity of the salt.

The D_2O could be added to the observation borehole by saturating a small sponge with the traced water. The RH of a sealed observation borehole in equilibrium with Na-Cl brine will be 75%. The D_2O will evaporate into the borehole air, elevating it above 75% RH (since it is pure water and therefore wants to equilibrate to 100% RH), and leading to deliquescence (dissolution of salt by condensation of moisture in the air).

Fractionation of the D_2O will occur in the test borehole during evaporation or boiling of the brine from a liquid into a vapor phase (Appendix A-3.1 and Stauffer et al. 2015, p. 73), as well as during the precipitation of any hydrous minerals in the borehole. The RH is equal to the activity of water, which primarily controls fractionation during evaporation, with less fractionation happening in a more humid environment. Evaporation into air with RH above 95% results in essentially no fractionation (Kendall & Caldwell 1998).

As with gas tracers, the initial breakthrough of liquid tracer can be related to transport velocities and effective porosity. Unlike the gas tracers, we can attempt a mass balance of D_2O distribution after the completion of the test. The sampling would need to estimate:

1) net loss of in D_2O in the source borehole,
2) mass of D_2O collected in vapor form in the test borehole during the length of the test,
3) mass of the D_2O precipitated in hydrous minerals in the test borehole, and
4) D_2O left in the formation (less the background concentration – estimated to be 3 ppm per gram of salt at Avery Island).

Post-test samples of salt will be cored between the source and test boreholes (adequately preserving the salt samples for evaporative losses and possible further fractionation during handling and transport to the laboratory), to estimate the spatial distribution of D_2O left in the formation (done at Avery Island, Appendix A-3.1).

Observed spatial and temporal distributions of D_2O will be used to calibrate THC models of flow and transport in the salt. This data will provide a unique calibration and validation dataset regarding brine transport through salt under both isothermal and heated conditions.

2.4.11 Acoustic Emission Monitoring

During heating and cooling, salt produces acoustic emissions (AE) related to micromechanical brittle deformation. AE sensors (i.e., sensitive piezoelectric microphones) will be installed into observation boreholes with grout or epoxy to ensure a good connection between the rock and sensors. A minimum of four sensors is required to estimate source locations of emissions in three dimensions, but due to effects of ambient noise six or more are preferred. The second borehole test will have one or two sensors emplaced in observation boreholes, to assess the ability to monitor and discriminate AE from the heating and cooling of salt, in the presence of ambient WIPP noise. Piezoelectric sensors will be placed in boreholes deep enough to be located beyond the access drift DRZ, where ultrasonic velocities are slower (Hardy & Holcomb 2000; Holcomb et al. 2001). If sufficient AE events are observed during the 120°C test, an arrangement of six or more AE sensors and higher-frequency observations may be justified for subsequent tests, to allow estimate source location estimation, especially with repeated heating and cooling episodes (Section 2.8.1).

AE would be useful for characterizing brine release micromechanical processes during heating and cooling (e.g., failure of fluid inclusions or micro-crack damage accumulation). Most macroscopic

mechanical or THMC models would not be able to use AE observations (timing or source locations) directly, but this dataset might be useful for building a physical understanding of the THMC processes going on in salt, especially during a rapid heating or cool-down period. This is not one of the primary goals of the test series, so these observations are lower priority than those directly related to brine availability, but the data may improve understanding of micromechanical and hydrological coupling in salt.

Piezoelectric sensors can double as ultrasonic sources to survey the distribution of wave velocities between sensor boreholes in the salt (i.e., cross-hole wave propagation tests). Estimating the distribution of faster and slower travel-time regions in the salt could help to estimate the distribution of the DRZ (Holcomb et al. 2001), and to better estimate the source locations of AE. Alkan et al. (2007) have used AE in the laboratory to investigate the onset of permeability enhancement in salt during triaxial compression tests. Active velocity surveys could be conducted before, during, and after heating, since the applicable wave propagation characteristics in the salt may change with temperature, damage, or healing.

If ambient WIPP noise levels are favorable, AE testing will collect full-waveform data for possible analysis of wave attenuation and dispersion. This data would also be useful for quality control, since the observations will change in character if the sensors de-bond from the salt in their boreholes. For subsequent tests, the sensor and source network should be installed to allow automatic execution of the velocity survey frequently during the test. As the bulk salt deforms and fractures the changes in seismic propagation can be significant, and associating the changes with AE events would be helpful, in place of more traditional geomechanical observations. Salt creep may complicate the survey process, because movement of the source relative to the receivers will appear just like changes to the speed of propagation between the sensors.

2.5 Expected Test Conditions and Processes

The following bulleted list summarizes important processes and conditions we expect to observe during the first two borehole tests (isothermal [~30°C] and 120°C) at WIPP. The expected conditions necessarily motivate the sequence of activities that will be conducted in the borehole (Appendix B), and the types of sensors to be used (Section 4).

- Boreholes will be drilled through the access room DRZ (gas flowrate testing will be used to delineate the extent of the DRZ surrounding the access room). If borehole test intervals are located deep enough into the salt to be outside the access drift DRZ, the salt will be low porosity, low permeability, and brine saturated as an initial condition.
    - Boreholes will each develop a small DRZ of approximately the same radius as the borehole.
        - Salt porosity will increase in the borehole DRZ due to dilation associated with stress redistribution from creating the borehole.
        - Salt permeability will increase in the borehole DRZ due to increased porosity.
        - Brine saturation of salt will decrease in the borehole DRZ due to increased porosity.
- Intergranular brine will flow to the test borehole down a pressure gradient (up the temperature gradient in the heated borehole). High brine pressure (~lithostatic) exists in the undisturbed far field, while the borehole will be maintained at nearly atmospheric pressure and constant humidity. There are porosity and permeability gradients, also (porosity and permeability of the salt are lowest in the far field and highest near the borehole). The brine inflow rate will be highest at first, and will decay exponentially with time (Figure 11).
- Brine will flow towards the borehole driven by thermal expansion of the brine in the pores (i.e., thermoporoelasticity, McTigue 1985), with slight changes in composition along the way. Salt

permeability will simultaneously decrease with expansion and accelerated creep deformation of the salt grains due to heating (Figure 32).

- Tracer (deuterated water) will be added in an observation borehole.
    - Tracer will travel through the brine-saturated porosity of the salt via diffusion (down a concentration gradient), and advection (down a pressure gradient towards the larger borehole).
    - Tracer may travel through the gas-saturated porosity of the salt (if a continuous gas-saturated path exists) as water vapor.
- Water will evolve in vapor form as hydrous minerals in the salt dehydrate at different temperatures. As different minerals dehydrate, there is typically a volume change associated with the dehydration, which may lead to additional porosity and permeability in the salt.
- Water vapor from mineral dehydration will migrate down minor air pressure and water vapor concentration gradients to the borehole, but it may condense and dissolve additional salt *en route*, depending on the temperature.
- Brine will evolve from the salt as fluid inclusions (i.e., intragranular brine) by migrating to grain boundaries and becoming "free" intergranular brine. Fluid inclusion composition is often different from intergranular brine (Figure 25) with higher concentrations of typically minor ionic species.
- Water vapor will be removed in the isothermal test borehole because dry N_2 will be circulated through the borehole.
    - Salts (mostly halite and sylvite, initially) will precipitate out of the brine as water vapor is removed, since the brine flowing into the borehole is at or near saturation already. Activity of H_2O will decrease below the 75% RH associated with saturated Na-Cl brine as the concentration of Mg increases (Figure 18).
    - The brine remaining in the borehole will evolve to a more Mg-rich brine, and hydrous magnesium chloride salts will precipitate as the system loses more water. This is brine evolution due to enrichment and salt precipitation (Appendix A-2.1).
    - Additional brine will flow into the borehole, which may or may not differ in composition from brine that will already have flowed into the borehole at that point. This may be a change in source composition (Appendix A-2.3).
    - Samples of gases collected from the borehole will include water vapor and the added deuterated water (D_2O) tracer. The D_2O may have fractionated in several ways (Appendix A-3.1):
        - D_2O will fractionate at the source, where it will migrate from the source into the salt via deliquescence and mixing with native formation brine.
        - D_2O will mix during flow through the salt via diffusion and dispersion with native brine (with concentration levels of D_2O).
        - D_2O will fractionate predictably after flowing into the test borehole, where the heavier D_2O will preferentially stay in the borehole and lighter H_2O will evaporate and be removed by the dry N_2 stream. The fractionation will be harder to predict if the temperature is above boiling, but there will be minimal fractionation if there is complete boiling. The volume of residual moisture may be small enough in a hot borehole to make fractionation less important in the overall mass balance of D_2O.
        - D_2O will fractionate, as precipitation of hydrous minerals in to borehole may take up D_2O at different rates than H_2O.
        - Microbial effects on fractionation should be small, since there are not significant communities of halophiles known to be viable in WIPP salt, especially heated salt.

  - The CMH and any downstream flow meters may require flushing or cleaning due to deposition of salt dust or precipitation of any condensable gases besides H_2O (e.g., $HCl_{(g)}$).
- Acid gas ($HCl_{(g)}$) will exist in equilibrium with the heated brine, especially as the brine evolves to become magnesium-rich. The effective pH of any condensate in the borehole will be low due to the presence of acid gas, and the reduced partial pressure of steam (availability of liquid water) from circulating dry N_2 gas (Appendix A-2.2).
- Acid gas will be generated in the heated borehole environment from a combination of:
  - decomposition of hydrous Mg salts (thermodynamically favored at higher temperatures and in presence of adequate oxygen), and
  - directly from a liquid brine by equilibrating $HCl_{(g)}$ above a strong chloride brine (Na-Cl or Mg-Cl) and moving that partial pressure of acid gas over distilled water.
- Magnesium chloride minerals will evolve differently depending on the humidity of the borehole environment. If the N_2 flowrate is too high and RH is low, minerals will dehydrate at lower temperatures than if the RH is in equilibrium with the salts (i.e., 75% RH for Na-Cl brine or lower for other brines – Greenspan 1976).
- In a heated borehole, the brine will evolve differently than in the isothermal borehole, since minerals have different stabilities with respect to temperature and RH (Wollmann 2010).
- In a heated borehole the fractionation of D_2O will be different than in the isothermal borehole, since fractionation between liquid and vapor and hydrous minerals is temperature dependent.
- The resistivity of the salt will change in space and time due to (Appendix A-8):
  - Resistivity of salt is a function of brine saturation
  - Resistivity of the brine is a function of temperature
  - Metal tools (including the heater, its power cables, rockbolts and chain-link fencing) in the boreholes and access drift will influence the effective resistivity (but this effect shouldn't change through time) – the magnitude of this effect will be examined in the initial isothermal test
  - Presence of brine-saturated clay layers outside the near field of the test interval could strongly affect the response, but should also not change significantly with time
  - Resistivity of the salt near the access drift, in the room DRZ, may fluctuate with the RH of the ventilation system air (i.e., dry vs. moist).
  - Formation factor may be a function of temperature due to temperature-driven changes in surface conductance, causing an apparent change in brine-saturated resistivity with temperature. This effect is stronger in clays, but the disseminated clays in MU-0 may produce a similar effect.
- Material added to the borehole may generate vapor, and may react with the brine and acid vapor evolving in the borehole. These materials may generate $HCl_{(g)}$ vapor and may interact with the acid brine, and may produce corrosion products and further change the system composition. Key system materials should be tested in the laboratory at expected temperatures to monitor their degradation and any byproducts they may produce. The materials in the borehole and directly exposed to the borehole will include:
  - Packer or plug seal materials (e.g., neoprene, viton, or silicone rubber). Neoprene may generate HCl vapor when heated; viton may genereate HF vapor when heated.
  - Gaskets or seals between packer and tubing (e.g., neoprene, silicone, or filler foam). Organic components could produce unexpected chemical results when heated.
  - Insulation on the heater side of the plug or packer (e.g., fiberglass).
  - Metal components of packers, brine sampling equipment, valves, and gas tubing (e.g., stainless steel or nickel-chromium based corrosion-resistant materials) will corrode.
  - Heater element and any "thermal ballast" added to surround the heater element will corrode.

  - Any cement samples added to the borehole will react with brine, acid gas, and heat.
- The test and observation boreholes will deform and creep closed.
  - Heating the test borehole will speed up borehole closure and creep closure of the access drift.
  - If the salt closes in on the heater or packers to prevent their removal, they will need to be overcored or destroyed to be removed.
  - The drift will only be heated from one side; it will creep closed asymmetrically.
- Acoustic emissions (AE) will be generated in the salt.
  - They may be difficult to discern faint emissions from background WIPP noise.
  - Rapid heating or cooling will cause micro-cracking due to extension or contraction, and will lead to AE.
  - Macroscopic cracking, spalling, and failure related to drift closure will cause AE.
  - Ultrasonic wave velocities are a function of the amount of damage in salt, with waves traveling faster in intact salt (Holcomb et al. 2001).
  - Ultrasonic wave velocities are more function of temperature and less a function confinement, with waves traveling slower in hot salt and faster in more strongly confined salt (Yan et al. 2014).
  - Both the travel times (i.e., first arrival) and the full observed waveforms from man-made cross-hole AE contain useful information for understanding changes to the salt and the sensor network.
  - Salt creep may change the relative positions of the AE sensors and sources with time. It may be difficult to discern the difference between changes in sensor network geometry from changes in material properties (including both damage and temperature effects).
- During cool-down of heated salt, a surge of brine will flow into the borehole.
  - At least two weeks of cool-down brine inflow data will be collected after the end of heating, with high-frequency data collected at changes in heater power (up or down).
  - Any unplanned fluctuations in heater power (i.e., power surges or brownouts) may lead to changes in brine inflow.
- Salt precipitate (i.e., efflorescence) will form on the borehole wall under isothermal and heated conditions. Salt will also precipitate in the formation once the boiling isotherm moves out into the formation. Precipitates will be collected from the test borehole during post-test sampling, to quantify the D_2O mass incorporated in hydrous minerals, and to determine its mineral makeup.

2.6 First Borehole Test Objectives

The first borehole test will be performed at ambient or isothermal (~30 °C) conditions. We will choose instrumentation and methods with high likelihood of success. A goal of this test will be not to over-complicate techniques or try too many new methods or equipment. Another important objective will be to enhance the test organization's experience with testing in the underground environment, with organizing and arranging activities, and assessing the efficacy methods and equipment at the conclusion of the test. The isothermal test will allow debugging of the data collection setup without the complication of the heater.

The isothermal test will provide a baseline of data to compare brine inflow, tracer transport, and brine chemistry against data collected from the second heated borehole. The main activities during this test will include gas flowrate testing for damage evaluation, installation of electrodes to gather ERT data, monitoring water vapor mass flowrate using recovery by circulation of dry N_2 gas, sampling liquid brine flowing into the test interval borehole, and observing migration of D_2O through the system. The first test will also assess the effectiveness of measures to control D_2O source containment and possible contamination of the access drift with deuterium. Table 4 is modified from Table 3 to only include practices utilized in the first test.

Features of the initial isothermal test include:

- Interval gas-flowrate rock damage testing sequence (constant pressure and falling-pressure tests with gas tracers) will be conducted in the borehole to evaluate damage along the length of the borehole by testing repeatedly and moving the packer deeper into the borehole (Appendix A-9). These tests should be conducted as quickly as possible, to install the borehole seal and quantify brine inflow before losing too much brine to the mine ventilation.
- Adding D_2O source to a packed-off portion of one observation borehole.
- The isothermal brine inflow test using dry N_2 may take 200 days or more to reach an approximate steady-state condition (e.g., see data reported in Appendix A-1).
- Experiment with multiple N_2 gas flowrates, to estimate the optimal gas flowrate for subsequent tests. Test should flush water vapor from the borehole, but N_2 flowrate should not be too high, which may create an artificially dry environment that might complicate the boundary condition applied at the borehole during model interpretation of data.
- Sample gases collected from the borehole, test water vapor samples from the borehole and the access drift air with CRDS for stable water isotopes.
- Sample liquid brine from borehole during test. Isothermal test may allow some sampling approaches not possible in heated boreholes (i.e., hot brine will precipitate salt in sampling tubes as it cools).
- After the test, gas flowrate damage testing will be conducted along the borehole (no need for tracer gases) to evaluate damage along the length of the borehole, to compare to the pre-test results.
- After the test, salt precipitate will be removed from the test borehole and tested for D_2O content and mineral identification.
- After the test salt cores will be examined in the laboratory to compare samples from before testing, to discern change that occurred to the salt pore network from the test.
- After the test, salt cores will be collected between the tracer and test boreholes to tests for D_2O content in the salt. Samples should be preserved to minimize evaporative losses and additional fractionation of D_2O in the cores.

Appendix B presents a proposed testing sequence for the first two tests.

Table 4. First borehole test components.

	Packer/plug equipment	Internal equipment	External equipment	Data collected
Borehole Test Interval	Inflow/outflow gas lines		Dry N_2 gas Gas flowmeters Data collector and power Chilled-mirror hygrometer Two-ended sample container	RH Gas composition
	Brine sampling access tube		One-use samplers	Liquid brine samples
Satellite Observation Borehole	Inflow/outflow gas lines		Gas source (w/ Ar & Xe tracers) Gas flowmeters Gas pressure & T Data collector and power	Characterization of DRZ extent and permeability of damaged regions
		Deuterated water tracer	In-drift sampling to assess D_2O leakage	Tracer breakthrough to test borehole and distribution
		ERT electrodes	ERT controller	Salt resistivity in space and time

2.7 Second Borehole Test Objectives

The objectives of the second (120 °C) borehole are to perform essentially the same tests conducted in the first borehole, but with the effects of added heat. This temperature was chosen to be above the lower-end gypsum and clay dehydration temperatures but below the lower polyhalite and bischofite dehydration temperatures (Table 2). Heat will speed up most processes in the salt (i.e., borehole closure, brine inflow, brine evaporation). Test activities will include the same measurements: gas flow tests, electrical resistivity tomography, brine and vapor sampling from the test interval borehole, and observations of D_2O tracer. This test will include preliminary deployment of a limited AE sensor network to quantify the timing of AE events in the presence of ambient WIPP noise. The initial deployment will not include enough sensors or high-frequency data acquisition rate to estimate source locations or conduct active surveys.

For comparison, tests 1 and 2 should be nearly identical right up to turning on the heater, including: 1) same borehole layout, especially in relation to access drift geometry; 2) borehole sealing system with pass-throughs and fixtures for heaters in the isothermal test; and 3) an initial baseline monitoring period without heating, in the second test. Appendix B lists a proposed chronology of tests in the first two boreholes.

2.8 Follow-on Borehole Test Objectives

Further tests will be conducted using the modular borehole plan, but we intend to take a break between tests two and three to re-assess the testing goals, instrumentation, and sampling strategies. Lessons learned from the first two boreholes may result in changes to instrumentation, heater design, or testing schedule (e.g., parallel *vs*. serial tests). We only present possible test ideas for boreholes 3-5 and possible subsequent tests, with the intention of updating the plan after the first two boreholes are complete.

2.8.1 Stepwise Heating

A follow-on experiment could include stepwise heating. In such a test the power would be increased in steps and cycled on and off several times, to monitor the brine inflow during repeated episodes of heating and cooling. The typical response of salt (both bedded and domal) is to produce large amounts of brine at the first significant decrease in temperature (i.e., beginning of cool-down; Avery Island Figure 28, Salt Block II Figure 34, and Asse – Rothfuchs et al. 1988). Previous field tests have sought to minimize this effect by stepping down the heater power gradually, but even the first minor decrease in heater power results in a large increase in brine inflow. At Avery Island, gas permeability tests were conducted during the cool-down period. Results showed the permeability of the salt increased during cool down (Appendix A-3.2, Figure 32).

We do not expect the "power" level of radioactive waste to drop suddenly, but no salt heater test (lab or *in situ*) has yet reduced heater power slowly enough to prevent this surge of cool-down brine inflow. The Asse brine migration test spread the cool-down phase out over a month (Appendix A-5.3, Figure 38) and it still produced half of the total brine inflow during the cool-down period. If the brine surge is due to cool-down tensile forces cracking the salt and increasing its permeability, the cool-down rate must be slow enough to allow salt creep (which does not produce damage to the salt) to dissipate any stresses due to cooling before they lead to tensile cracking.

This proposed follow-on test will generate data for validating the coupled hydromechanical mechanisms in THMC models. We will cycle one of the tests through multiple hot/cold cycles and multiple temperature steps to collect a dataset for investigating the physical mechanism behind this widely observed (but still yet un-modeled) behavior. During this temperature cycling test, it will be important to measure borehole closure (and possible expansion), measure high-frequency brine inflow (including collecting samples of brine and gases), monitor AE, conduct active ultrasonic surveys to characterize DRZ development, and estimate the gas permeability of satellite boreholes through time.

2.8.2 Sealed Borehole Test

Another follow-on test of interest would involve conducting a hotter borehole heater test (i.e., above the brine boiling point), but under sealed conditions, without flowing dry N_2 through the borehole to remove brine. This test would be more representative of the conditions around a waste package. The cool-down phase would have to be quite drawn out (i.e., like radioactive decay) to reduce damage and brine release at the end of heating from completely wiping out the evidence left in the system that evolved during heating. The main information from this type of test would be the post-test coring and sampling to determine the final distribution of moisture and estimation of salt permeability and porosity surrounding the heater. This type of test would reveal information about the fate of brine in a sealed heated borehole or drift, where water is not continually removed. The interaction of brine migration down a pressure gradient, thermal expansion of brine, and water vapor recirculation and heating may be significantly different from in tests where the water is removed.

Brady et al. (2013) prepared their survey of remaining equipment as part of a re-entry plan to collect cores and heater samples from still-in-place Room A and B heaters in WIPP (emplaced in the 1980s). Most of these WIPP heaters were sealed (i.e., did not have N_2 circulated through them) and achieved temperatures above boiling.

2.8.3 Long-term Brine Availability

Once the brine collection and borehole packer system designs have been tested, a follow-on low-temperature heated (~50 °C) test could be conducted for a longer period of time (≥3 years) in a deeper borehole (≥20 m [65']). The point of this type of experiment would be to monitor the availability of brine over a longer time scale, to possibly see boundary effects associated with the edge of the DRZ for the repository excavation (i.e., a decline in the production of brine). The initial planned tests are short duration and are expected to reach an essentially steady-state brine production rate. The reservoir of brine and permeable salt that these shorter tests will draw from appears infinite in previous *in situ* tests. From the point of view of long-term performance of a salt repository, it would be useful to quantify the extent of the DRZ associated with the excavation of the repository facility and possibly assess the ultimate quantity of brine that could flow into a repository excavation.

2.8.4 Other Follow-on Measurement Types

Cement and brine interaction tests will be conducted in later borehole tests (possibly during tests listed above), as they will likely affect brine chemistry. Geomechanical observations beyond possibly simple borehole closure will also be conducted in subsequent tests.

3. LABORATORY INVESTIGATIONS

Along with in-situ testing, laboratory experiments and laboratory investigations of samples from the test intervals will also be coordinated. These include microscopic observational studies and flow properties on cores, estimating the coefficient of thermal expansion of salt and brine, and analyzing captured brine and gas samples from the boreholes. These experiments require preservation of samples. All core should be sealed to prevent dry-out. If samples are properly preserved, analyses can be run in subsequent years, based on the availability of funding.

3.1 Pre-Field Test Materials Interaction Experiment

Materials to be utilized in the elevated temperature field tests should be tested first in the laboratory to monitor for significant produced gases or liquids. Neoprene rubber gaskets or seals may produce HCl vapor, and silicone or fiberglass may produce silane (SiH_4) vapor. These by-products should be evaluated to assess whether they will meaningfully interfere with the planned measurements, including: CRDS interference, CMH condensate, and tracer gas detection via gas chromatography.

Laboratory exposures of cement and metal samples in heated brine would also help to better understand their impacts on brine composition, but would not require laboratory testing before execution of the field test.

3.2 Core Analysis

Classical microscopic observational studies will include examination of thin sections to determine mineral distributions and microstructural features. Mineral distributions will require accurate descriptions of hydrous minerals that influence brine and gas samples collected during the test, as well as deformation mechanisms. Microstructural features provide details of deformation characteristics ongoing in salt structures before and after testing. The evolution of micro-mechanical processes is important to the long-term performance of heat-generating repositories and model validation (Hansen 2014). Pressure solution processes, dislocation creep, and plasticity are micro-mechanical processes that are sensitive to thermal exposure and have a direct impact on the structural state of salt. The effects from hot brine or steam on these micromechanical processes have not been explored directly. Exposed samples from the near-borehole region can be analyzed for precipitated salts or damage associated with heat and vapor transport.

Flow and pore properties of the intact salt are also desired. Laboratory analyses will be conducted on samples obtained before and after heating. Laboratory analyses will include total porosity (e.g., He

porosimetry), and pore size distribution (i.e., Hg-injection porosimetry). The three-dimensional pore morphology, connectivity, pore-grain dihedral angle (Ghanbarzadeh et al. 2015), and elemental composition will be investigated using serial imaging methods, including: micro –CT scanning, focused ion beam-scanning electron microscopy (FIB-SEM), multi-beam SEM, and scanning transmission electron microscopy (STEM). Small-angle neutron scattering (SANS) will be used to characterize pore network and brine distribution. These methods have been used to classify pore types and reconstruct pore networks in shales (Dewers et al. 2012), and may reveal microstructural changes to the salt due to heating not revealed by more classical methods. FIB-SEM digital reconstructions can have resolution of 10 nm/voxel and allow quantification of pore structure and topology.

Sandia's automated robotic polishing and imaging instrument, the Robo-Met.3D, has multiple options for polishing and etching of samples (Madison et al. 2017). The Robo-Met.3D can obtain optical bright or dark field image resolutions of 2.1 micron/pixel (at 5×) to 0.21 micron/pixel (at 50×). Automated polishing, etching, and imaging may achieve new understanding of 3D micro-structural deformation in salt and the connectivity of associated pore networks. The combination of FIB-SEM, STEM, SANS, and Robo-Met.3D will allow for multiscale examination of the coupled deformation and flow properties of the salt samples and the effects heating and in situ salt precipitation has on the network.

The water and EDTA-insoluble fractions of salt samples will be estimated. Dissolving away the water-soluble portions of the salt samples reveals the silicate, sulfate, and carbonate fraction of the salts. Boiling this water-insoluble residue from salt in 0.25 molar EDTA for 4 hours further removes the sulfate and carbonate minerals (Stein 1985). These methods allow rapid estimation of bulk silicate, carbonate, and sulfate composition of the salt. The insoluble fractions isolated from water dissolution will be tested via TGA and SEM to further quantify their composition.

3.3 Brine Evaporation Experiment

To provide relevant data for TC model validation, samples of brine collected from MU-0 will be concentrated in the lab via evaporation (both at 30 °C and 120 °C). Fluid samples will be collected from the experiment for compositional analysis during their dry-out process to confirm predictions of numerical TC models, and confirm field observations. Krumhansl et al. (1991a) essentially performed this experiment at room temperature, using fluid collected from a vertical borehole across MB139 (Appendix A-2.1).

The heated sample will be held at a constant temperature and the RH will be monitored during the evaporation process, rather than increasing temperature through time, typical to TGA. Especially at higher temperatures, thermochemical database entries for relevant salts have significant uncertainty (Jové Colón et al. 2013). The minerals in equilibrium with brine are strongly a function of temperature, and the behavior of multi-component brine systems at elevated temperatures is complex (Wollmann 2010). Precipitation of different salts at different temperatures will lead to different pathways along which the brine will evolve.

3.4 Gas and Brine Analysis

Gas samples will be analyzed in the laboratory for major gases and key noble gases (e.g., He and Ar) using gas chromatography. Sampling and analysis will need to account for condensate that may form in gas sample containers, once the high-RH warm gas moves into the relatively cold container. Some gases will dissolve into the condensate (e.g., HCl), and should be accounted for in the analyses. Individual gases of concern (e.g., HCl) could be tested directly in the field using gas-specific detection equipment.

The distribution of brine in sub-samples from cores will be examined by thermal-gravimetric analysis (TGA) before and after the borehole test. This will allow for the estimation of inter- and intra-granular brine as well as moisture associated with different minerals and their phases. Multiple sub-samples will be analyzed to characterize the heterogeneity of the salt. Based on available capabilities, a gas

chromatograph can be connected to the TGA to provide information on the composition of gases released during heating. This can also be used to confirm any gases observed during field test sampling.

Brine samples will be analyzed by ion chromatography and inductively coupled plasma mass spectrometry for major ions (i.e., Na^+, K^+, Mg^{2+}, Ca^{2+}, Cl^-, Br^-, SO_4^{2-}, CO_3^{2-}, and BO_3^{3-}) and minor substituting ions (NH_4, I, F, Fe, and Rb), based on analysis of data from previous samples collected from WIPP boreholes. Samples tested for ionic composition will require significant dilution (>1,000×) before analysis, but chloride levels can be tested without dilution using a chlorimeter. Stable water isotopes will be tested via CRDS. Brine electrical conductivity, pH, alkalinity, total dissolved solids, and density will be measured in the laboratory using appropriate methods. Meaningful estimates of pH are difficult in brines, requiring development of pH standards with similar salinity of the brine (Marcus 1989; Nir et al. 2014). Quantitative analysis will be done on precipitated salts, including X-ray diffraction, X-ray fluorescence, and TGA to quantify the composition and minerology of salts precipitated in the borehole. CRDS analysis will be used to estimate the isotopic composition of hydrated minerals.

Preserved salt samples will be dissolved in the laboratory using de-aerated water inside a sealed container put under an initial vacuum. The gases that develop in the head space will be analyzed using gas chromatography to estimate the gases that exist dissolved in the brine and trapped in the salt crystal structure (e.g., He, Ar and other noble gases). This data will help explain some observations during the field test. Some gases will come from the rock directly, while other gases will evolve from thermal decomposition of various materials in the borehole.

4. TESTING AND MEASURING EQUIPMENT

4.1 Plug and Packer Types

Sealing the borehole from the access drift and its DRZ, and isolating discrete borehole intervals is important to the success of several of the proposed tests and observations.

A wide variety of plugs or packers for borehole applications exist. However, there are several factors to consider for this field test. Factors include: ease of implementation, seal effectiveness, cost, dimensions, and corrodibility. The ideal packer system would be easy to implement with multiple ports, good sealing against a possibly creeping borehole wall, diameter close to the borehole diameter, low cost, and constructed of non-corrosive material that can withstand the saline environment, elevated temperature, and acidic vapors.

Sewer plugs are made from aluminum or plastic plates that sandwich a neoprene membrane. They are commonly used in industry and are straightforward to implement. They are relatively inexpensive and come in an assortment of sizes and materials. Sewer plugs seal a short interval (2” to 3”) and have a limited capacity to seal when the borehole wall is even slightly irregular. Because their plates must be turned against one another to expand the neoprene membrane, they are difficult to install at more than an arm’s length into the borehole. This twisting can also create complication for tubing and power cords running through the ports. Neoprene may also emit HCl vapor when heated above ~100 °C.

Commercial inflatable and mechanical packers are being investigated and would create a much better seal than sewer plugs for a reasonable increase in price. Inflatable packers require pumps or gas cylinders to apply and maintain fluid pressure to create a seal. Packers come in various sealing lengths and can create a good seal against most borehole conditions. Packer elements can be made of different types of rubber; all packer construction materials should be compatible with heat, brine, and acidic vapor.

Packers or plugs must have inflow, outflow, instrumentation, and heater pass-throughs to accommodate a variety of measurements and the heater. In inflatable packers, packer inflation pressure would be monitored throughout the test, and in mechanical packers/plugs, the torque associated with the closure of the tools would be monitored through the test. It would be more straightforward to monitor pressure automatically during the test than to monitor torque.

The test program is currently considering both inflatable packers and mechanical packers. Mechanical packers could be based on the design used by Blankenship & Stickney (1983) at Avery Island (see drawing in Figure 31b), or a commercially available equivalent. A mechanical packer is simpler to install than an inflated packer (no need for pumps to apply or maintain pressure), but the seal may not be as good in an irregular borehole. In a mechanical packer, the sealing rubber is shortened axially, and the sealing is provided by its radial expansion. In inflatable packers, a fluid is used to radially expand the seal directly. The sealing element on a mechanical or inflatable packer would be several times longer than a sewer-type plug, and allow simpler installation of the packer at depth into the borehole (not just within arm's reach). Since the gas flowrate damage testing is not planned at high operating pressures, or to estimate permeability of salt below approximately a microdarcy (similar to the approach of Stormont et al. 1987), a relatively simple mechanical or inflatable packer would likely be sufficient for the project's needs.

4.2 Heater Element

For the heated borehole test intervals, a resistive heater element is proposed. Resistive heater elements have better thermal properties and require less on/off cycling to maintain a specified temperature if the heater element is embedded in a block of thermally conductive and chemically inert material. Quartz lamp type heaters have been used successfully in bedded and domal salt (Appendix A-7.1), but resistive heaters are familiar to the WIPP testing organization and they are simple. Curved flat resistive heater elements could be installed directly on the surface of the borehole and backfilled inside, but this arrangement would be more difficult to test in the laboratory and set up.

The heater element and surrounding heater block should be non-corrosive in a wet, briny, acidic, hot environment. The heater block should isolate the heater element from the borehole environment. The temperature sensor for control of the power should be on the outside of the heater block (assuming the heater block is made of reasonably conductive materials), but temperatures at the heater element should also be monitored to record the hottest temperatures experienced in the borehole. The hottest temperature in the borehole may have significant ramifications on the stability of some mineral phases (e.g., Krumhansl 1986).

The test borehole heater assembly will be put together in a pipe on a lab bench with all instruments, wiring, pass-throughs and packers. The assembly will be tested in the laboratory before being inserted into the borehole in the field.

WIPP site electrical standards require electrical components to be listed with a testing laboratory (e.g., UL listed) or have an electrical safety inspection and plan developed. These aspects of heater and electrical component design are being considered in laboratory and preliminary field testing being conducted in FY17.

4.3 Thermocouples/Resistance Temperature Devices

Previous WIPP thermal experiments used premium grade, Type-E thermocouples with ungrounded junctions, high purity magnesium oxide insulation, and Inconel 600 sheathing (Munson et al. 1997b). A lesson learned from use of this type of thermocouple at WIPP involved numerous unidentified sensor failures (i.e., a break or short in the lead wires). It was not always clear the gauges failed until looking at the sensors after the experiment. A robust option for temperature sensors is the resistance temperature device (RTD), which relies on resistance being a function of temperature in a specific element of the circuit. It is more obvious during testing when these types of sensors have failed. It will be imperative the temperature detectors are well sealed to prevent brine from invading the insulation.

Thermal gauges will be installed by mounting them on a non-conducting rod to be inserted into the borehole as part of the heater/packer system. In the heated borehole it would be informative to also measure temperature at different angular locations around the borehole, at a given radius (e.g., thermal

gauges attached to an expandable non-conductive ring). This would provide some information regarding the development of convection or thermal stratification of the air during the test.

4.4 Multi-Point and Single-Point Borehole Extensometers

Used previously in Asse and WIPP thermal tests (Bollingerfehr et al. 2004; Munson et al. 1997b), rod or wire borehole extensometers monitor rock mass deformation by measuring relative displacement between anchors in a borehole, and the borehole collar. This can be done with a single anchor or multiple anchors set at different depths. Borehole extensometers are typically installed in an array around the room or access drift, with anchors set at varying depths up to 15 m [50’].

Room closure is important for calibrating drift-scale creep closure models, but is deferred to subsequent tests because these measurements would complicate setup of the initial testing boreholes. During later tests it would be useful to install a single extensometer set in a recently mined access drift between multiple borehole locations, so the response of the salt surrounding the access drift can be observed across multiple tests.

4.5 Borehole Pressure Cells

BPCs have been used to measure stress change in a wide variety of rock types (Bechthold et al. 2004). A BPC typically consists of a flat metal chamber filled with incompressible fluid connected to a transducer by a tube; the transducer converts fluid pressure into a measurable electrical output. The cell is grouted into the borehole, and pumped up to create contact with the material in which stress changes are to be measured. The BPC responds primarily to stresses acting perpendicular to the plane of the fluid chamber, but also has small sensitivity to stress changes in the perpendicular direction. Two cells installed in a borehole at right angles to each other will provide orientations of the principal stresses in the plane perpendicular to the axis of the borehole.

The evolution of stress redistribution around the rooms is not a measurement of primary importance and is deferred to subsequent test. It would provide useful information to corroborate extensometry, characterize the evolution of salt deformation around the access drift, and how it responds to heating.

4.6 Acoustic Emission Monitoring

The deformation induced by heating and cooling the salt will likely result in some brittle failure in the surrounding salt. During initial heating, small-scale deformation might occur along cracks or fracture planes, either by crack growth or by slippage along pre-existing planes of weakness. These discrete events will result in very small microseismic or AE. As heating progresses, large-scale fracturing can occur in the access drift walls, roof, and floor. Data from these events can be used to characterize the development of the DRZ, including the extent of fracturing and information about the fracture mechanism. A passive AE monitoring system will provide insight into the presence and source of brittle phenomena. The brine migration test at Asse recorded AE at multiple locations through time (Appendix A-5.3).

Only one AE sensor is needed to get the timing of events (but data can be interpreted jointly from multiple sensors to eliminate some noise). Observation of natural AE could be made in conjunction with observations of a known active source to assist in interpretation of the data, and to estimate the distribution and evolution of the DRZ. More than four (likely six) sensors recording at a high frequency (higher than the inverse of the expected travel time from the source or heated interval to the closest sensor) would be required to accurately estimate event location. Beyond the minimum, the number of sensors is tied to the objective. What volume of salt needs to be characterized? How many boreholes are present?

4.7 Electrical Resistivity Tomography

Electrical Resistivity Tomography (ERT) will be used to infer water content from electrical measurements made between electrodes in two observation boreholes. An electric current is induced into the test bed through two electrodes, and voltage is monitored between other pairs of electrodes. The data from a collection of measurements are then processed tomographically to image the resistivity distribution. Based on the calibration curves (determined in the laboratory) of electrical resistivity as a function of water saturation, the correlation of water saturation to electrical resistivity has about 1% precision in saturation levels below 40% (Appendix A-8). ERT has been successfully used to monitor brine injection in the DRZ at Asse, Germany (Jockwer & Wieczorek 2008) and the distribution of damage around drifts at WIPP (Skokan et al. 1989).

4.8 Air Humidity Sensors/Chilled Mirror Hygrometers

Whereas air humidity sensors (i.e., capacitive thin-film polymer sensors) are reliable, stable, and accurate in most applications, past experience using them in salt has resulted in early failures of the instrument and erroneous readings resulting from salt dust buildup on the sensor (e.g., a constant reading of ~75% RH). CMHs will likely be a more robust and accurate measurement in these underground conditions for measuring the humidity of the dry N_2 circulating through the test borehole. The CMH makes a direct measurement of the dew point temperature of a gas by allowing a sample of gas of unknown water vapor content to condense on an inert, chilled, mirror-polished metal surface. Thermoelectric modules are typically used to chill the surface. A beam of light is reflected from the surface into a photo-detector. A typical CMH, in contrast to many other humidity sensors, can be made very inert, rendering it virtually indestructible and minimizing the need for recalibration. However, salt dust deposition on polished surfaces can lead to erroneous CMH measurements, and may require periodic inspection and cleaning.

4.9 Other Sensors and Instruments

Linear variable differential transformer (LVDT) gauges are high-resolution linear displacement sensors that have been used to observe isothermal borehole closure at WIPP (Roberts et al. 1999). LVDTs could be placed at three locations (spaced 120°) around the heater block, or attached to a centralizer to allow initial contact with the borehole wall. Alternative emplacement strategies and measurement approaches are also being investigated.

Gas flowrate will be measured accurately upstream and downstream of the test borehole to develop a water mass balances. The upstream gas flowmeter will only need to measure flow of dry N_2 from a cylinder at ambient temperature, while the downstream gas flowmeter will need to measure flow of humid, hot gas, with acidic vapor components. Flowmeters that depend on the composition of the gas remaining constant (i.e., mass or density-based flowmeters), or depend on a dry gas stream will not work for the downstream gas flowrate measurement. Rotameter or turbine-style flow meters are economical, robust, tolerant of water vapor content, and work with a compositionally variable stream of gases. The instantaneous flowrate measurement will be used with the estimate of absolute humidity to estimate the total water inflow rate, so the accuracy of the downstream gas flowrate is important (i.e., should be better than 1%).

Gas pressure will be measured upstream and downstream of the test borehole. Gas pressure will be measured at the same time and locations with gas temperature, to allow estimation of the gas budget going into and coming out of the borehole. Gas pressure should be measured with accurate gauges that will be able to resolve expected differences in air pressure expected during the test (i.e., a few tens of kPa [few psi] higher gas pressure upstream of the borehole compared to downstream). Like the downstream gas flowmeter, the downstream gas pressure transducer should be tolerant of a hot, humid, acidic environment. Rather than differencing two pressure transducers measured relative to an atmospheric or vacuum standard, a differential pressure transducer could be used to accurately measure the pressure

difference between the upstream and downstream gases. Downstream gas pressure and temperature observations should be close to one another and at or very near the CMH, to allow accurate estimation of the absolute humidity of the gas stream. Pressure, temperature, and RH measurements should be collocated, because the pressure and temperature of the downstream gas may be changing rapidly as the gas leaves the borehole environment.

Sensors are available to quantify concentrations of individual specific gases (e.g., HCl vapor) directly via sampling. This analyte can be added to the downstream sampling system, but water vapor will tend to condense as the temperature of the outflow gas drops. HCl vapor will tend to go into the condensate, rather than stay in the gas phase.

4.10 Instrumentation Lessons Learned in a Salt Environment

Munson et al. (1997a, 1997b) presented lessons learned and details of instruments used in the drift-scale defense high-level waste mockup heater tests in Rooms A and B at WIPP. They detailed room closure gauges, extensometers, stress gauges, inclinometers, borehole strain gauges, thermocouples, thermal flux meters, and power meters used in WIPP. They present experience learned during testing and maintenance of the gauges over 10 years. Several instruments types had issues with corrosion of particular metal parts.

Howard et al. (1993) detailed much of the instrumentation used in the Room Q large-scale brine inflow and mine-by experiment. This test notably included multiple types of slim-hole packer test tools for both brine and gas permeability testing of the salt. Hydraulic test intervals contained LVDT borehole closure and thermocouple observations.

Roberts et al. (1999) detailed the instrumentation used in brine permeability packer testing, and brine/gas sampling from MB140. These instruments included multipacker systems with thermocouples and LVDT borehole closure observations, differential pressure measurements, and a fracture dilation test tool to observe fracture opening and closing during hydraulic testing.

Brady et al. (2013) presented an analysis of the heaters and canisters used in the Room A and B WIPP experiments, illustrating what heater and sample materials were left in place and still exist underground at WIPP.

Krumhansl et al. (1991b) analyzed precipitated salts and metal corrosion products observed in vertical heaters retrieved from WIPP Room B. They found stainless steel and nickel-based metals corroded readily in the acidic environment. Krumhansl (1986) discussed heater failures in brine-filled vertical boreholes as part of the Materials Interface Interactions Test (MIIT) test at WIPP.

Bechthold et al. (2004) and Bollingerfehr et al. (2004) presented observations about corrosion of instrumentation during the 10 years of the Asse drift-scale heater test. Krause (1983) included an appendix discussing issues and adjustments made while implementing the brine collection test plan at Avery Island (Appendix A-3). The Project Salt Vault report (Bradshaw & McClain 1971) presented a large amount of information learned during the first set of large-scale *in situ* heater tests in salt (Appendix A-6).

5. SUMMARY AND NEXT STEPS

This report presents the background and an initial conceptualization of the proposed FY18 DOE-NE intermediate-scale heater test at WIPP. This report summarizes relevant previous tests and data collected at salt research sites around the world, to support the design of the test, and is intended to represent an initial consensus on test design. The scientific focus of the tests is on brine availability, brine transport, and brine chemistry. The technical goals of the project are to create a validation dataset for coupled THMC numerical models of salt, as well as to provide the means for a new generation of salt science researchers to build upon the long successful history of underground testing in salt.

There have been several heater tests with brine collection in both bedded and domal salt, but the proposed suite of tests is unique because:

- the horizontal heater will not intersect major clay or anhydrite layers;
- the test will track deuterated water to better quantify intergranular brine transport in salt;
- liquid brine samples will be collected during progression of the test; and
- a straightforward test design is chosen to be executed at both ambient and elevated temperatures;
- the test of a modular design to facilitate adding similar, future tests with different test conditions (e.g., maximum temperature and thermal cycling and sealed or long-duration tests) and data collection activities (e.g., more intensive studies of AE, geomechanical observations, and cement exposure tests).

Proposed tests will be designed in more detail through FY17, to allow FY18 implementation, including the development of cost estimates, procedures, and quality assurance/quality control documentation as required. The tests should provide a better understanding of the relevant THMC processes in salt under controlled circumstances, which may better allow numerical model predictions before testing and validation after testing. Hopefully, the data collected from these proposed field and laboratory tests will result in further DOE and international collaboration on numerical model benchmarking and validation.

6. REFERENCES

Alkan, H., Y. Cinar and G. Pusch, (2007). Rock salt dilatancy boundary from combined acoustic emission and triaxial compression tests, *International Journal of Rock Mechanics and Mining Sciences* 44(1):108-119.

Beauheim, R.L. and R.M. Holt, (1990). "Hydrogeology of the WIPP Site" *in* Powers, Holt, Beauheim and Rempe, [eds.] *Guidebook 14*, pp. 131-179. Dallas, TX: Geological Society of America (Dallas Geological Society).

Beauheim, R.L. and R.M. Roberts, (2002). Hydrology and hydraulic properties of a bedded evaporate formation, *Journal of Hydrology* 259(1):66-68.

Beauheim, R.L., A. Ait-Chalal, G. Vouille, S.-M. Tijani, D.F. McTigue, C. Brun-Yaba, S.M. Hassanizadeh, G.M. van der Gissen, H. Holtman and P.N. Mollema, (1997). *INTRAVAL Phase 2 WIPP 1 Test Case Report: Modeling of Brine Flow Through Halite at the Waste Isolation Pilot Plant Site*. SAND97-0788. Albuquerque, NM: Sandia National Laboratories.

Bechthold, W., T. Rothfuchs, A. Poley, M. Ghoreychi, S. Heusermann, A. Gens, and S. Olivella, (1999). *Backfilling and Sealing of Underground Repositories for Radioactive Waste in Salt (BAMBUS Project)*. EUR 19124 EN, Commission of the European Communities.

Bechthold, W., E. Smailos, S. Heusermann, W. Bollingerfehr, B. Bazargan Sabet, T. Rothfuchs, P. Kamlot, J. Grupa, S. Olivella and F.D. Hansen, (2004). *Backfilling and Sealing of Repositories for Radioactive Waste in Salt (BAMBUS II Project)*. EUR 20621 EN, Commission of European Communities.

Blankenship, D.A. and R.G. Stickney, (1983). *Nitrogen Gas Permeability Tests at Avery Island*. ONWI-190(3), Rapid City, SD: RE/SPEC, Inc.

Bollingerfehr, W., S. Heusermann, J. Droste, and T. Rothfuchs, (2004). "Reliability and accuracy of geotechnical instruments during 10 years of in situ application" in *EURADWASTE '04. EUR 21027* EN, Brussels, Belgium: Commission of the European Communities.

Borns, D.J. and J.C. Stormont, (1988). *An Interim Report on Excavation Effect Studies at the Waste Isolation Pilot Plant: The Delineation of the Disturbed Rock Zone.* SAND87-1375, Albuquerque, NM: Sandia National Laboratories.

Bradshaw, R.L. and W.C. McClain [Eds.], (1971). *Project Salt Vault: A Demonstration of the Disposal of High-Activity Solidified Wastes in Underground Salt Mines*. ORNL-4555. Oak Ridge, TN: Oak Ridge National Laboratory.

Brady, P., C. Herrick, K. Kuhlman, B. Malama, M. Schuhen, and B. Stenson, (2013). *Sandia Experimental Programs Background and Targeted Activities for Forensic Investigation of Rooms B and A1*. Carlsbad, NM: Sandia National Laboratories.

Caporuscio, F.A., H. Boukhalfa, M.C. Cheshire, A.B. Jordan and M. Ding, (2013). *Brine Migration Experimental Studies for Salt Repositories*, LA-UR-13-27240, FCRD-UFD-2013-000204. Los Alamos, NM: Los Alamos National Laboratory.

Carslaw, H.S. and J.C. Jaeger, (1959). Conduction of Heat in Solids, Second Edition, Oxford.

Clynne, M.A., R.W. Potter, and L.D. White, (1981). *Analytical Results of Tagged Synthetic Brine Migration Experiments at Avery Island, Louisiana*. USGS Open File Report 81-1137. Menlo Park, CA: US Geological Survey.

Cosenza, Ph., M. Ghoreychi, (1993). "Coupling between mechanical behavior and transfer phenomena in salt" in *Proceedings of the Third Conference on the Mechanical Behavior of Salt*, September 14-16, 1993, Ecole Polytechnique Palaiseu, France, pp. 271-293.

Coyle, A.J., J. Eckert, and H. Kalia, (1987). *Brine Migration Test Report: Asse Salt Mine, Federal Republic of Germany*, BMI/ONWI-624, Office of Nuclear Waste Isolation, Battelle Memorial Institute, Columbus, OH.

Deal, D.E., R.J. Abitz, D.S. Belski, J.B. Case, M.E. Crawley, R.M. Deshler, P.E. Drez, C.A. Givens, R.B. King, B.A. Lauctes, J. Myers, S. Niou, J.M. Pietz, W.M. Roggenthen, J.R. Tyburski, and M.G. Wallace, (1989). *Brine Sampling and Evaluation Program 1988 Report*. DOE-WIPP-89-015, Carlsbad, NM: Westinghouse Electric Corporation.

Deal, D.E., R.J. Abitz, J. Myers, D.S. Belski, M.L. Martin, D.J. Milligan, R.W. Sobocinski and P.P.J. Lipponer, (1993). *Brine Sampling and Evaluation Program 1991 Report*. DOE-WIPP 93-026, Carlsbad, NM: Westinghouse Electric Corporation.

Deal, D.E., R.J. Abitz, D.S. Belski, J.B. Case, M.E. Crawley, C.A. Givens, P.P.J. Lipponer, D.J. Milligan, J. Myers, D.W. Powers and M.A. Valdivia, (1995). *Brine Sampling and Evaluation Program 1992-1993 Report and Summary of BSEP Data since 1982*. DOE-WIPP 94-011, Carlsbad, NM: Westinghouse Electric Corporation.

de Bakker, J., J. Lamarre, J. Peacey and B. Davis, (2012). The phase stabilities of magnesium hydroxychlorides, *Metallurgical and Materials Transactions B*, 43:758.

Dewers, T.A., J.E. Heath, R. Ewy, and L. Duranti, (2012). Three-dimensional pore networks and transport properties of a shale gas formation determined from focused ion beam serial imaging. *International Journal of Oil, Gas and Coal Technology*, 5(2):229-248.

DOE Carlsbad Field Office (CBFO), (2011). *A Management Proposal for Salt Disposal Investigations with a Field Scale Heater Test at WIPP*. DOE/CBFO-11-3470. Carlsbad, NM: US Department of Energy Office of Environmental Management.

DOE Carlsbad Field Office (CBFO), (2013). *Test Specification for the Salt Defense Disposal Investigations Thermal Test in WIPP*. DOE/CBFO-13-3510. Carlsbad, NM: US Department of Energy Office of Environmental Management.

Ewing, R.I. (1981a). *Test of a Radiant Heater in the Avery Island Salt Mine*. SAND81-1305, Albuquerque, NM: Sandia National Laboratories.

Ewing, R.I. (1981b). *Preliminary moisture release experiment in a potash mine in southeastern New Mexico*. SAND81-1318, Albuquerque, NM: Sandia National Laboratories.

Finley, S.J., D.J. Hanson, and R. Parsons, (1992). *Small-scale brine inflow experiments – data report through 6/6/91*. SAND91-1856, Albuquerque, NM: Sandia National Laboratories.

Ghanbarzadeh, S., M.A. Hesse, M. Prodanovic and J.E. Gardner, (2015). Deformation-assisted fluid percolation in rock salt, *Science*, 350(6264):1069-1072.

Greenspan, L., (1976). Humidity fixed points of binary saturated aqueous solutions. *Journal of Research of the National Bureau of Standards – A. Physics and Chemistry*, 81A(1):89-96.

Hansen, F.D., (2003). *The Disturbed Rock Zone at the Waste Isolation Pilot Plant*. SAND2003-3407, Albuquerque, NM: Sandia National Laboratories.

Hansen, F.D., (2014). "Micromechanics of isochoric salt deformation" in *American Rock Mechanics Association 48th Annual Meeting*, ARMA14-7012.

Hansen, F.D., T. Popp, K. Wieczorek, and D. Stührenberg, (2014). *Granular Salt Summary: Reconsolidation Principles and Applications*. SAND2014-16141R, FCRD-UFD-2014-000590. Albuquerque, NM: Sandia National Laboratories.

Hansen, F.D., W. Steininger and W. Bollingerfehr, (2016a). *Proceedings of the 6th US/German Workshop on Salt Repository Research, Design, and Operation*. SAND2016-0194R, FCRD-UFD-2016-000069. Albuquerque, NM: Sandia National Laboratories.

Hansen, F.D., S. Sobolik and P.H. Stauffer, (2016b). *Intermediate Scale Testing Recommendation Report*, SAND2016-9041R, FCRD-UFD-2016-000030, Albuquerque, NM: Sandia National Laboratories.

Hansen, F.D., W. Steininger and W. Bollingerfehr, (2017). *Proceedings of the 7th US/German Workshop on Salt Repository Research, Design, and Operation*. SAND2017-1057R, SFWD-SFWST-2017-000008. Albuquerque, NM: Sandia National Laboratories.

Hardy, R.D., and D.J. Holcomb, (2000). "Assessing the Disturbed Rock Zone (DRZ) around a 655 meter vertical shaft in salt using ultrasonic waves: An update" in *4th North American Rock Mechanics Symposium*. American Rock Mechanics Association. SAND2000-0668C.

Hess, H.H., J.N. Adkins, W.B. Heroy, W.E. Benson, M.K. Hubbert, J.C. Frye, R.J. Russell, and C.V. Theis, (1957). *The Disposal of Radioactive Waste on Land, Report of the Committee on Waste Disposal of the Division of Earth Sciences*. Publication 519, Washington, D.C.: National Academy of Sciences - National Research Council.

Hohlfelder, J.J., (1979). *Salt Block II: Description and Results*. SAND79-2226, Albuquerque, NM: Sandia National Laboratories.

Hohlfelder, J.J., A.G. Beattie, and H.C. Shefelbine, (1981). *Water Release and Mechanical Failure in Heated Geologic Salt*. SAND81-1488. Albuquerque, NM: Sandia National Laboratories.

Holcomb, D.J., T. McDonald, and R.D. Hardy, (2001). "Assessing the disturbed rock Zone (DRZ) at the WIPP (Waste Isolation Pilot Plant) in salt using ultrasonic waves" in *DC Rocks 2001, The 38th US Symposium on Rock Mechanics (USRMS)*. American Rock Mechanics Association. SAND2001-13055C.

Howard, C.L., A.L. Jensen, R.L. Jones, and T.P. Peterson, (1993). *Room Q Data Report: Test Borehole Data from April 1989 through November 1991*. SAND92-1172, Albuquerque, NM: Sandia National Laboratories.

IT Corporation, (1995). *Summary of Brine Investigations at the Waste Isolation Pilot Plant, Southeastern New Mexico*. DOE/WIPP 96-2161. Carlsbad, NM: Westinghouse Electric Corporation.

Jockwer, N. and K. Wieczorek, (2008). *ADDIGAS: Advective and Diffusive Gas Transport in Rock Salt Formations Final Report*. GRS-234, Cologne, Germany: Gesellschaft für Anlagen- und Reaktorsicherheit (GRS).

Jové Colón, C.F., P.F. Weck, T. Hadgu, J.E. Bean, M.J. Martinez, J.G. Argüello, C.D. Leigh, and F.D. Hansen, (2012). *Thermomechanical, Hydrological and Chemical (THMC) Model Development*. SAND2013-1412P, FCRD-UFD-2013-000064, Albuquerque, NM: Sandia National Laboratories.

Kendall, C. and E.A. Caldwell, (1998). "Fundamentals of Isotope Geochemistry" in *Isotope Tracers in Catchment Hydrology*, C. Kendall and J.J. McDonnell [Eds.], Elsevier, Amsterdam pp. 51-86.

Krause, W.B., (1979). *Avery Island Test Site Procedure for Installation and Operation of Brine Movement Experiments and Prototype Test Site*. RSI-0090. ONWI/SUB-79-E512-02200/10, Rapid City, SD: RE/SPEC, Inc.

Krause, W.B., (1983). *Avery Island Brine Migration Tests: Installation, Operation, Data Collection, and Analysis*. ONWI-190(4). Rapid City, SD: RE/SPEC, Inc.

Krumhansl, J.L., (1986). *MIIT Heater Failure: Geochemical Analysis*. April 1, 1986 Memo to M.A. Molecke (Obtained as attachment to Molecke 1986; ERMS-303090), Carlsbad, NM: Sandia National Laboratories WIPP Records Center.

Krumhansl, J.L., K.M. Kimball, C.L. Stein, (1991a). *Intergranular Fluid Compositions from the Waste Isolation Pilot Plant (WIPP), Southeastern New Mexico*. SAND90-0564, Albuquerque, NM: Sandia National Laboratories.

Krumhansl, J.L., C.L. Stein, G.D. Jarrell, and K.M. Kimball, (1991b). Summary of WIPP Room B Heater Test Brine and Backfill Material Data. SAND90-0626, Albuquerque, NM: Sandia National Laboratories.

Kuhlman, K.L., (2014). *Summary Results for Brine Migration Modeling Performed by LANL, LBNL, and SNL for the UFD Program*. SAND2014-18217R, FCRD-UFD-2014-000071. Albuquerque, NM: Sandia National Laboratories.

Kuhlman, K.L. and B. Malama, (2013). *Brine Flow in Heated Geologic Salt*. SAND2013-1944, Carlsbad, NM: Sandia National Laboratories.

Kuhlman, K.L. and B. Malama (2014). *Assessment of Contaminated Brine Fate and Transport in MB139 at WIPP*. SAND2014-16153, Albuquerque, NM: Sandia National Laboratories.

Kuhlman, K.L. and S.D. Sevougian, (2013). *Establishing the Technical Basis for Disposal of Heat-Generating Waste in Salt*. SAND2013-6212P, FCRD-UFD-2013-000233. Albuquerque, NM: Sandia National Laboratories.

Kuhlman, K.L., S. Wagner, D. Kicker, R. Kirkes, C. Herrick, D. Guerin, (2012). *Review and Evaluation of Salt R&D Data for Disposal of Nuclear Waste in Salt*. SAND2012-8808P, FCRD-UFD-2012-000380, Carlsbad NM: Sandia National Laboratories.

Lambert, S.J., (1979). *Mineralogical Aspects of Fluid Migration in the Salt Block II Experiment*. SAND79-2423, Albuquerque, NM: Sandia National Laboratories.

Lambert, S.J., (1992). Geochemistry of the Waste Isolation Pilot Plant (WIPP) site, southeastern New Mexico, U.S.A., *Applied Geochemistry*, 7(6):513-531.

Lappin, A.R., (1988). *Summary of Site-Characterization Studies Conducted from 1983 through 1987 at WIPP, Southeastern New Mexico*, SAND88-0157. Albuquerque, NM: Sandia National Laboratories.

Madison, J.D., O.D. Underwood, G.A. Poulter and E.M. Huffman, (2017). Acquisition of real-time operation analytics for an automated serial sectioning system. *Integrating Materials and Manufacturing Innovation, 224.*

Marcus, Y., (1989). Determination of pH in highly saline waters. *Pure and Applied Chemistry*, 61(6):1133-1138.

McTigue, D.F., (1985). *A Linear Theory for Porous Thermoelastic Materials*. SAND85-1149. Albuquerque, NM: Sandia National Laboratories.

McTigue, D.F., (1993). *Permeability and Hydraulic Diffusivity of WIPP Repository Salt Inferred from Small-Scale Brine Inflow Experiments*. SAND92-1911, Albuquerque, NM: Sandia National Laboratories.

McTigue, D.F. and E.J. Nowak, (1987). *Brine Transport Studies in the Bedded Salt of the Waste Isolation Pilot Plant (WIPP)*. SAND87-1274C, Albuquerque, NM: Sandia National Laboratories.

Molecke, M.A., (1983). *A Comparison of Brines Relevant to Nuclear Waste Experimentation*. SAND83-0516, Albuquerque, NM: Sandia National Laboratories.

Molecke, M.A., (1986). *Measurement of Hydrochloric Acid Vapors in WIPP from In Situ Experiments – SAFETY ASPECTS*. ERMS-303090, May 8, 1986 Memo of Record. Carlsbad, NM: Sandia National Laboratories WIPP Records Center.

Molecke, M.A., (1992). *Results from Simulated Remote-Handled Transuranic Waste Experiments at the Waste Isolation Pilot Plant (WIPP)*. SAND92-1003C, Albuquerque, NM: Sandia National Laboratories.

Morgan, K.Z., (1963). *Health physics division annual progress report for period ending July 31, 1963*. ORNL-3492, Oak Ridge, TN: Oak Ridge National Laboratory.

Munson, D.E., S.J.V. Petney, R.M. Clancy, J.R. Ball, R.L. Jones and C.L. Northrop-Salazar, (1991). *18 W/m^2 Mockup for Defense High-level Waste (Rooms A): In situ Data Report: Vol. 1 – Mechanical response gages (February 1985-June 1990), Waste Isolation Pilot Plant (WIPP) Thermal/Structural Interactions Program*. SAND90-2748, Albuquerque, NM: Sandia National Laboratories.

Munson, D.E., R.L. Jones, C.L. Northrop-Salazar and Woerner, S.J. (1992a). *Multipass Mining Sequence Room Closures: In situ Data Report. Waste Isolation Pilot Plant (WIPP) Thermal-Structural Interactions Program*. SAND87-2687, Albuquerque, NM: Sandia National Laboratories.

Munson, D.E., S.J.V. Petney, T.L. Christian-Frear, J.R. Ball, R.L. Jones and C.L. Northrop-Salazar, (1992b). *Geomechanical Evaluation (Room G): in situ Data Report (December 1984-November 1990), Waste Isolation Pilot Plant (WIPP) Thermal/Structural Interactions Program*. SAND92–0582, Albuquerque, NM: Sandia National Laboratories.

Munson, D.E., D.L. Hoag, D.A. Blankenship, R.L. Jones, S.J. Woerner, G.T. Baird and R.V. Matalucci, (1997a). *Construction of the Thermal/Structural Interactions in situ Tests at the Waste Isolation Pilot Plant (WIPP)*. SAND87-2685, Albuquerque, NM: Sandia National Laboratories.

Munson, D.E., D.L. Hoag, D.A. Blankenship, W.F. DeYonge, D.M. Schiermeister, R.L. Jones, and G.T. Baird, (1997b). *Instrumentation of the thermal/structural interactions in situ tests at the Waste Isolation Pilot Plant (WIPP)*. SAND87-2686, Albuquerque, NM: Sandia National Laboratories.

Nir, O., E. Marvin, and O. Lahav, (2014). Accurate and self-consistent procedure for determining pH in seawater desalination brines and its manifestation in reverse osmosis modeling, *Water Research*, 64:187-195.

Nowak, E.J., and D.F. McTigue, (1987). *Interim Results of Brine Transport Studies in the Waste Isolation Pilot Plant (WIPP)*. SAND87-0880. Albuquerque, NM: Sandia National Laboratories.

Powers, D.W., S.J. Lambert, S.E. Shaffer, L.R. Hill, W.D. Weart, (1978). *Geological Characterization Report: Waste Isolation Pilot Plant (WIPP) Site, Southeastern New Mexico.* (2 Volumes) SAND78-1596, Albuquerque, NM: Sandia National Laboratories.

Powers, D.W., (2017). *Reference Stratigraphy Applied to Rock Mechanics Studies for the Waste Isolation Pilot Plant: A Review – Jan 11, 2017*. ERMS-567705. Carlsbad, NM: Sandia National Laboratories WIPP Records Center.

Roberts, R.M., R.L. Beauheim, P.S. Domski, (1999). *Hydraulic Testing of the Salado Formation Evaporites at the Waste Isolation Pilot Plant: Final Report*. SAND98-2537, Albuquerque, NM: Sandia National Laboratories.

Roedder, E., and R.L. Bassett, (1981). Problems in determination of the water content of rock-salt samples and its significance in nuclear-waste storage siting, *Geology*, 9:525-530.

Rothfuchs, T., K. Wieczorek, H.K. Feddersen, G. Staupendahl, A.J. Coyle, H. Kalia, and J. Eckert, (1988). *Brine Migration Test: Asse Salt Mine Federal Republic of Germany Final Report*, GSF-

Bericht 6/88, Joint project between Office of Nuclear Waste Isolation (ONWI) and Gesellschaft für Strahlen- und Umweltforschung Munchen (GSF).

Rothfuchs, T., H.-K. Feddersen, K.-P. Krohn, R. Miehe, and K. Wieczorek, (1999). *The DEBORA Project: Development of Borehole Seals für High-Level Radioactive Waste – Phase II Final Report*. GRS-161, Braunschweig, Germany: Gesellschaft für Anlagen-und Reaktorsicherheit (GRS) mbH.

Saulnier, Jr., G.J., P.S. Domski, J.B. Palmer, R.M. Roberts, W.A. Stensrud, and A.L. Jensen, (1991). *WIPP Salado Hydrology Program Data Report #1*. SAND90-7000, Albuquerque, NM: Sandia National Laboratories.

Sevougian, S.D., R.J. MacKinnon, B.A. Robinson, C.D. Leigh, and D.J. Weaver, (2013). *RD&D Study Plan for Advancement of Science and Engineering Supporting Geologic Disposal in Bedded Salt—March 2013 Workshop Outcomes*. FCRD-UFD-2013–000161, Albuquerque, NM: Sandia National Laboratories.

Shefelbine, H.C., (1982). *Brine migration: A summary report*. SAND82-0152, Albuquerque, NM: Sandia National Laboratories.

Skokan, C.K., M.C. Pfeifer, G.V. Keller, and H.T. Andersen, (1989). *Studies of Electrical and Electromagnetic Methods for Characterizing Salt Properties at the WIPP Site, New Mexico*. SAND87-7174, Albuquerque, NM: Sandia National Laboratories.

Sonnenfeld, P. and J.-P. Perthuisot, (1989). *Brines and Evaporites*, American Geophysical Union.

Stauffer, P.H., A.B. Jordan, D.J. Weaver, F.A. Caporuscio, J.A. Ten Cate, H. Boukhalfa, B.A. Robinson, D.C. Sassani, K.L. Kuhlman, E.L. Hardin, S.D. Sevougian, R.J. MacKinnon, Y. Wu, T.A. Daley, B.M. Freifeld, P.J. Cook, J. Rutqvist and J.T. Birkholzer, (2015). *Test Proposal Document for Phased Field Thermal Testing in Salt*. LA-UR-15-23154, FCRD-UFD-2015-000077. Los Alamos, NM: Los Alamos National Laboratory.

Stein, C.L., (1985). Mineralogy in the Waste Isolation Pilot Plant (WIPP) Facility Stratigraphic Horizon. SAND85-0321, Albuquerque, NM: Sandia National Laboratories.

Stein, C.L. and J.L. Krumhansl, (1986). *Chemistry of Brines in Salt from the Waste Isolation Pilot Plant (WIPP), Southeastern New Mexico: A Preliminary Investigation*. SAND85-0987, Albuquerque, NM: Sandia National laboratories.

Stein, C.L. and J.L. Krumhansl, (1988). A model for the evolution of brines in salt from the lower Salado Formation, southeastern New Mexico, *Geochemica et Cosmochimica Acta*, 52:1037-1046.

Stickney, R.G. and L.L. Van Sambeek, (1984). *Summary of the Avery Island Field Testing Program*. RSI-0225, Rapid City, SD: RE/SPEC, Inc.

Stormont, J.C., (1988). *Test Plan: WIPP Horizon Gas Flow/Permeability Measurements*. Albuquerque, NM: Sandia National Laboratories.

Stormont, J.C., E.W. Peterson, P.L. Lagus, (1987). *Summary and Observations About WIPP Facility Horizon Flow Measurements Through 1986*. SAND87-0176, Albuquerque, NM: Sandia National Laboratories.

Stormont, J.C., (1997a). Conduct and interpretation of gas permeability measurements in rock salt. *International Journal of Rock Mechanics and Mining Sciences*, 34(3–4):303.e1–303.e11.

Stormont, J.C., (1997b). In situ gas permeability measurements to delineate damage in rock salt. *International Journal of Rock Mechanics, Mineral Science & Geomechanics Abstracts*, 34(7):1055-1064.

Sugimoto, K., R.E. Dinnebier, and J.C. Hanson, (2007). Structures of three dehydration products of bischofite from in situ synchrotron powder diffraction data ($MgCl_2 \cdot nH_2O$; n=1,2,4), *Acta Crystallographica Section B*, 63(2):235-242.

Tyler, L.D., R.V. Matalucci, M.A. Molecke, D.E. Munson, E.J. Nowak, and J.C. Stormont, (1988). *Summary report for the WIPP technology development program for isolation of radioactive waste.* SAND88-0844, Albuquerque, NM: Sandia National Laboratories.

Ucok, H., I. Ershaghi, and G.R. Olhoeft, (1980). Electrical resistivity of geothermal brines. *Journal of Petroleum Technology*, 32(04), 717-727.

Van Sambeek, L.L., D.D. Luo, M.S. Lin, W. Ostrowski, and D. Oyenuga, (1993). *Seal Design Alternatives Study*. SAND92-7340, Albuquerque, NM: Sandia National Laboratories.

Westinghouse Electric Corporation, (1987). *Brine Migration Test for Asse Mine, Federal Republic of Germany: Final Design Report*, BMI/ONWI-651, Office of Nuclear Waste Isolation, Battelle Memorial Institute, Columbus, OH.

Wollmann, G., (2010). *Crystallization Fields of Polyhalite and its Heavy Metal Analogues*, PhD. Dissertation, Technische Universität Bergakadamie Frieberg, Frieberg, Germany.

Yan, F., D.-H. Han, Q. Yao, and H. Li, (2014). "Seismic Velocities of Halite Salt: Anisotropy, Dispersion, Temperature, and Stress Effects." in *SEG Denver Annual Meeting Technical Program Expanded Abstracts.* (pp. 2783-2787). Society of Exploration Geophysicists.

Appendix A RELEVANT HISTORICAL TESTS

A-1. Horizontal Boreholes in MU-0 at WIPP

A series of horizontal boreholes was monitored for brine inflow at WIPP in the late 1980s and early 1990s. The relevant aspects of these data include:

1) Isothermal brine inflow observations were made over several years at WIPP in MU-0 salt
2) Modeling was done to match brine inflow fluxes observed with time
3) Non-salt components of MU-0 samples were characterized from Room L4

Finley et al. (1992) reported brine inflow measured in vertical and horizontal boreholes at WIPP. Brine was manually sampled from boreholes by technicians who breached the borehole seal, and used a vacuum pump to remove brine from the borehole. Humidity was monitored in the boreholes with capacitance-type hygrometers, but this data was only used to assess the quality of the borehole seal.

The horizontal boreholes in room L4 (L4B01 and L4X01) of the North Experimental Area were completed in MU-0 (Figure 9). Vertical boreholes near room Q (QPB0{1,2,3,4,5}) intersected MB139, while vertical boreholes from the higher-elevation experimental drifts (DBT1{0,1,2,3,4,5} and DBT3{1,2}) intersected Clay F. Nearly horizontal boreholes completed in Map Unit 9 (DBT16 and DBT17) would be difficult to reach from currently accessible excavations within WIPP (i.e., the North Experimental Area is currently inaccessible).

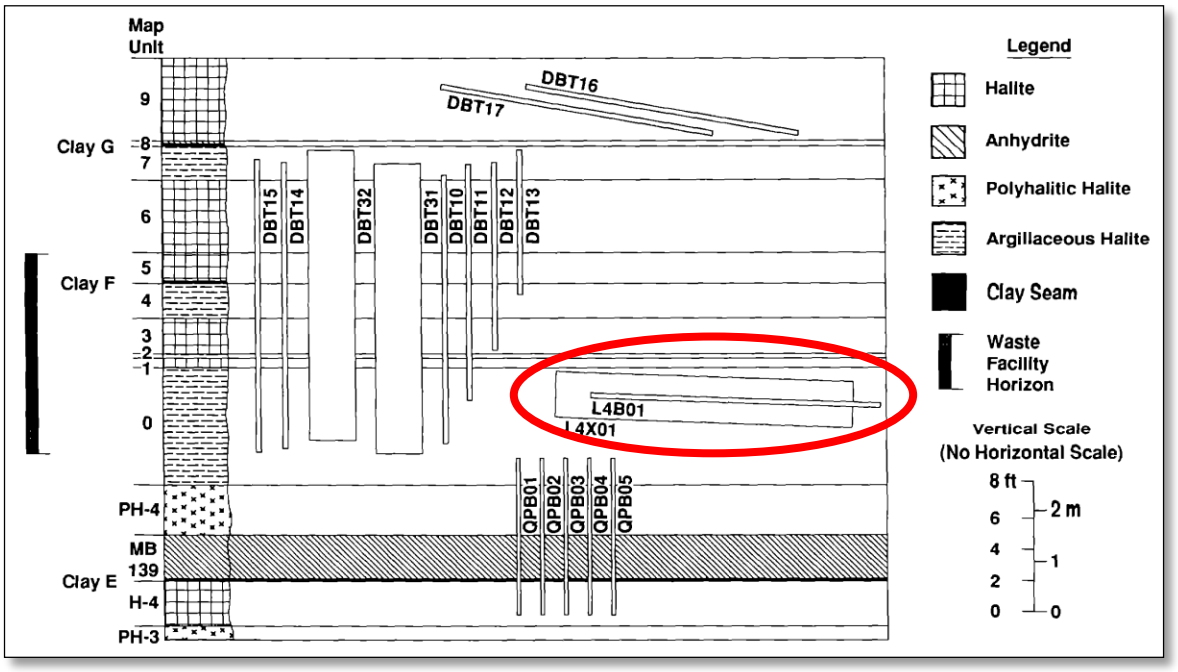

Figure 9. Boreholes at WIPP monitored for isothermal brine inflow and idealized stratigraphy (Figure 2 of Finley et al. 1992).

The boreholes in Room L4 were similar in stratigraphic location to the planned intermediate-scale heater test boreholes, and the smaller borehole is similar in diameter (10.2 cm) and length (5.8 m) to the planned boreholes.

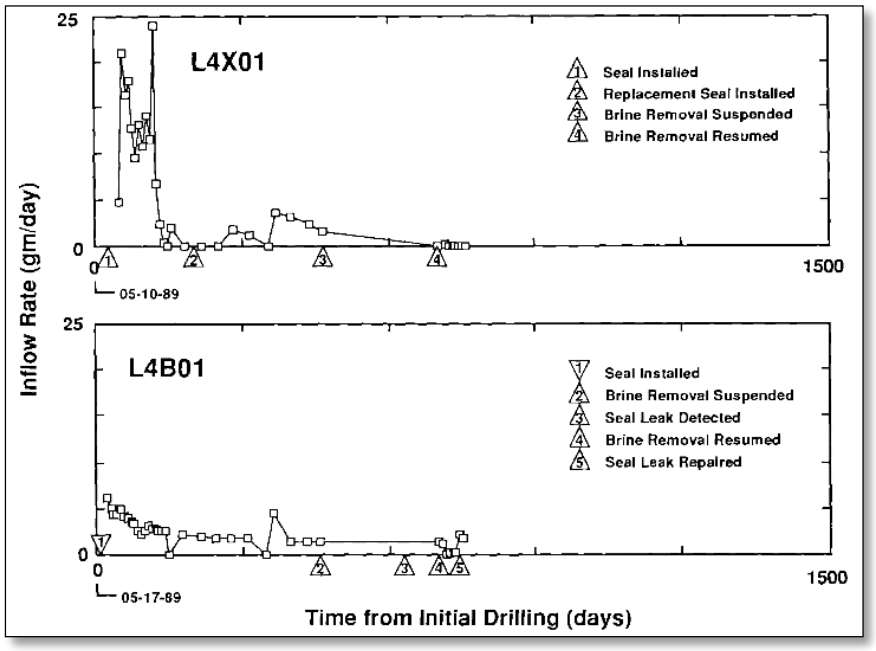

Figure 10. Brine inflow to horizontal boreholes in Room L4. (Figure 11 of Finley et al. 1992).

A-1.1 Isothermal Brine Inflow into Horizontal MU-0 Boreholes

Brine inflow data (Figure 10) indicate boreholes L4B01 collected approximately 2 to 5 grams of brine per day over approximately 2 years, with the largest amount collected in the first few months after drilling the borehole. The larger-diameter borehole L4X01 collected more brine and the pattern of inflow was less regular. Scaling the inflow data in Figure 10 by the borehole surface area reveals the normalized inflow into L4X01 was less than L4B01 (Figure 14). This difference might be due evaporative losses through a larger DRZ existing around the larger borehole, since the borehole DRZ should be proportional in size to the borehole diameter.

This brine inflow data was used in the INTRAVAL model validation exercise. Multiple analytical solutions and numerical models tried to match observed data (Beauheim et al. 1997). McTigue (1993) developed a pressure-gradient driven analytical flow solution, which was fit to observations (Figure 11 and Figure 12).

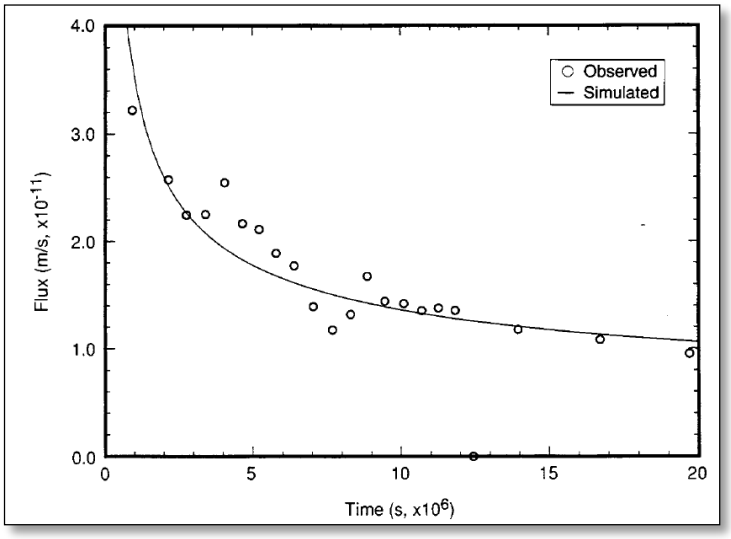

Figure 11. Comparison of McTigue (1993) model to data from L4B01 over 230 days (Figure 4-31 of Beauheim et al. 1997).

Table 4-4. Parameters Derived from Fits to Flux through January 1990

Hole	Perm. x Press. kp_∞ (m^2Pa, x 10^{-15})	Permeability* k (m^2, x 10^{-21})	Diffusivity c (m^2/s, x 10^{-10})	Specific Capacitance* C_s (Pa^{-1} x 10^{-9})
DBT10	3.84 ± 0.24	0.380 ± 0.024	0.47 ± 0.078	3.870 ± 0.69
DBT11	14.92 ± 0.55	1.490 ± 0.055	35.09 ± 6.29	0.200 ± 0.037
DBT12	8.40 ± 0.94	0.840 ± 0.094	101.73 ± 65.33	0.039 ± 0.025
DBT13	2.29 ± 0.35	0.230 ± 0.035	0.59 ± 0.23	1.850 ± 0.77
L4B01	0.88 ± 0.56	0.088 ± 0.056	0.58 ± 0.91	0.730 ± 1.24
	—	—	—	—

* Assumes p_∞ = 1.0 x 10^7 Pa, μ = 2.1 x 10^{-3} Pa·s, ρ = 1200 kg/m^3.

Figure 12. Results from model-data fit for borehole L4B01 (Table 4-4 of Beauheim et al. 1997).

The WIPP management and operations contractor (initially Westinghouse) monitored brine inflow to WIPP for several years, and the inflow rates and brine composition data are available from Deal et al. (1995). Figure 13 shows brine inflow data for a period of approximately 1,700 days in 46-m long horizontal boreholes completed in MU-0 at the entrances to Panels 7 and 8, and OH45 was completed in S400 (see Figure 3 for borehole locations). The first 15 m of these boreholes are completed above the orange marker band (MU-1, Figure 5), but the boreholes dip down, and the back 2/3 of these boreholes are completed in MU-0. Deal et al. (1993) hypothesized the brine collected in these boreholes originated mostly from thin clay layers above MU-1.

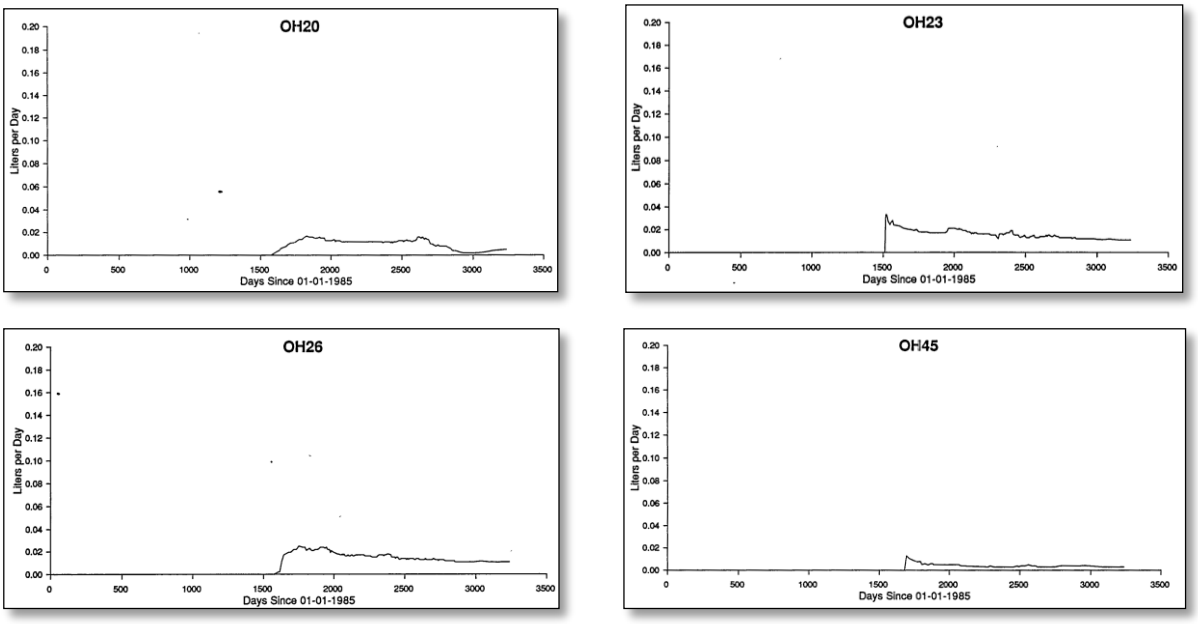

Figure 13. Isothermal brine inflow rates to horizontal boreholes completed predominantly in MU-0 (Appendix B of Deal et al. 1995).

Figure 14 shows normalized brine inflow data for both datasets (Finley et al. 1992 and Deal et al. 1995), assuming a brine density of 1.16 g/cm^3 to convert the volumetric rates reported in Deal et al. 1995 into mass rates. The fluxes are normalized by the area of salt open to the borehole, consisting of the surface of a cylinder (minus the end open to the access drift). The data from Deal et al. (1995) illustrate a long period (>2 years) of nearly constant brine inflow, while data from OH20 shows decline in brine production after 1,200 days. Multi-year heated brine inflow tests have been proposed to investigate the long-term stability of brine inflow to excavations (Section 2.8.3). The data from these boreholes do not adequately capture the early brine inflow peak after completion of the borehole. The data from L4B01 best capture the early time peak in inflow and the subsequent decline; this is why these data were used in the INTRAVAL project.

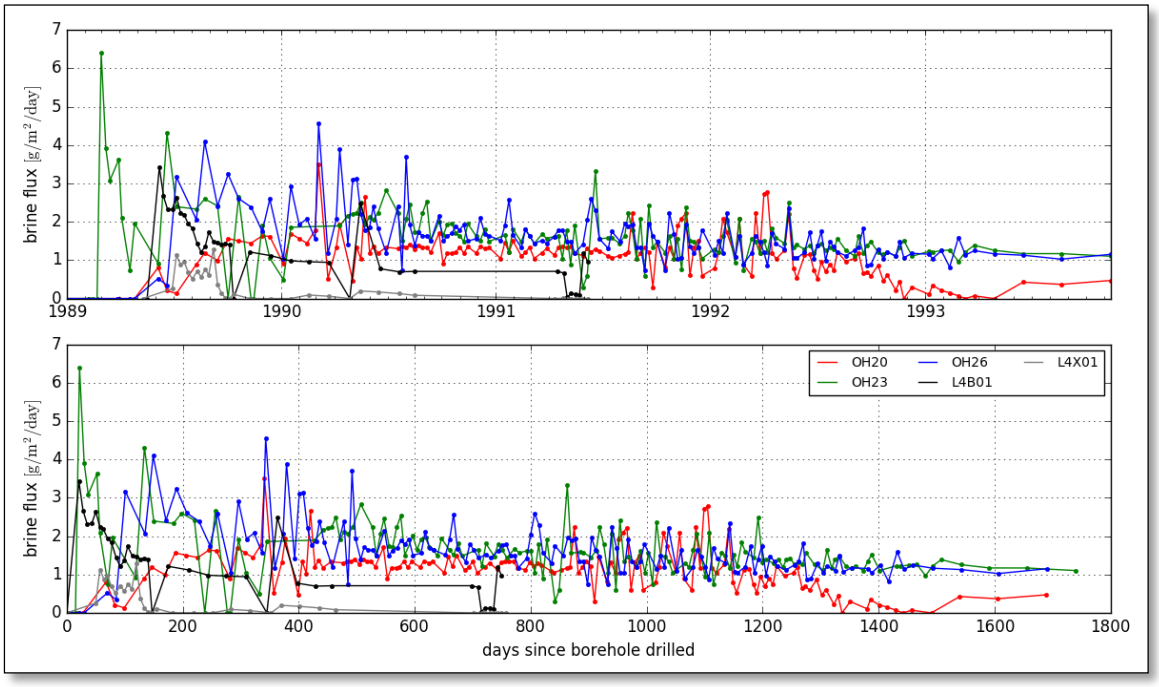

Figure 14. Normalized brine inflow data for boreholes completed in MU-0. Mass flowrate normalized by borehole wall area. Data from Finley et al. 1992 and Deal et al. 1995.

Using the normalized data plotted in Figure 14, we would expect between 1 and 2 g/m^2/day brine inflow to the test borehole under isothermal conditions (3 to 5 g/m^2/day immediately after borehole completion). A 6.1-m [20'] long, 15.2-cm [6"] diameter borehole has an inner area of 3 m^2, resulting in a scaled steady-state brine inflow of 3 to 6 g/day in the test borehole, with early peaks as high as 9 to 15 g/day. Appendix C relates the predicted brine inflow rates to minimum nitrogen consumption rates in the planned isothermal moisture extraction system.

A-1.2 MU-0 Insoluble Mineral Composition

Cores from L4B01 were analyzed in the laboratory for water content and insoluble residue content (Appendix D of Finley et al. 1992). Insoluble residue was less than 2 wt-% of the total sample and was mostly comprised of silicates (clay and quartz), with some sulfates (anhydrite, gypsum, and polyhalite), and trace feldspar (Figure 17). These or similar analyses would likely be run again on new cores collected (associated with the activities described in Appendix B-2).

Four samples (each with three sub-samples) from Borehole L4B01 were tested for total insoluble residue and weight change upon heating (Appendix D of Finley et al. 1992). The results (Figure 15) indicate MU-0 in Room L4 contains on average 0.51 wt-% water and 1.3 wt-% insoluble residue. These data are consistent with previously reported values of 0.22 wt-% and 0.75 wt-% water content in clean and argillaceous WIPP salt, respectively. The amount of weight change correlates well with total insoluble residue (Figure 16), indicating a significant part of the water content is associated with clays and hydrated sulfates. Figure 17 lists the relative major, minor, and trace content of insoluble minerals in these cores (hydrous minerals are highlighted).

In general agreement with geologic descriptions of MU-0 (Section 2.1.1), all samples 1, 2, and 3 have smectite as their primary hydrous insoluble mineral, while sample 4 includes sulfate minerals (polyhalite and gypsum) as the primary hydrous insoluble mineral. Although Finley et al. (1992) do not report the

locations of the samples in the boreholes, it might be inferred that samples 1-3 came from the upper, more clay-rich portions of MU-0, while sample 4 came from the lower, more polyhalite-rich portions of MU-0.

Sample number	Sample weight (g)	Weight change (g)	Weight change (wt.%)	Insol. Res. wt. (g)	Insol. Res. wt. %
1-1	84.052	0.574	0.68	1.424	1.69
1-2	76.239	0.418	0.55	0.930	1.22
1-3	84.099	0.534	0.64	1.241	1.48
2-1	84.817	0.250	0.30	0.510	0.60
2-2	93.658	0.233	0.25	0.388	0.41
2-3	89.234	0.186	0.21	0.309	0.35
3-1	76.300	0.502	0.66	1.317	1.73
3-2	86.290	0.627	0.73	1.655	1.92
3-3	90.536	0.645	0.71	1.688	1.86
4-1	67.768	0.280	0.41	1.237	1.82
4-2	66.763	0.318	0.48	0.902	1.35
4-3	49.102	0.263	0.54	0.677	1.38

Figure 15. Data from lab analyses on core from MU-0 in Room L4 (Appendix D of Finley et al. 1992).

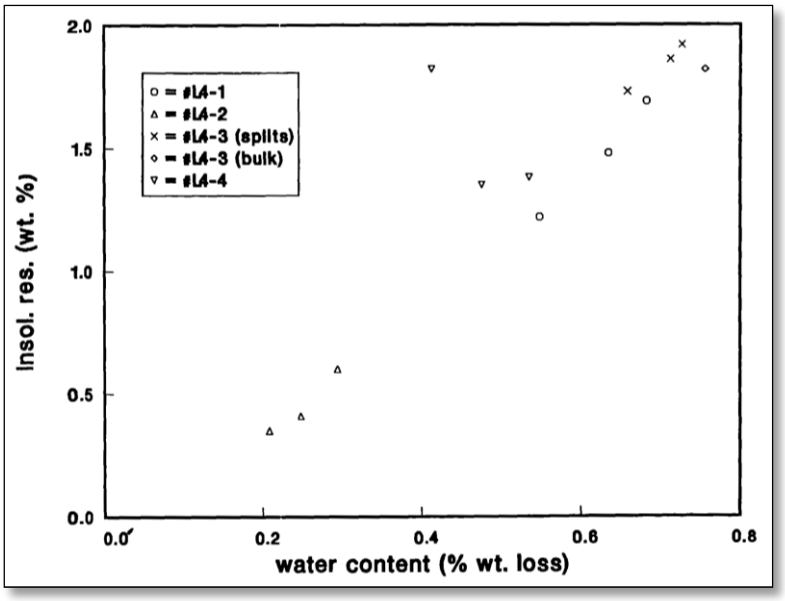

Figure 16. Water content vs. insoluble residue for MU-0 samples from Room L4 (Appendix D of Finley et al. 1992).

Sample	Major	Minor	Trace
1-1	quartz anhydrite	magnesite smectite	illite
1-2	quartz anhydrite	magnesite smectite	illite
1-3	quartz	magnesite smectite	illite anhydrite
2-1	quartz	magnesite smectite	illite anhydrite
2-2	quartz	magnesite smectite	illite anhydrite
2-3	quartz	magnesite smectite	illite anhydrite
3-1	quartz anhydrite smectite	magnesite illite	microcline
3-2	quartz anhydrite smectite	magnesite illite	microcline
3-3	quartz anhydrite smectite	magnesite illite	microcline
4-1	polyhalite gypsum	quartz anhydrite magnesite	illite
4-2	quartz	magnesite calcite gypsum anhydrite	microcline
4-3	quartz	magnesite anhydrite	illite smectite gypsum

Figure 17. Observed insoluble minerals in MU-0 samples from Room L4 (Appendix D of Finley et al. 1992). Hydrous minerals highlighted.

A-2. Observations of WIPP Salado Brine Chemistry

Observations have been made of brine chemistry at WIPP (IT Corporation 1995), both from boreholes collecting brine under isothermal conditions (in the targeted MU-0), and during heater tests (in vertical boreholes completed across Clay F). Understanding the expected brine chemistry and its evolution during concentration from evaporation and heating is important to designing the sampling and testing program.

It is important to note some brines reported in WIPP publications may not represent typical brine encountered in the underground. Some are believed to be strongly affected by WIPP construction efforts and contain components of groundwater from the overlying Culebra Member of the Rustler Formation (see stratigraphy in Figure 1) that flowed into the air intake shaft during and soon after construction. Shallow perched groundwater surrounding the WIPP surface facilities is still observed to drip down the exhaust shaft (Kuhlman & Malama 2014), and may impact brine composition samples collected in the vicinity of the shafts or in MB139. Other brines used commonly in WIPP performance assessment modeling include WIPP-12 and ERDA-6, which are not Salado Formation brines, but are Castile Formation brines (from wells that encountered pressurized brine pockets in the underlying Castile – see stratigraphy in Beauheim & Holt 1990 and Figure 1). This brine composition is important for WIPP performance assessment, but is not representative of Salado brine chemistry. Finally, the synthetic "Brine A" and "Brine B" were used in both laboratory and in situ experiments at WIPP (Molecke 1983), but are different from most brines observed at WIPP.

Brine chemistry of fluid inclusions and brines collected from boreholes and weeps show distinctive composition, indicating the source of available brine accumulating in boreholes is not purely from fluid inclusions. The marker beds at WIPP include MB139, which is a 1-m thick anhydrite and clay unit 1.5-m below the repository horizon, and MB140, a 4-m thick anhydrite and clay unit 15.5-m below the repository horizon. These marker beds have a distinct fluid composition compared to fluid inclusion brine and brines from boreholes completed only in halite units.

A-2.1 Brine Evolution During Isothermal Evaporation

Krumhansl et al. (1991a) described an experiment where they monitored the composition of WIPP brine (collected from a vertical borehole in floor near Room Q intersecting MB139) as it was left out to evaporate at room temperature for several months. The brine evolved into a magnesium-rich brine as the sample evaporated more than 50% (see red and green highlighting in last 4 samples of Figure 18). The evolution of these brines is discussed further in Appendix A-2.4.

Figure 19 illustrates the isothermal evaporation data and the salt mineral species in equilibrium at different relative quantities of SO_4, K_2, and Mg. The inset figure is from Wollmann (2010) and illustrates the potential complexities of these multicomponent (hexary: Na^+, K^+, Mg^{2+}, Cl^-, SO_4^{2-}, H_2O) brine systems (in Figure 19 inset: ph=polyhalite, anhy=anhydrite, goerg=görgeyite, and glaub=glauberite), beyond that portrayed in the Krumhansl et al. (1991a) figure. This indicates the brines used in the Krumhansl et al. (1991a) analysis were likely in equilibrium with polyhalite (which is consistent with the polyhalite content of MU-0 and PH-4 immediately above MB-139 where the samples were collected). Wollmann (2010) also presents these data at different temperatures, which would be useful for future heated evaporation experiments, that could be run to better understand field observations of brine composition.

Sample #	% Evap.	Na	Cl	Mg	K	Li	B	SO_4	Br	Ca	K/Mg	Na/Cl
1	0.0	67	163	17	14	23.5	1.45	13	1.2	0.30	0.86	0.41
2	1.1	66	163	17	14	23.2	1.44	13	1.5	0.30	0.86	0.40
3	2.0	67	164	17	14	25.9	1.45	13	1.4	0.30	0.84	0.41
4	2.9	67	164	17	15	23.7	1.46	13	1.4	0.31	0.84	0.41
5	4.3	67	164	18	15	25.2	1.52	14	1.4	0.32	0.84	0.41
6	9.6	65	164	19	16	24.7	1.56	14	1.5	0.34	0.84	0.40
7	9.7	62	164	19	16	25.2	1.58	15	1.5	0.33	0.84	0.38
8	14.1	61	164	21	17	28.3	1.68	16	1.6	0.36	0.82	0.37
9	16.7	59	165	22	18	30.1	1.79	16	1.6	0.37	0.83	0.36
10	20.0	57	166	23	19	23.7	1.89	18	1.7	0.30	0.82	0.34
11	24.9	52	166	25	20	30.1	2.08	19	1.8	0.27	0.82	0.32
12	40.7	33	172	39	28	45.5	3.02	27	2.7	0.16	0.72	0.19
13	57.0	7.4	193	69	18	98.3	5.61	47	5.2	0.04	0.26	0.038
14	61.6	1.5	245	107	0.6	127	4.51	29	7.8	0.03	0.006	0.006
15	65.8	1.2	248	89	0.5	172	5.62	211	79	0.02	0.006	0.005
16	66.0	1.3	245	91	0.5	199	6.35	285	100	0.02	0.006	0.005

Figure 18. Isothermal evaporation experiment brine compositions in g/L (Table 4 of Krumhansl et al. 1991a). Significant increases are green; significant decreases are red.

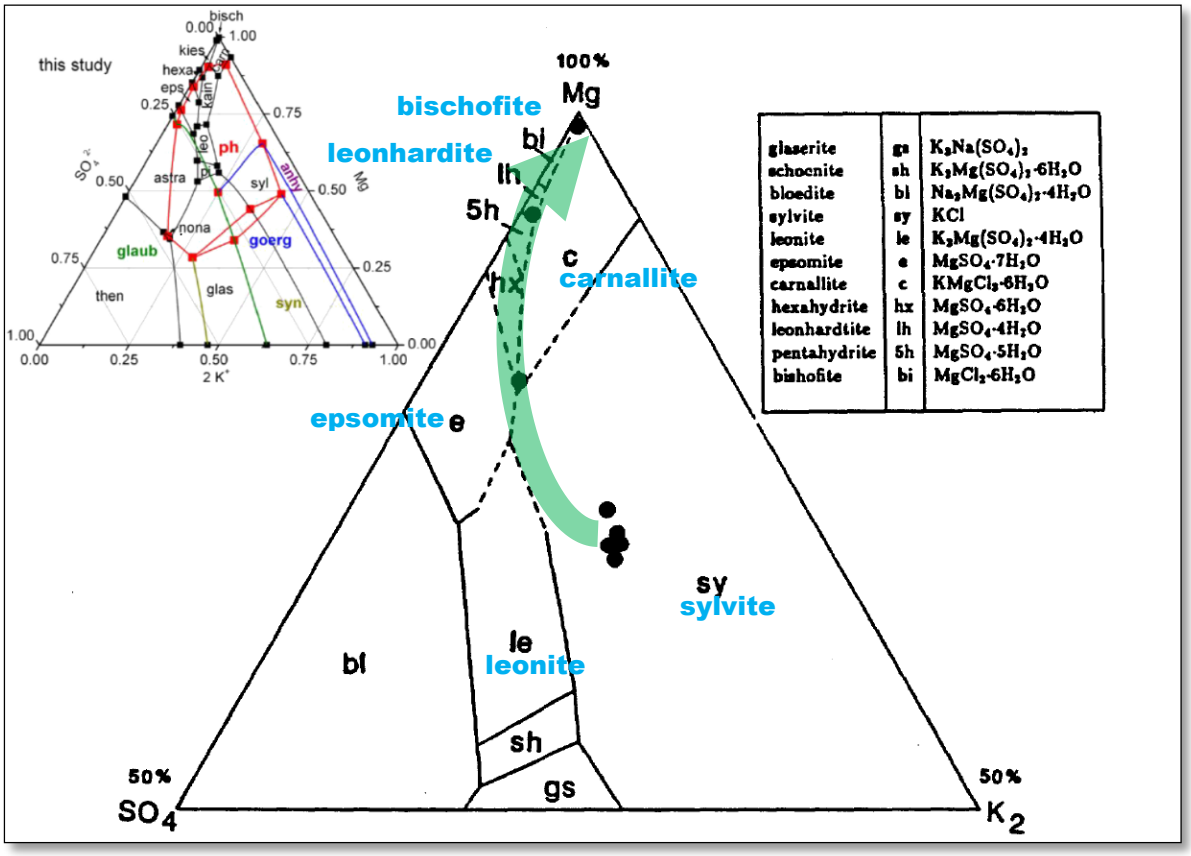

Figure 19. Jänecke diagram of isothermal brine evaporation data plotted as Mg-K_2-SO_4 (Figure 12 from Krumhansl et al. 1991a; inset Figure 100 from Wollmann 2010). Brine from MB139 (Room Q vertical borehole).

Roberts et al. (1999) presented results from geochemical modeling analyses that showed which minerals would precipitate from MU-0 waters: primarily halite, but with significant amounts of the hydrous chloride minerals carnallite [$KMgCl_3 \cdot 6(H_2O)$] and bischofite [$MgCl_2 \cdot 6(H_2O)$] (Figure 19 and Figure 20), which is largely consistent with the precipitation reaction path discussed in Appendix A-2.4.

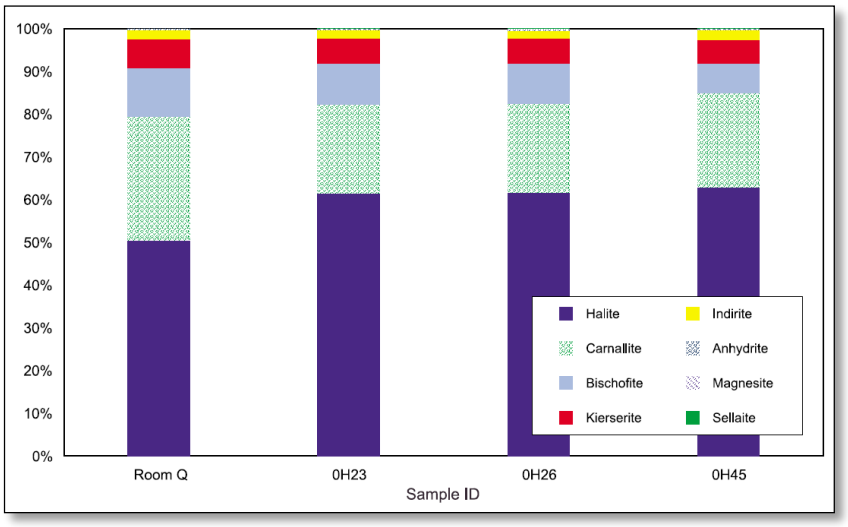

Figure 20. Normative salt assemblages for MU-0 brines (Figure 9-27 of Roberts et al. 1999).

Figure 21 illustrates the evolution of the equilibrium RH and specific gravity over a brine as it concentrates due to precipitation of salts. The path indicated on this figure is similar to that shown in Figure 19. Magnesium chloride salts tend to deliquesce much more readily than halite, since they equilibrate at a lower RH (<50%, compared to 75% RH). Greenspan (1976) summarizes laboratory data on equilibrium RH for several binary salts across a range of temperatures. Jové Colón et al. (2013) compared the TC model EQ3/6 to observations and showed the equilibrium RH for hydrous magnesium chloride salts decreases below 20% for temperatures above 100 °C.

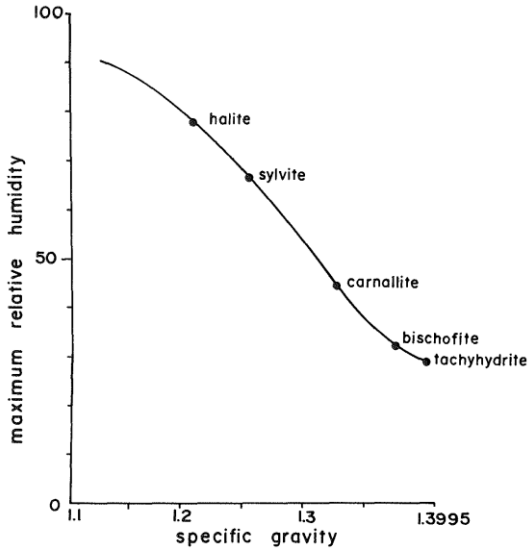

Figure 21. Equilibrium RH and specific gravity during brine concentration by evaporation (Figure 1 from Sonnenfeld & Perthuisot 1989)

A-2.2 Salt Precipitate During Heating

Krumhansl et al. (1991b) analyzed precipitated salts found on post-test exhumed heaters in Room B at WIPP (Figure 22 and Figure 23). Heater B042 was studied post-test via a 94 cm [37”] diameter overcore. Initially it was a 91.4 cm [36”] diameter vertical hole with a 61 cm [24”] heater placed in it without backfill. Maximum hole temperature was 130 °C. During the first 600 days of testing, B042 produced 35 liters of brine. The rind of salts observed between the heater and the creep-closed borehole only accounted for 20 to 23 liters of brine (e.g., see Figure 22 showing heater removal at WIPP – both heaters from Room B, but not necessarily heater B042). The rest of the salts were assumed to have been deposited in the formation, once the boiling isotherm moved out into the formation. The effect of hot steam migration through the intact salt (i.e., from the boiling point in the formation to the moisture collection system in the borehole) near the borehole was never examined. A combination of borehole closure and salt precipitation (Figure 21) filled the initial 15.24 cm [6”] annular space between the heater and the borehole wall.

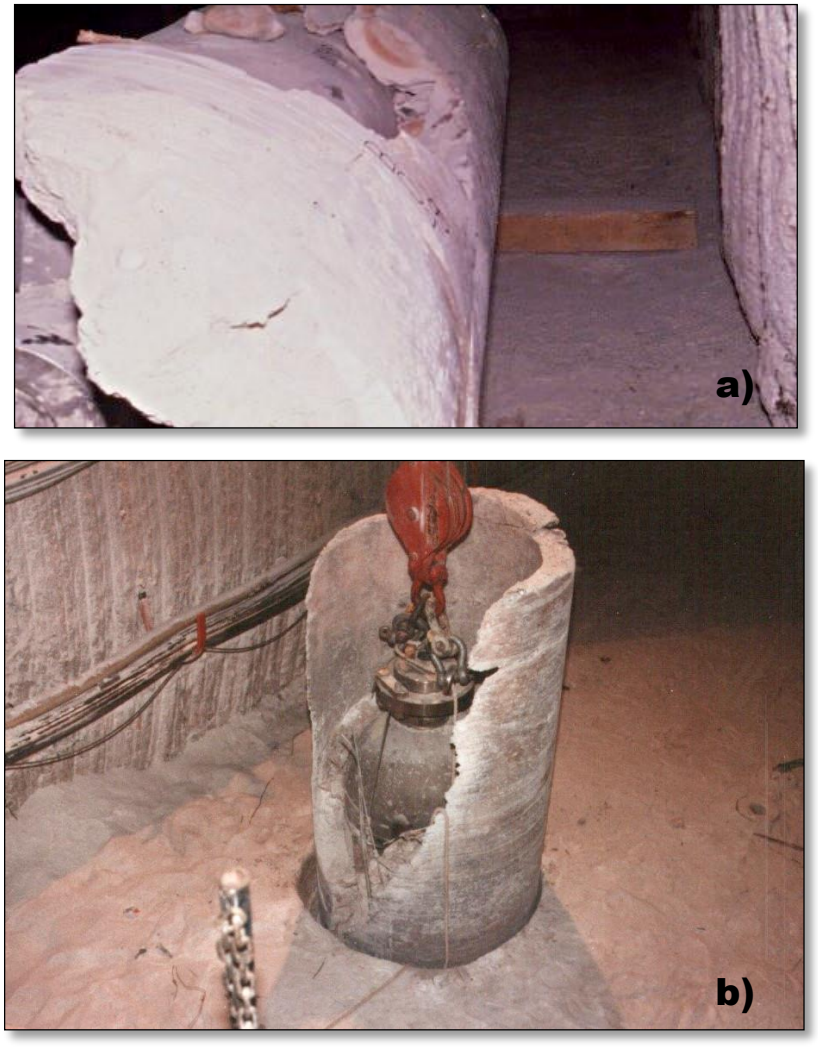

Figure 22. Post-test condition of heaters in WIPP Room B (a Figure 2.5 of Hansen et al. 2014; b Figure 2.2.1.2 of Brady et al. 2013).

Mineralogy of B042 Heater Scale
(Distance are downward from the top of the heater)

JS 57	From 0 to 1 foot down - halite.
JS 58	From 1 to 2 feet down - mostly halite and traces of bischofite and sylvite.
JS 59	From 2 to 3 down - mostly halite, a few good carnallite x-ray diffraction peaks (a few important ones missing between 24 and 26.5°). Possibly traces of kieserite, bischofite and sylvite.
JS 60	From 3 to 4 feet down - mostly halite but the carnallite x-ray diffraction peaks are well represented in this sample; possibly a trace of bischofite also.
JS 61	From 4 to 5 feet down - halite, carnallite and sylvite.
JS 62	From 5 to 6 feet down - some small clear gemmy non-cubic crystals which proved to be pure carnallite. The bulk of the sample was halite with a lesser, but significant, amount of carnallite. May contain traces of bischofite as well.
JS 63	From 6 to 7 feet down - halite and probably a little carnallite.
JS 64	From 7 to 8 feet 4 inches down - halite and a definite, though minor, amount of carnallite. (This sample originated from the junction between the bottom of the weep salt accumulations and the top of the crushed salt filling the hole bottom)
JS 65	From 8 feet 4 inches to the heater bottom. Essentially pure halite.
JS 66	Hardpan heater scale taken from the dense salt - halite and possibly a little bischofite.

Figure 23. Mineralogy of observed B042 heater scale (Table 3 of Krumhansl et al. 1991b). Hydrous minerals highlighted.

A-2.3 Acid Gas Generation at Elevated Temperatures

Acidic vapors have been observed several times in heater tests in both bedded and domal salt, including:

- WIPP Room B vapor collection system (pH 0.93 – Molecke 1986) and during overcoring of Room B heaters (10 ppm HCl vapor – Brady et al. 2013);
- WIPP Room J Materials Interface Interactions Test (MIIT). This test used artificial brine, likely experienced a significant heater over-temperature event, and was not carried out in N_2 gas (Krumhansl 1986);
- Lab experiments involving salt, brine, and candidate waste package materials (Molecke 1983); and
- Asse during the large-scale brine migration experiment (Coyle et al. 1987; see Appendix A-5.2).

Krumhansl et al. (1991b) and Molecke (1986) proposed HCl was generated by decomposition of solid magnesium chloride bearing salts to produce periclase (MgO). The proposed reactions are:

$$MgCl_2 + H_2O \longrightarrow MgO + 2HCl$$

$$MgCl_2.H_2O \longrightarrow MgO + 2HCl$$

$$MgCl_2.2H_2O \longrightarrow MgO + 2HCl + H_2O$$

$$MgCl_2.4H_2O \longrightarrow MgO + 2HCl + 4H_2O$$

These reactions from Krumhansl (1986) are correct, but thermodynamic data indicate they might not be likely under expected borehole conditions (40 to 75% RH and ≤150 °C). MgO does not form except at elevated temperatures of several hundred degrees Celsius (Sugimoto et al. 2007; de Bakker et al. 2012). Trace MgO was observed on the MIIT heaters (Krumhansl 1986), but not on the Room B heaters (Figure 23). The MIIT heaters also showed evidence of molten halite (sample 4), which indicate the heaters likely shorted or experienced significant over-temperature (several hundred degrees Celsius) before failing. The MIIT heaters were in vertical boreholes filled with synthetic brine (i.e., Brine A – see Figure 25), and were not being flushed with dry N_2; ample oxygen was present to form oxides.

Under the expected conditions, the first thing to precipitate is likely a magnesium hydroxychloride phase, $Mg_x(OH,Cl)_{2x}{:}YH_2O$. Anhydrous phases include Mg(OH)Cl and $Mg_2(OH)_3Cl$, but multiple hydrous phases with different (OH):Cl ratios or degrees of hydration have been reported (de Bakker et al. 2012), that precipitate from concentrated magnesium chloride solutions as base is added, or if the solution is heated. Reaction to form these would also produce acid. For instance, for the simplest anhydrous phase:

$$H_2O + Mg^{2+} + 2Cl^- \rightarrow Mg(OH)Cl + HCl_{(g)}$$

but it is not clear under what temperature and pH conditions these phases will form, or which ones will be stable. Magnesium-hydroxychlorides precipitate readily from Salado brines, under high pH conditions they will form Sorel cement.

Another possible mechanism for acid gas generation produces HCl vapor directly from the liquid phase. It relies on presence of a concentrated Na-Cl or Mg-Cl brine and a downstream relatively pure H_2O condensate. This mechanism is consistent with the conditions where acid brines in heated salt have been observed to form. Molecke (1986) indicated the most acidic brine observed in the Room B moisture release experiments was "previously assumed to be essentially condensed, distilled water."

For a chloride-rich brine at any pH a non-trivial amount of HCl will exist in the atmosphere above the brine. As the atmosphere moves to a downstream cold trap or outlet and cools, the partial pressure of HCl gas does not change. Thus, at the location where condensate forms, the P_{HCl} will be the same as was present in the atmosphere over the brine, and will be in equilibrium with the condensate as it forms.

A Na-Cl brine begins to precipitate halite at ionic strength of about 5 molar, while a Mg-Na-Cl brine can reach higher molarities (e.g., see increasing brine specific gravities associated with Mg-Cl salts in Figure 21), and therefore drive the acidity even lower. The ionic strength of the brine will increase due to evaporation, precipitation of halite, and due to temperature effects.

A secondary goal of the intermediate scale borehole heater test is to gather field data to better understand the mechanisms for acid gas generation (i.e., decomposition of hydrous magnesium chloride minerals and acidification of condensate in the presence of a strong Na-Cl or Mg-Cl brine). The mechanism occurring in the field may be a combination of the two processes given above, and to further understand them would likely require carefully designed laboratory experiments and numerical modeling (Jové Colón et al. 2013).

A-2.4 WIPP Salado Brine Composition Survey

Figure 24a shows the variability in composition of brines from the repository horizon at WIPP. Two groups of halite fluid inclusions are presented. Group II (open squares) is closer to being a direct result of seawater evaporation (heavy arrow and upper stippled area marked "Brantley et al, 1984"). Group I (partially filled squares) are likely the result of polyhalite conversion from anhydrite or gypsum, which lowers K levels relative to Mg levels (Figure 24b). This suggests that disseminated polyhalite in the repository horizon, and in stratigraphically lower portions of MU-0, may be an alteration product of gypsum rather than a primary deposit. The halite containing the fluid inclusions likely re-crystallized about the same time the polyhalite was formed. Age dates for polyhalite in WIPP are approximately 200 million years (Stein & Krumhansl 1986), indicating these transformations likely happened soon after

deposition. Stein & Krumhansl (1988) presented these similar plots with additional data, which further supported these same proposed relationships (data from Stein & Krumhansl, 1988, Roberts et al. 1999, and Deal et al. 1995 are summarized in Figure 25).

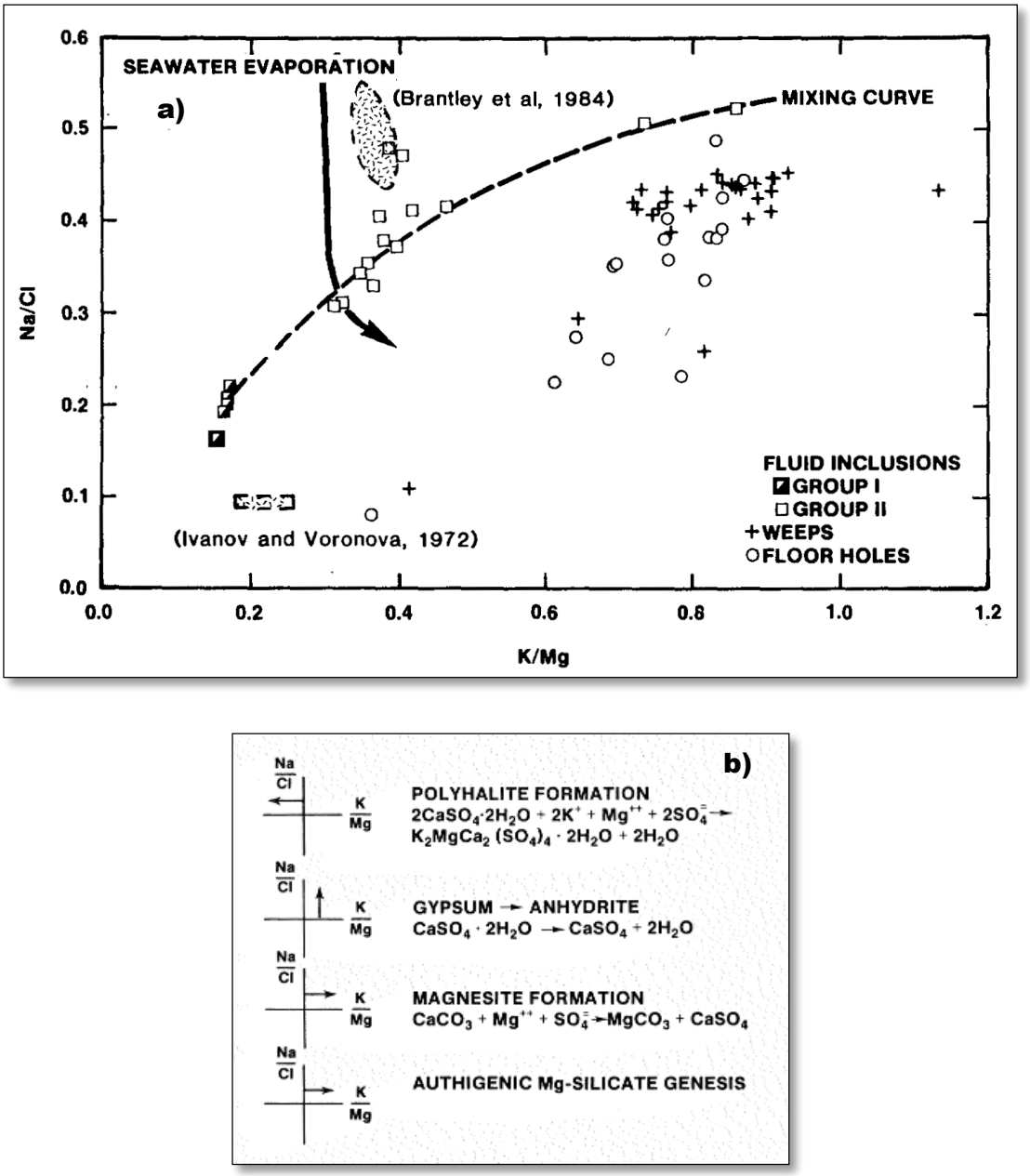

Figure 24. WIPP Salado brines a: K/Mg vs. Na/Cl (by weight) in WIPP brines (Figure 2 of Stein & Krumhansl 1986). b: qualitative effect of different mineral transformations on relative position (Figure 3.10 of Lappin 1988).

Table 2 shows that the gypsum dehydration temperature range (75-175 °C) is much lower than the "uncontaminated" polyhalite dehydration range (340-360 °C), so this proposed *in situ* transformation is significant from a brine availability point of view. Dehydration of polyhalite typically only occurs at

temperatures significantly above the brine inclusion decrepitation temperature, and would therefore make this water unavailable for migration into excavations.

Weeps and floor holes in Figure 24 have an apparently different composition from fluid inclusions, likely because most floor holes at WIPP cross MB139, which is a significant anhydrite and clay layer (about 1 m thick and 1.5 m below the repository horizon). Brines from MB139 (orange circles) and MB140 (blue circles) are in some ways quite different from fluid inclusion brines and different from each other.

Brines collected from MU-0 (pink triangles) are shown in Figure 25 to be markedly different in composition compared to Group I and all but possibly 2 samples from Group II fluid inclusions (open black triangles). MU-0 brines are much closer to MB139 and Room Q brines. MU-0 is located stratigraphically between Room Q (which followed the orange marker band [MU-1] and intersected MU-0 along the bottom of the room) and MB139 (approximately 1 m below the bottom of MU-0 – unit PH-4 lies between them – see Figure 5). GSEEP brine in Figure 25 is likely derived from MB140 brine (Roberts et al. 1999). Data for many of the "weeps" and "floor holes" in Figure 25 may have experienced significant evaporation, starting from a composition closer to MB139 and MU-0. The isothermal evaporation line is data from the Krumhansl et al. (1991a) evaporation experiment, which started with brine collected from a vertical borehole near Room Q (i.e., in MB139). Brine A (Molecke 1983) and typical seawater composition are plotted for comparison.

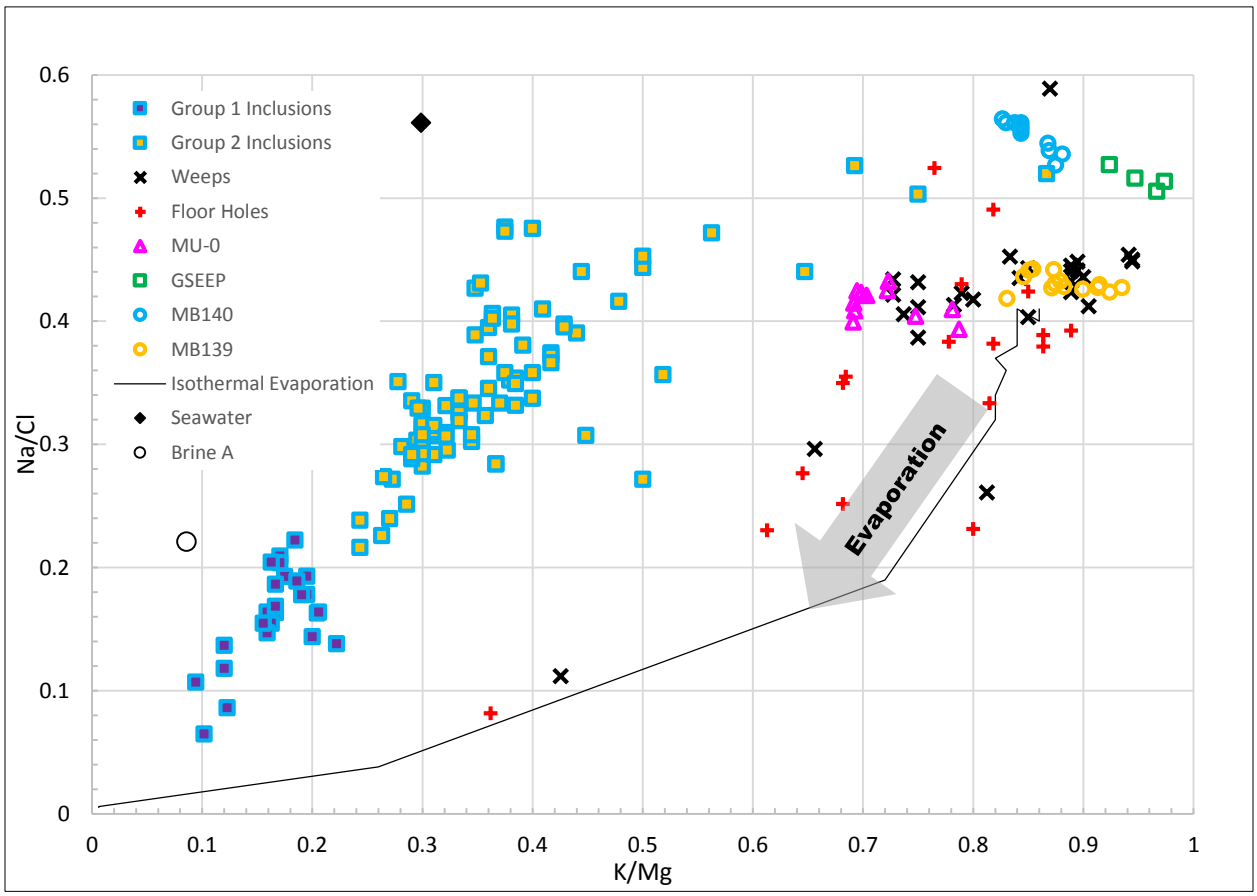

Figure 25. Salado brine chemistry summary plot (data from Molecke 1983, Stein & Krumhansl 1988, Krumhansl et al. 1991a, Deal et al. 1995, and Roberts et al. 1999).

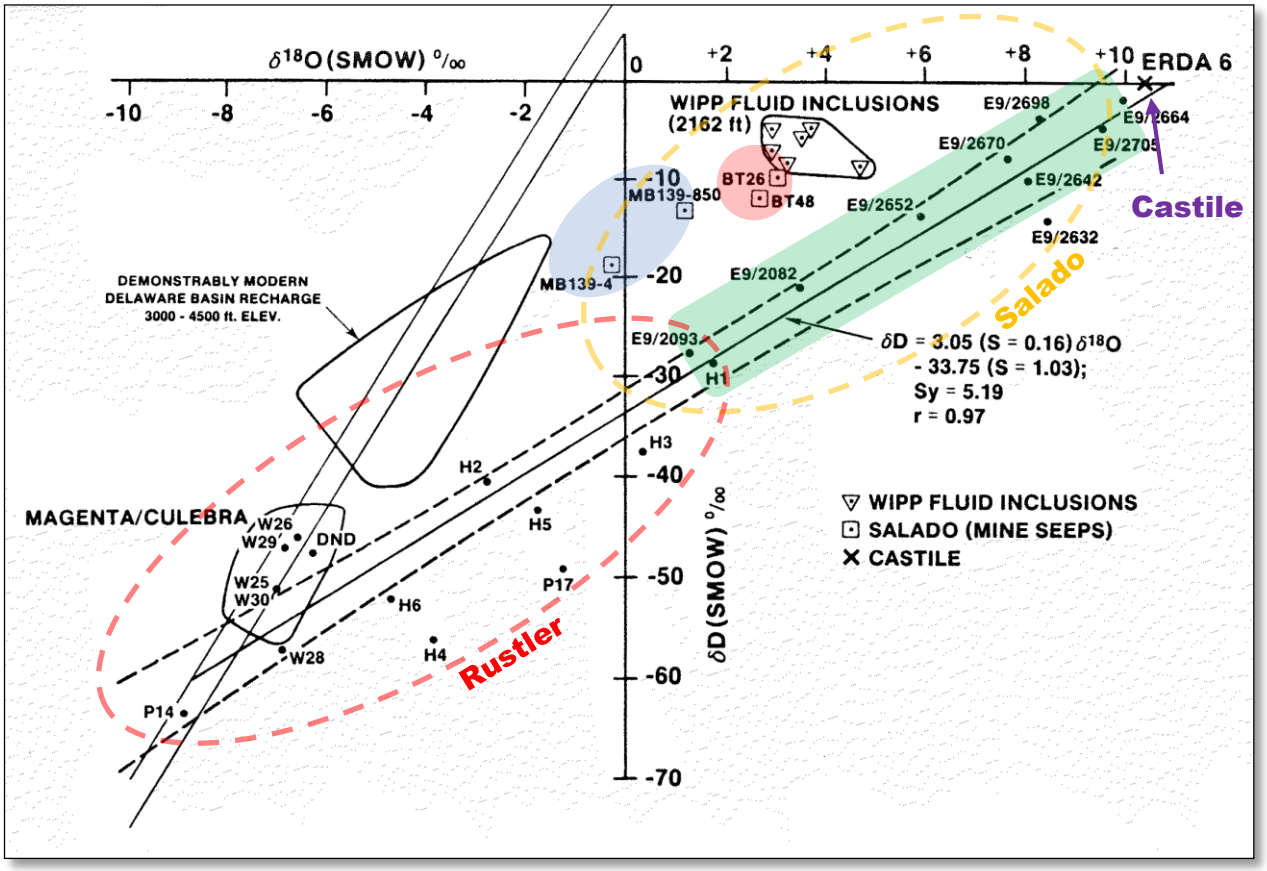

Figure 26. Stable-isotope composition of fluids from WIPP-relevant horizons (Figure 3.11 of Lappin 1988). Samples BT26 & BT48 from Duval potash mine (McNutt Potash Zone; Figure 1); blue shaded samples are from MB139.

A-2.5 WIPP Salado Stable Isotope Data

Figure 26 shows the relative levels of oxygen and hydrogen isotopes in WIPP waters, including Salado brines. The small isotopic difference between Salado halite fluid inclusions and MB139 brine (inverted triangles and squares) is not completely understood (Lappin 1988; p. 60), but this is relatively small compared to the compositional differences among these waters (Figure 24). The ERDA-6 sample in Figure 26 is from the Castile Formation (below the Salado Formation, the source of high-pressure brine pockets – Figure 1). The ERDA-9 samples are from a range of depths across the Salado (green shaded box), and seem to span from the deeper ERDA-6 sample to the shallower Rustler Formation (Figure 1) samples (i.e., H-, P-, and W-series samples circled with red dashed line).

Samples collected from boreholes generally follow an indicated trendline on Figure 26, while samples from mined excavations do not. This distinction is not completely understood, and may be an artifact of sample collection methods or contamination from drilling fluid in boreholes. Lambert (1992) presented stable isotope data similar to those in Figure 25.

A-3. Avery Island Brine Migration Tests

A series of isothermal and heated vertical borehole brine inflow tests were conducted at Avery Island (domal salt) in the late 1970s and early 1980s (Stickney & Van Sambeek 1984). The relevant test details include:

- Utilizing deuterated water as an introduced tracer
- Salt gas permeability observations were made:
  - At different temperatures, and
  - During cool-down period after brine migration heater test

A-3.1 Deuterium Tracer in a Salt Heater Test

Three identical groups of boreholes (see Figure 27 for layout of a typical group) were monitored for bine inflow (one unheated, two heated). Test design is documented in Krause (1979) and test results are summarized in Krause (1983) and Stickney & Van Sambeek (1984). One of the heated boreholes utilized a traced synthetic brine (SB), where the heater and tracer boreholes were later overcored and analyzed post-test. The synthetic brine composition introduced into boreholes B2, B4 and B8 was 25 g/l D_2O, approximately 2 wt-% D_2O (Clynne et al. 1981).

The results of the isotopic analysis of water samples and desiccant cartridges by the USGS were not easily interpretable, but Clynne et al. (1981) had the following observations about the fractionation processes in the heater test at Avery Island:

> "(1) Evaporation of the brine arriving at the heater hole fractionates deuterium. In the Avery Island situation, where vapor is continually removed from the system and the brines are very saline, evaporation initially enriches the residual solution in deuterium. As evaporation proceeds a reversal takes place and the residual solution is depleted in deuterium. The point of reversal is dependent upon evaporation rate, temperature and brine chemistry (Sofer and Gat, 1975).
>
> (2) A second fractionation in the brine arriving at the heater hole involves the crystallization of hydrated minerals. The volumetrically important hydrated minerals crystallizing from NaCl-saturated WIPP-A at 55°C are carnallite ($KMgCl_3 \cdot 6H_20$) and bischoffite [*sic*] ($MgCl_2 \cdot 6H_20$) (D'Ans, 1933). There is a deuterium fractionation between water of hydration in minerals and the solution from which they crystallized, and the process is temperature and composition dependent. Although the crystallization of hydrated minerals normally enriches the residual brine in deuterium, minerals that deplete brine deuterium are known. No data exist for the effect of carnallite and bischoffite [*sic*] crystallization on isotopic composition."

These discussed fractionation effects would be going on in the planned heater test, and should be considered in the test design and interpretation. On the order of 35,000 ppm D_2O was observed in the desiccant canisters associated with the SB heated borehole at the conclusion of the test, showing the tracer did flow into the heated borehole. Additional fractionation mechanisms were observed related to the desiccant canisters and their treatment in the laboratory, which precluded their use in a quantitative analysis.

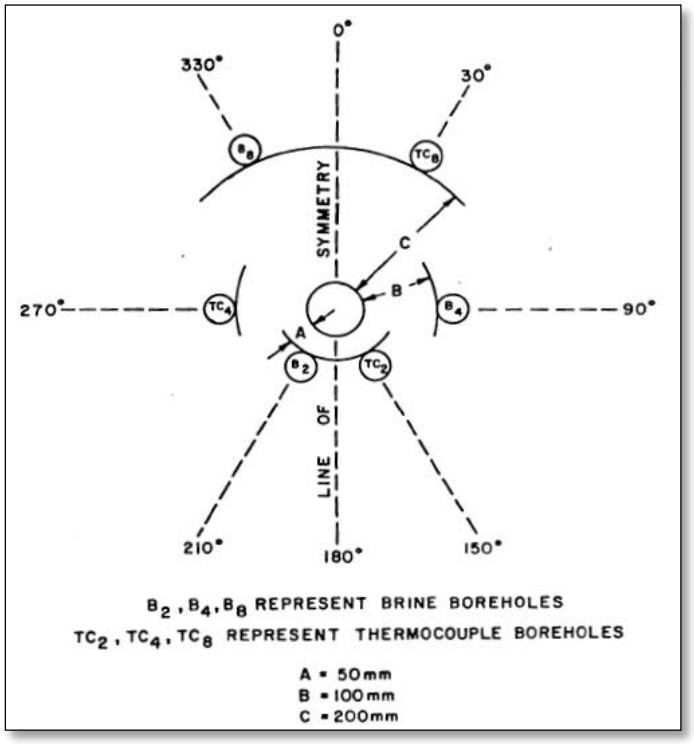

Figure 27. Layout of typical Avery Island brine inflow experiment (Figure 2 of Krause 1983).

Brine inflow at all three sites was monitored for several months, showing stable brine inflow rates after approximately one month of monitoring (Figure 29). Brine inflow rates were approximately 100 times lower in domal salt at Avery Island than in bedded salt at WIPP; comparing unheated site AB from Figure 28 with Figure 10.

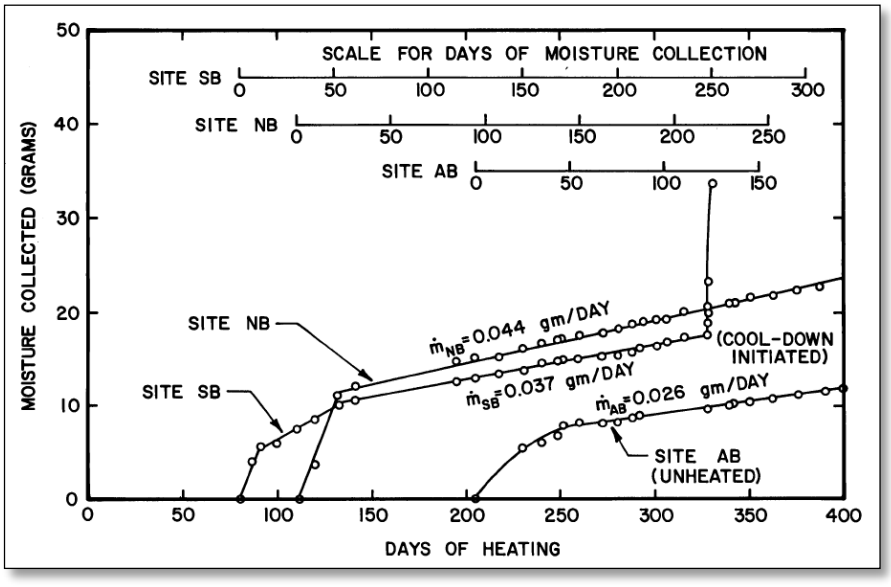

Figure 28. Brine inflow through time in Avery Island vertical boreholes (Figure 20 of Krause 1983).

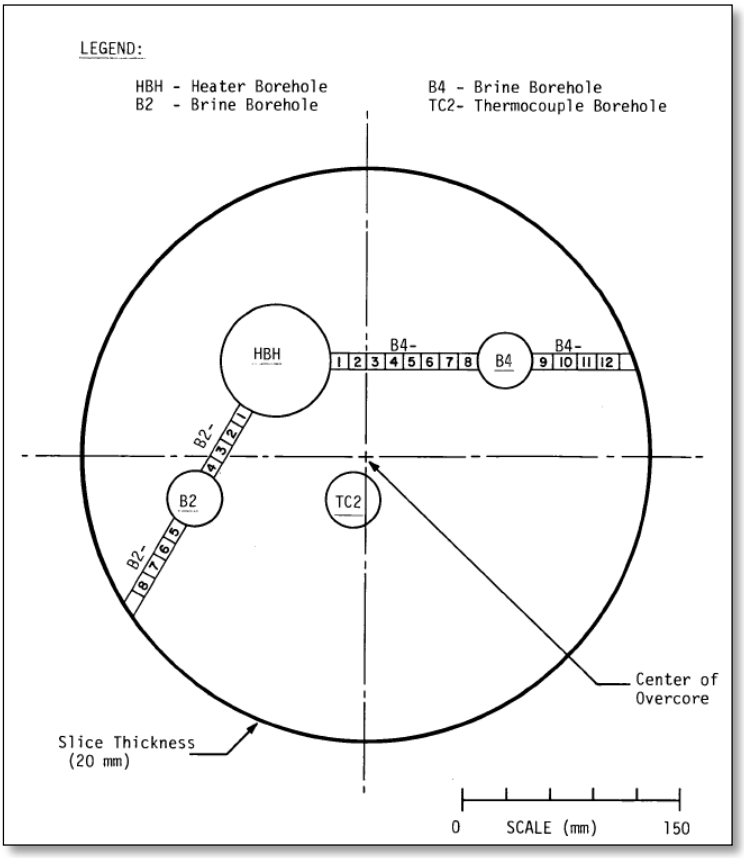

Figure 29. Illustration of over-coring and profiles of lab D_2O samples between boreholes (Figure 34 of Krause 1983).

The distribution of D_2O through space in the salt (after the end of heating) was estimated by overcoring around the smaller-diameter borehole B2 (50 mm [2”] to edge of heater borehole) and the heater borehole, and testing small samples along profiles between the boreholes (Figure 29).

The distribution of D_2O in the intact salt after heating is shown in Figure 30. The observed values were low, within a factor of 5 of the background level. The background level was estimated to be 3 ppm/gram salt D_2O by quadrupole mass spectrometer at SD School of Mines (see sample preparation description on p. 46 of Krause 1983), which would correspond to 300 ppm for 1% porosity. All the planned analyses were not carried out “because of the low concentration of D_2O in the synthetic brine” (p. 49 Krause 1983). A Mg tracer was also added to the traced brine, but interpretation of Mg data was harder, because of low spatially heterogeneous background levels of Mg in the salt.

Based on this information, a high enough level of D_2O should be spiked in the satellite borehole to ensure the signal in the water flowing to the main/heated borehole is detectable, but the fractionation of deuterium during evaporation and precipitation of hydrous minerals will complicate interpretation.

Given how much deuterium was added to borehole B2 (25,000 ppm or 2% by weight – Clynne et al. 1981), and how much was collected in the desiccant canisters (on the order of 35,000 ppm – Krause 1983, p. 52), the low levels of D_2O in the salt are a function of the low advective porosity of the salt.

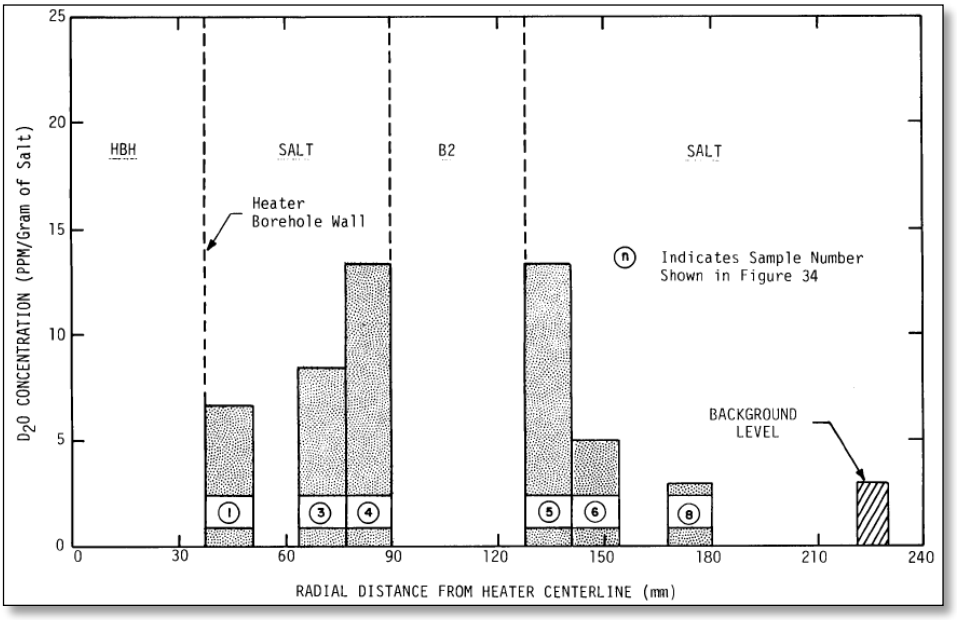

Figure 30. Results showing distribution of D_2O in lab samples from overcored salt at Avery Island (Figure 35 of Krause 1983).

A-3.2 Salt Gas Permeability During Cooling

Gas permeability measurements were made in small-diameter vertical boreholes at Avery Island, using a pipe-based neoprene compression plug as the isolation tool Figure 31b). Additional borehole sealing was achieved by placing grout above the plug in the borehole (Stickney & Van Sambeek 1984; p. 32). Both constant-head and falling-head permeability tests were conducted using the same setup, and produced results which agreed with one another. The tests were conducted at different radial distances away from a long-term heater tests (i.e., distance from the heater was proportional to salt temperature). Figure 32b shows permeability was observed to decrease with an increase in temperature. Since these tests were run in shallow boreholes in the floor of the mine, the heat from the long-term heater test at Site C was causing the salt to expand and close up micro- and macro-fractures in the DRZ.

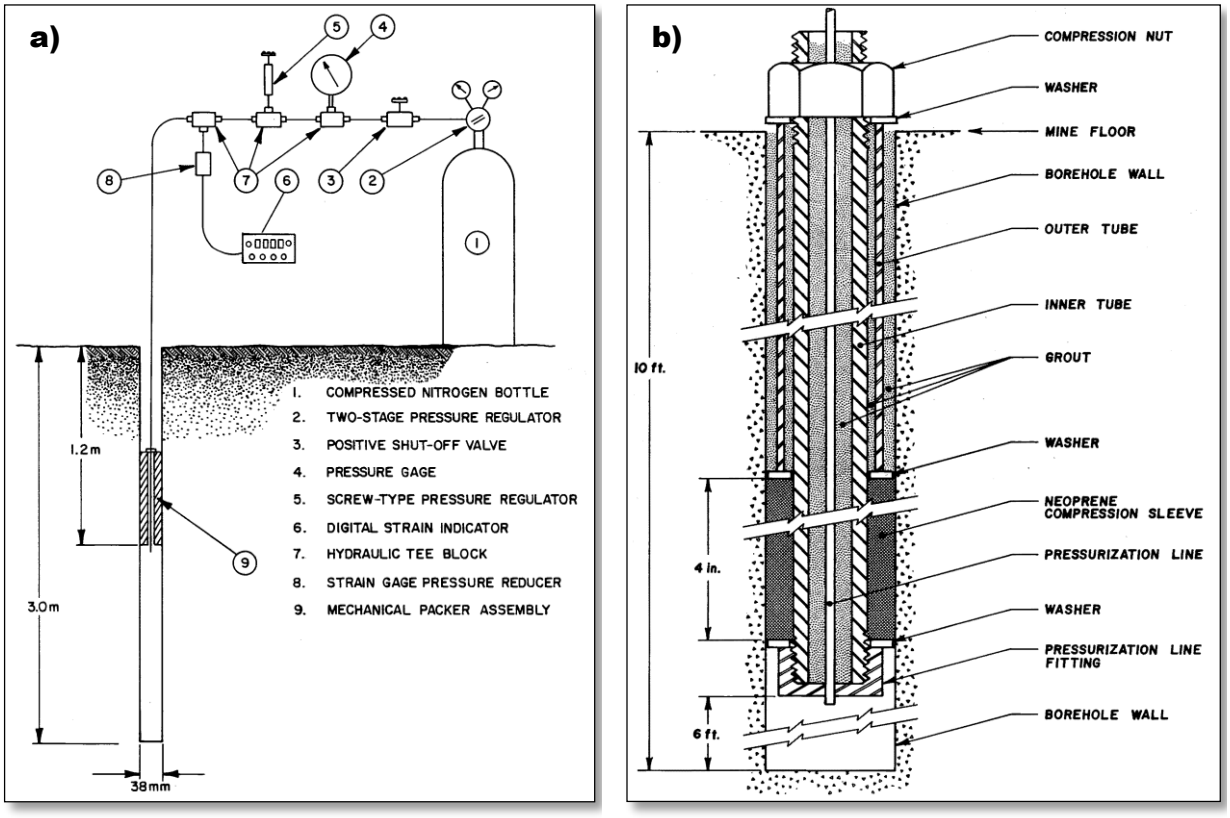

Figure 31. Salt gas permeability testing apparatus used at Avery Island (a: Figure 4-1 of Stickney & Van Sambeek 1984; b: Figure 1 of Blankenship & Stickney 1983).

Approximately half the total brine inflow at site SB occurred during the cool-down period (Figure 28). In conjunction with brine collection, further nitrogen gas permeability tests were conducted. Salt permeability was observed to increase by as much as five orders of magnitude (to 1.2×10^{-16} m^2 from 2.0×10^{-21} m^2) while heater power was stepped down over a period of five days (Figure 31a).

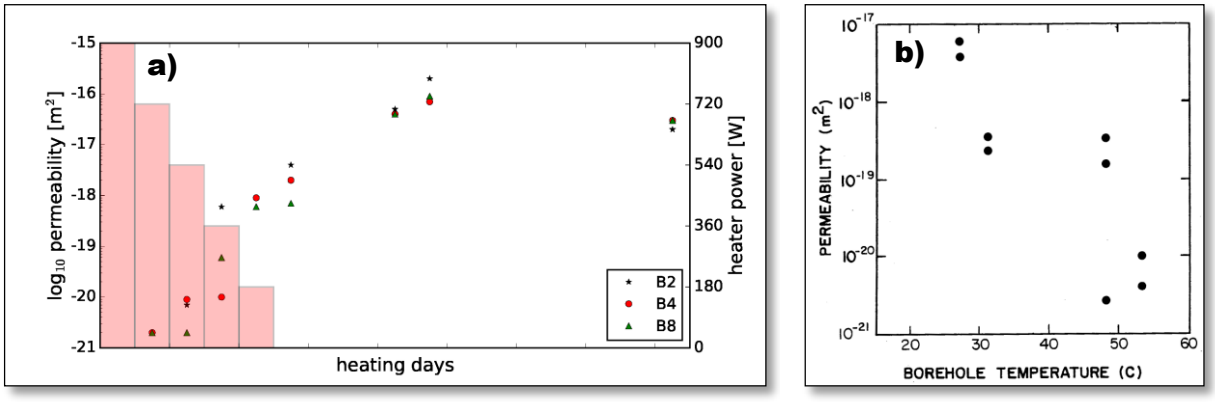

Figure 32. Avery Island borehole gas permeability. a: during cool down at site SB (Figure 4.4 of Kuhlman & Malama 2013); b: near heater Site C (Figure 4-2 of Stickney & Van Sambeek 1984).

A-4. Salt Block II: High-Frequency Brine Inflow

The Salt Block II experiment (Figure 33) included a large (1-m diameter) block of bedded salt from the MCC potash mine in the McNutt Potash Zone (Figure 1), located stratigraphically above WIPP in the Salado Formation (Hohlfelder 1979; Lambert 1979). The block was heated axially, and brine inflow to the heater was monitored via N_2 circulation through chilled mirror hygrometers (CMHs) and desiccant canisters. This large-scale lab experiment was unique with respect to the high-frequency brine inflow measurements made via CMH.

This high-frequency data allowed observation of additional shorter timescale trends and details of behavior not observed with daily weighing of desiccant canisters seen in most field salt heater tests.

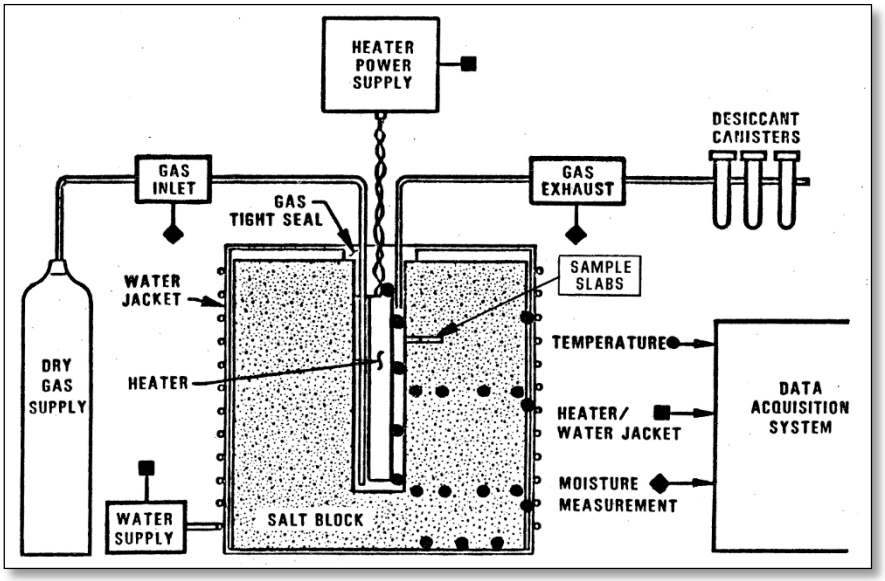

Figure 33. Salt Block II laboratory experiment setup (Figure 1 of Hohlfelder, 1979).

For the first portion of the experiment (Figure 34), both the CMH and the downstream desiccant canisters were used to measure brine inflow. The two methods agreed within 10%. The CMH approach was abandoned after approximately 83 days after the data became unreliable due to fouling of the mirrors.

This experiment showed that measuring brine inflow by two methods would be useful to assure data quality. This was one of the few datasets with high-frequency water inflow data during heating at different temperatures and during cooling. This also illustrates the large amount of brine released after the heaters were shut down (>40% of total brine collected). Steady state brine inflow is plotted in Figure 2 as a function of borehole temperature.

There was a temperature drift in the experiment due to uncontrolled conditions in the laboratory where the experiment was conducted, which also shows that large scale experiments require careful environmental control.

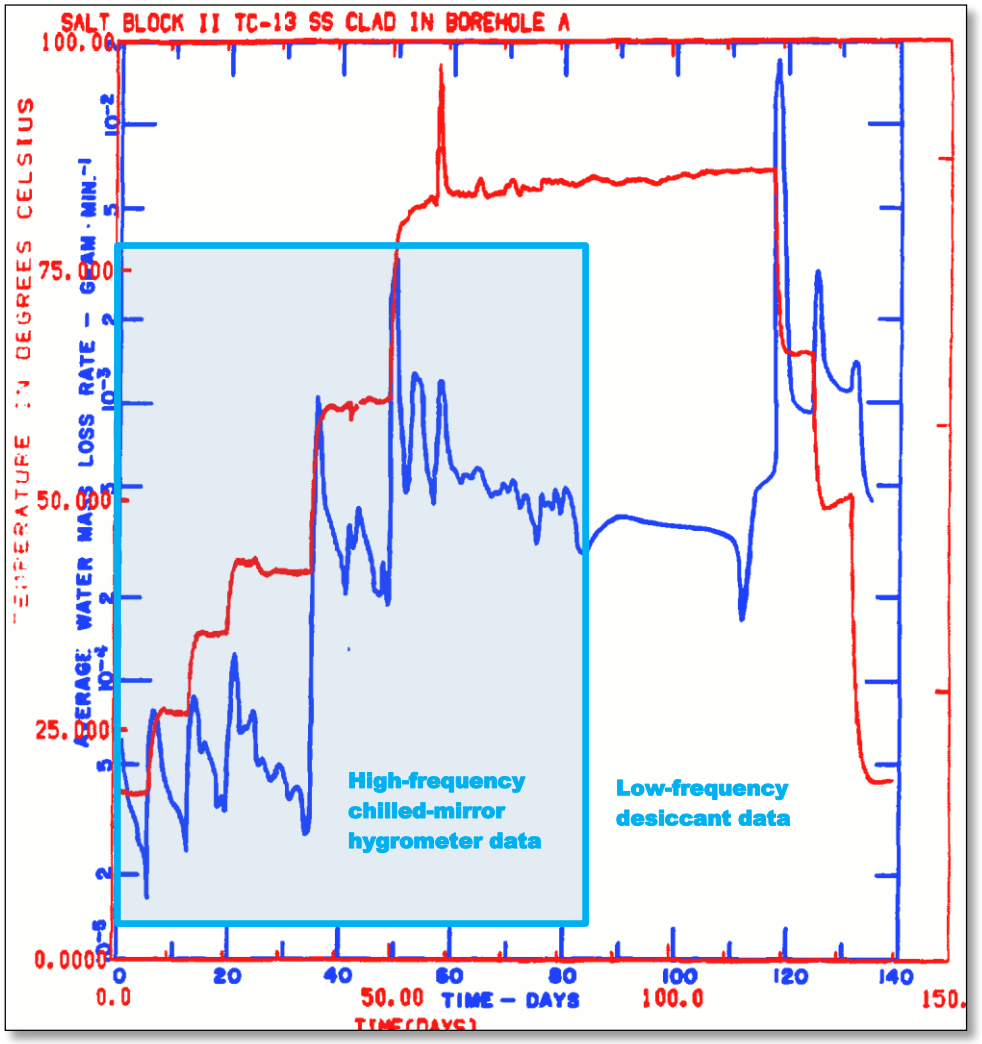

Figure 34. Water mass loss rate (blue line) and temperature (red line) observed in Salt Block II test. Blue box highlights high-frequency CMH data, other data are from daily weighing of desiccant canisters (Figures 17 & 27 of Hohlfelder, 1979).

A-5. Asse Brine Migration Experiments

The Asse Brine Migration test was jointly conducted by Westinghouse (US) and then West Germany (Federal Republic of Germany) in the Asse salt mine (Westinghouse 1987; Rothfuchs et al. 1988). The test included four identical sets of heated boreholes and observation holes. Two of the boreholes included radioactive ^{60}Co (other two had no radioactive material), and two were sealed during heating (while the other two had gas continuously extracted from them). Relevant observations or techniques used during testing included:

- Sampling and analysis of gases during testing,
- Use of a cold-trap type of brine collection system,
- AE monitoring.

This test was a very complex test with significant engineering design (Westinghouse 1987) and budget, but the tests produced some unique data. Four sites were established (Figure 36), with one sealed radioactive, one unsealed radioactive, and two more non-radioactive sites (sealed and unsealed).

A-5.1 Cold Trap Moisture Collection

The moisture collection system was similar to that proposed in this report, with dry nitrogen pumped through the two unsealed sites to flush any inflow of moisture, but instead of using desiccant or a CMH, they used a cold trap to condense all the liquid out of the gas stream (Figure 36). This is an alternative approach to using desiccant canisters (cheapest and most robust, but labor intensive and low-frequency) or inline hygrometers (higher frequency data, but more expensive and less robust). Maintaining a cryogenic cold trap in the underground would be relatively expensive and complex.

A-5.2 Gas Sampling While Heating Salt

Gas samples were collected from two of the four sites (the unsealed ones). The following statement from Coyle et al. (1987, p. 71) discusses the gases collected (example data shown in Figure 37).

> "These gases also contribute to the total pressure increase. It is of interest that hydrogen is observed in the nonradioactive sites as well as in the radioactive sites. The hydrogen in the nonradioactive sites is probably produced by corrosion reactions of the released brine. It will be of great interest to retrieve those different metal samples, which were attached to the thermocouple cage for corrosion investigations. The production of small amounts of hydrocarbons, carbon dioxide, and carbon monoxide is not surprising since it is known from former investigations that these components usually occur in rock salt. *The production of hydrogen chloride (HCl), observed in four measurements at sites 1 and 2, is possibly due to hydrolysis of bischofite ($MgCl_2 \cdot 6H_2O$).* This mineral could occur in small traces in the salt. In order to prove this assumption, special chemical analyses will need to be performed on salt samples of the test formation after the tests are completed."

> "Since *hydrogen production at the nonradioactive test sites is considered to be due to corrosion reactions*, it should be expected that the hydrogen production would decrease when either the brine release rates decrease or the metal surfaces are protected by oxide coatings. And in fact, it can be observed at test site 2 … that the hydrogen production decreased approximately 400 days after start-up of operation when the brine release rates became very small. Since the same effect can be observed at test site 1 where the water vapor is kept in the borehole, it can be concluded that the hydrogen production is also reduced because of the oxidized metal surfaces."

We would expect less production of hydrocarbons, the presence of any injected tracers, and possibly additional different gases due to differences between bedded and domal salt. This dataset of gases produced during the Asse Brine Migration test has not been generated for bedded salt.

Gas sampling was conducted downstream of the cold trap (Figure 36), so other condensable components in the gas phase (e.g., HCl) would likely have condensed out of the gas stream with the H_2O.

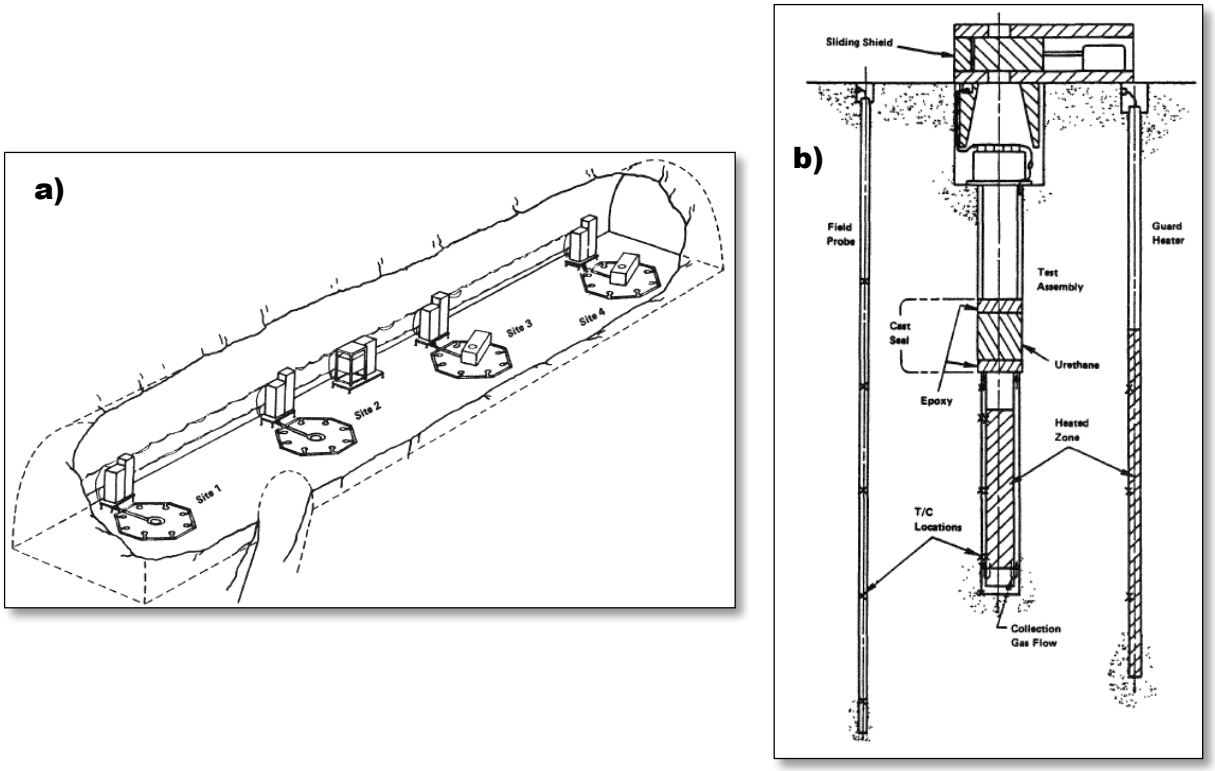

Figure 35. Layout of brine migration test at Asse (Figures 4-1 (a) and 4-2 (b) of Coyle et al. 1987).

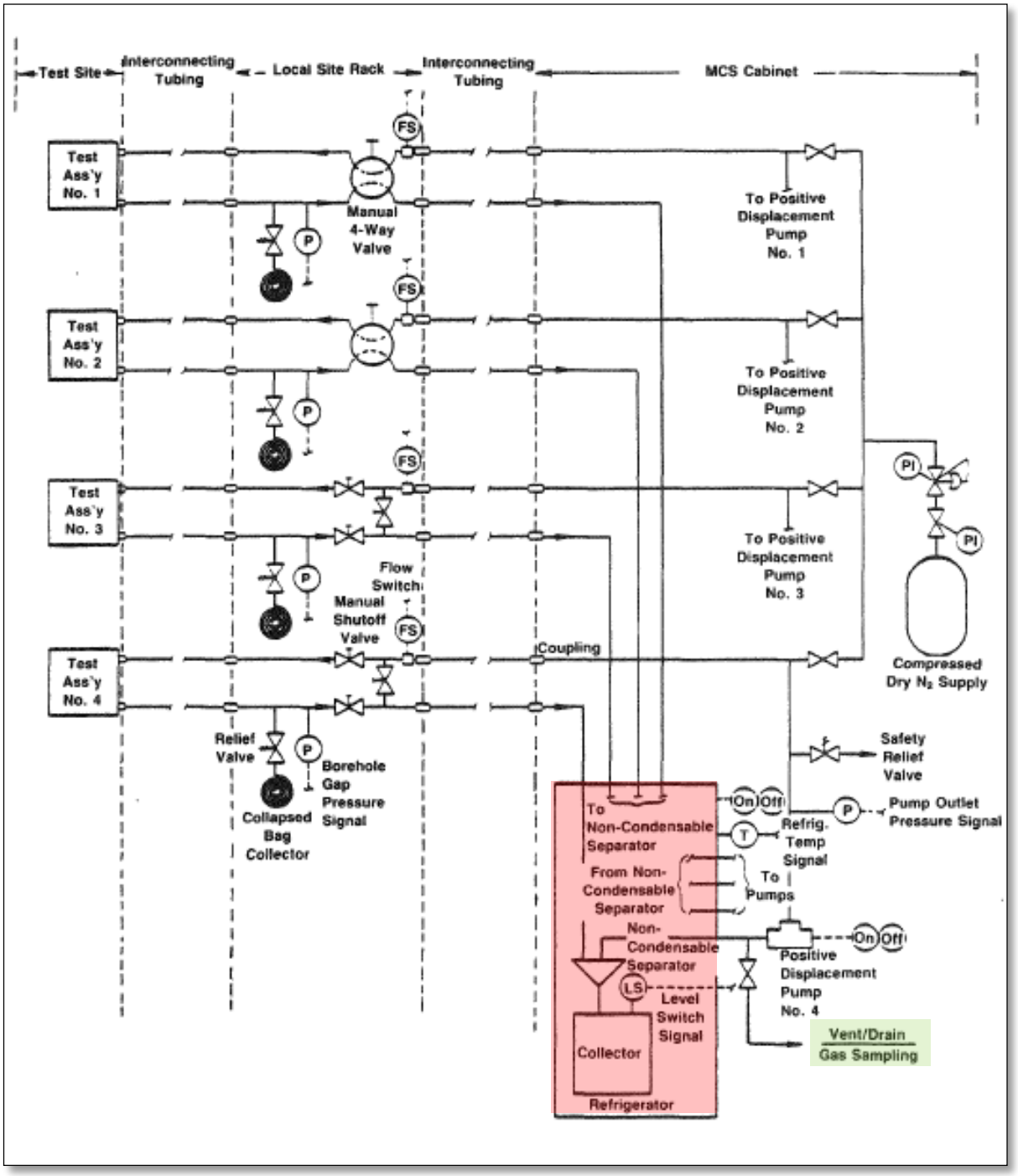

Figure 36. Moisture collection system at Asse (Figure 4-9 of Coyle et al. 1987). Cold trap and sample port highlighted.

Date of Sampling	Test Day	Sample No.	Component (Vol. %) H_2	O_2	N_2	CO_2	CO	CH_4	C_2H_6	C_3H_8
May 25, 83	0	1/1	-	0.9	98.9	0.034	-	0.0005	-	-
June 15, 83	21	1/3	-	0.4	99.3	0.69	-	0.02	0.005	0.0063
July 20, 83	56	1/4	0.01	1.04	-	1.5	0.096	0.033	0.0027	-
Aug. 23, 83	90	1/5	0.45	2.8	94	3.1	0.052	0.06	0.0287	0.164
Sept. 23, 83	121	1/6	0.6	0.74	93.6	4.04	0.32	0.0678	0.04	0.195
Oct. 25, 83	153	1/7	1.43	0.56	91.4	7.1	0.51	0.1140	0.00495	0.216
Nov. 23, 83	182	1/8	1.34	1.1	89.9	7.0	0.27	0.123	0.073	0.163
Dec. 19, 83	208	1/9	1.94	1.1	89.8	6.8	0.31	0.167	0.0715	0.159
Jan. 17, 84	237	1/10	1.47	0.84	93.1	4.1	0.30	0.152	0.058	0.125
Feb. 15, 84	266	1/11	1.40	0.51	93.8	4.7	0.26	0.167	0.027	0.13
March 14, 84	294	1/12	1.72	0.59	90.6	6.0	0.40	0.18	0.015	0.072
April 17, 84	328	1/13	2.21	0.24	91.4	5.46	0.39	0.22	0.03	0.10
May 15, 84	357	1/14	1.84	0.72	92.7	4.30	0.24	0.185	0.024	0.075
June 16, 84	386	1/15	2.31	0.28	91.8	4.95	0.29	0.18	0.024	0.075
July 13, 84	415	1/16	1.54	0.26	92.5	4.70	0.30	0.20	0.025	0.061
Aug. 16, 84	449	1/17	1.05	0.38	92.7	4.70	0.31	0.214	0.022	0.068
Sept. 17, 84	481	1/18	0.74	0.39	92.0	5.19	0.30	0.25	0.02	0.07
Oct. 15, 84	509	1/19	0.58	0.28	93.5	5.3	0.31	0.24	0.02	0.06
Nov. 8, 84	537	1/20	0.23	2.3	93.1	4.1	0.14	0.2	0.02	0.05
Dec. 14, 84	569	1/21	0.27	0.72	93.2	4.2	0.16	0.18	0.02	0.02
Jan. 15, 85	601	1/22	0.26	0.28	93.6	4.6	0.22	0.21	0.022	0.035

Figure 37. Example of non-condensable gases collected in samples from Asse brine migration test (Table 6-16 of Coyle et al. 1987).

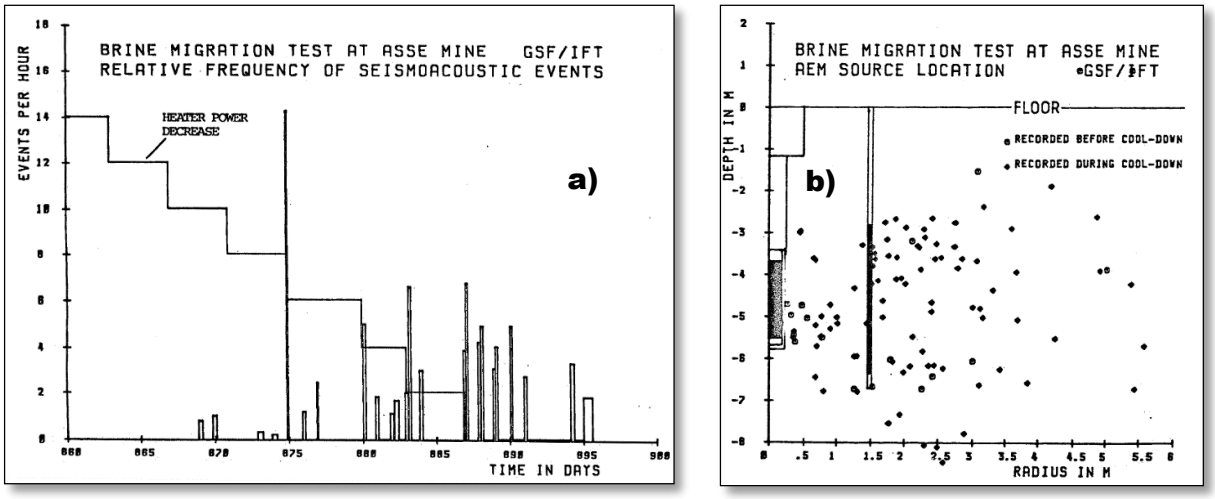

Figure 38. Acoustic emissions a: through time (during cool-down) and b: projected onto cross-section (Figures 6-54 and 6-56 of Rothfuchs et al. 1988).

A-5.3 Acoustic Emissions During *in situ* Heating

AE were monitored at multiple locations during heating and cooling. Figure 38 shows the distribution of AE events in time (during cool-off and heater step-down in power) and in space (near guard heaters). AE had been successful in SNL laboratory tests (Hohlfelder et al. 1981), but this is one of the only large-scale observations of AE during a field-scale salt heater test.

A-6. Project Salt Vault: Brine Collection

The first major *in situ* effort to characterize salt for disposal of radioactive waste was performed by ORNL in bedded salt deposits in Kansas as part of Project Salt Vault (Bradshaw & McClain 1971). This testing is relevant because:

- Several approaches were investigated to collect and quantify the moisture release of the salt, and
- Both vertical and horizontal borehole heater tests were conducted.

A-6.1 Brine Collection System Design

The following statement from Section 10.5.2 of Bradshaw & McClain (1971, p. 128) summarizes the issues encountered in the bedded salt of Lyons, KS:

> "Several special experiments were carried out in an effort to accurately measure the rate at which moisture was entering the array holes due to the migration of brine inclusions in the salt … The difficulty with these measurements was due to the moisture already in the mine air (40 to 60% relative humidity) and the low rate of moisture production from the salt in the array holes. These special experiments included the use of Drierite columns in the off-gas lines; cold traps using ice and brine, dry ice, and liquid nitrogen; *and one series of experiments (the most successful) where dry nitrogen gas was swept through the hole and off-gas system*."

More from Project Salt Vault on brine collection can be found in Section 11.2.2 (Bradshaw & McClain 1971, p. 168), indicating the importance of using *very* dry nitrogen:

> "By about the middle of June 1967 (shortly before shutdown) the total condensate collection in room 1 was about 1.7 liters, and in room 4 it was about 0.8 liter. … Several attempts were made to determine if water was migrating into the holes during the periods between the sporadic collections. These included the use of Drierite columns and the determination of the dew point by means of the refrigeration units on the condenser systems. However due to the fact that the mine air normally ran about 40 to 60% relative humidity (a rough average moisture content of about 11 g/m^3) these methods were unsuccessful. *Several tests using dry nitrogen gave the most reliable estimates*, although even these were good only for upper limit values. The best test was performed in room 1 on January 19-20, 1967 (about 70 days since there had been any condensate collection). In this test there was a 1-hr sweep of dry nitrogen through hole IV at 7 liters/min. This should produce more than three volume changes of the gas in the hole (greater than 95% removal of the original gas, if complete mixing is assumed), so that a negligible amount of water vapor (less than 0.1 ml) should remain in the hole. After this the hole was closed off for 24 hr to permit the diffusion of water from the salt into the hole. Then nitrogen at a flow rate of 2.1 liters/min for about 3½ hr was passed through the hole and into a system of traps at a temperature ranging from about 0 to 5° F. About ½ ml of liquid was collected in the traps. This meant that, if the nitrogen was absolutely dry when it entered the hole, it picked up enough moisture in the hole to become saturated at around 12°F. If that was the case, then the total emission of water from the salt into the hole during the 24-hr period was no more than 1 ml. *On the other hand, a test on the nitrogen alone (without its passing through the array hole) produced some traces of condensate at similar temperatures. (This was in spite of the fact that the nitrogen supplier said that the dew point should be below -20°F.)* Thus it must be concluded that the water collected from the array hole after the 24-hr period of no off-gas flow may not have come from the salt at all, so that the maximum inflow rate from the salt at that time must have been between 0 and 1 ml/day."

A-6.2 Brine Collection in Horizontal vs. Vertical Boreholes

Morgan (1963, p. 29-30) discussed some early efforts at heated boreholes in bedded salt:

> "Cylindrical heaters, 6 in. in diameter by 4 ft long, were used in 10-in. diameter holes in the floor and in a column of the mine to investigate the physical properties of salt in situ at temperatures above 300°C. Instrumentation was provided to measure floor rise around the heater in the floor and column expansion about the wall installation and to collect water vapor from the holes. Both the floor- and wall-cylinder tests began on July 18, 1962, with a power input of 3500 w each. Salt-temperature rises in the plane perpendicular to the center of the heater are shown … [Figure 39 of this report], along with theoretical curves based on the 100°C salt thermal properties. After 45 and 49 hr operation of the wall test and the floor test, respectively, the power was turned off for 3 hr, during which time the heater was removed from the hole and the hole diameter was calipered at 1-ft intervals. Both heaters were restarted at 5000 w; and the power remained constant, with the exception of a 5- to 10-min daily period (to record heater temperatures) and one period of about 45 min (to inspect the wall heater hole)."

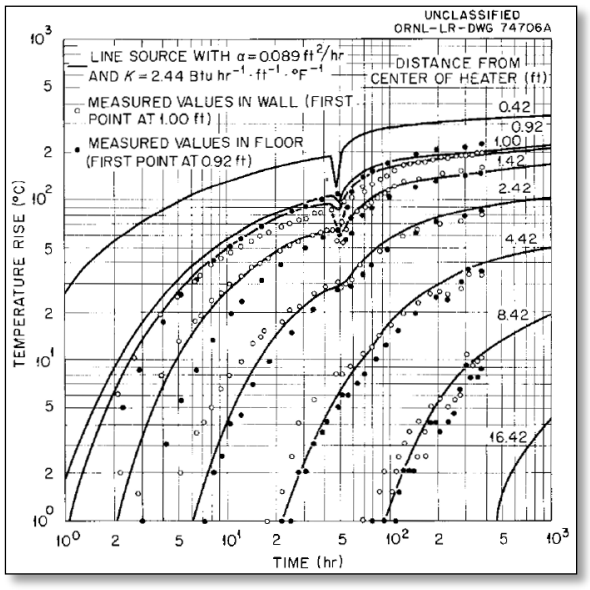

Figure 39. Comparison of temperature rise in horizontal and vertical boreholes to analytical solution (Figure 3.9 of Morgan et al. 1963).

> "Although the salt shattered at an estimated 280°C, it did not seem to have significantly affected heat transfer … Water evaporated from shale partings or released by salt shattering was condensed at mine temperature in air-cooled condensers. *About 15.5 liters from the floor heater hole and 250 ml from the wall heater hole were recovered*. One-gallon samples of the water from the floor hole, together with a reference sample of known recent water, were submitted to the laboratory of the U. S. Geological Survey for tritium dating."

A-7. Carlsbad Potash Mine Heater Tests

Preparing for the first shafts to be constructed at WIPP, *in situ* tests were conducted at the nearby MCC potash mine (Shefelbine 1982). This relatively shallow mine (350 m level) allowed access to the Salado Formation, but in the McNutt Potash zone (stratigraphically above the WIPP horizon; Figure 1). These tests were in some ways a "dry run" for the *in situ* tests being planned at WIPP. At least two borehole heater tests were conducted in the MCC mine. These tests demonstrated:

- Use of radiative "quartz lamp" heaters,
- One of a small number of horizontal borehole heater tests in bedded salt,
- Photography of salt crust growth during heater test,
- Heated boreholes to several different temperatures and monitored brine inflow, and
- Brine collected in unheated "observation" boreholes.

A-7.1 Quartz Lamp Radiative Heaters

Quartz lamp radiative heaters were first tested in a vertical borehole at Avery Island (Ewing 1981a), and the same lamps were then re-used in two different tests at MCC (Figure 40). One was a horizontal heated borehole configuration with nine lamps (Ewing 1981b), and the other was a vertical three-borehole configuration with one lamp in each (Shefelbine 1982).

Applying radiative heat directly to the borehole wall is efficient through air, and may lead to some convection, but does not rely on convection to heat the salt.

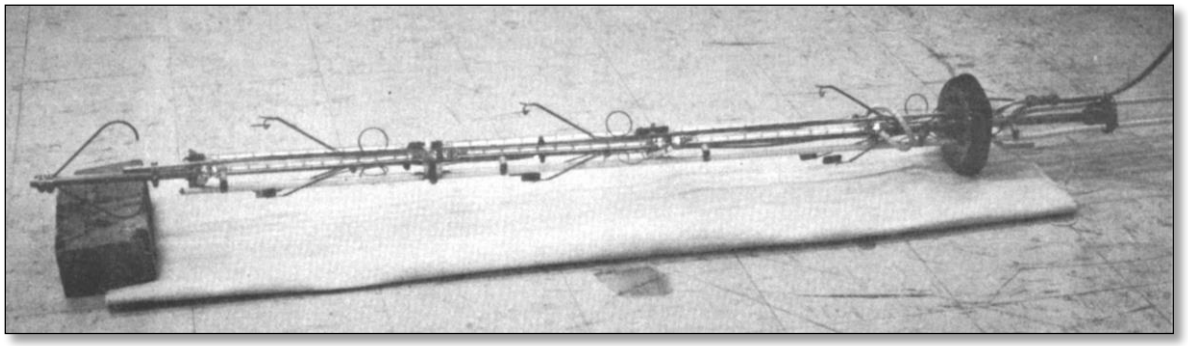

Figure 40. Nine-element quartz lamp radiative heater (Figure 2 of Ewing 1981a).

A-7.2 Horizontal Heater Test in Bedded Salt

The horizontal heater test at MCC was documented by Ewing (1981). This test was mostly a dry-run for testing to be done at WIPP (but this arrangement of quartz lamp heaters was not used at WIPP). There were electrical problems (power outage across the entire mine and a power overage to the test that brought borehole temperatures to 270 °C and led to decrepitation). But the general test design was successful. During nominal operation, the borehole wall temperature was 200 °C and brine was collected at approximately 2 grams per day.

The horizontal borehole was only 1.88 m [74"] long (Ewing 1981b; p. 18), with the heater placed near the end of the borehole (Figure 41). This means the access drift DRZ likely intersected the test interval.

Figure 41. Installation of heater in horizontal borehole at MCC (Figure 5 of Ewing 1981b).

A-7.3 Photography of Salt Crust Growth

The quartz lamp heater allowed photography of salt encrustation growth during the experiment (Figure 42). The photos were captured with a low-resolution VHS system, and the photos are not of high quality. This approach might allow additional diagnostic information during testing, if conducted with modern equipment.

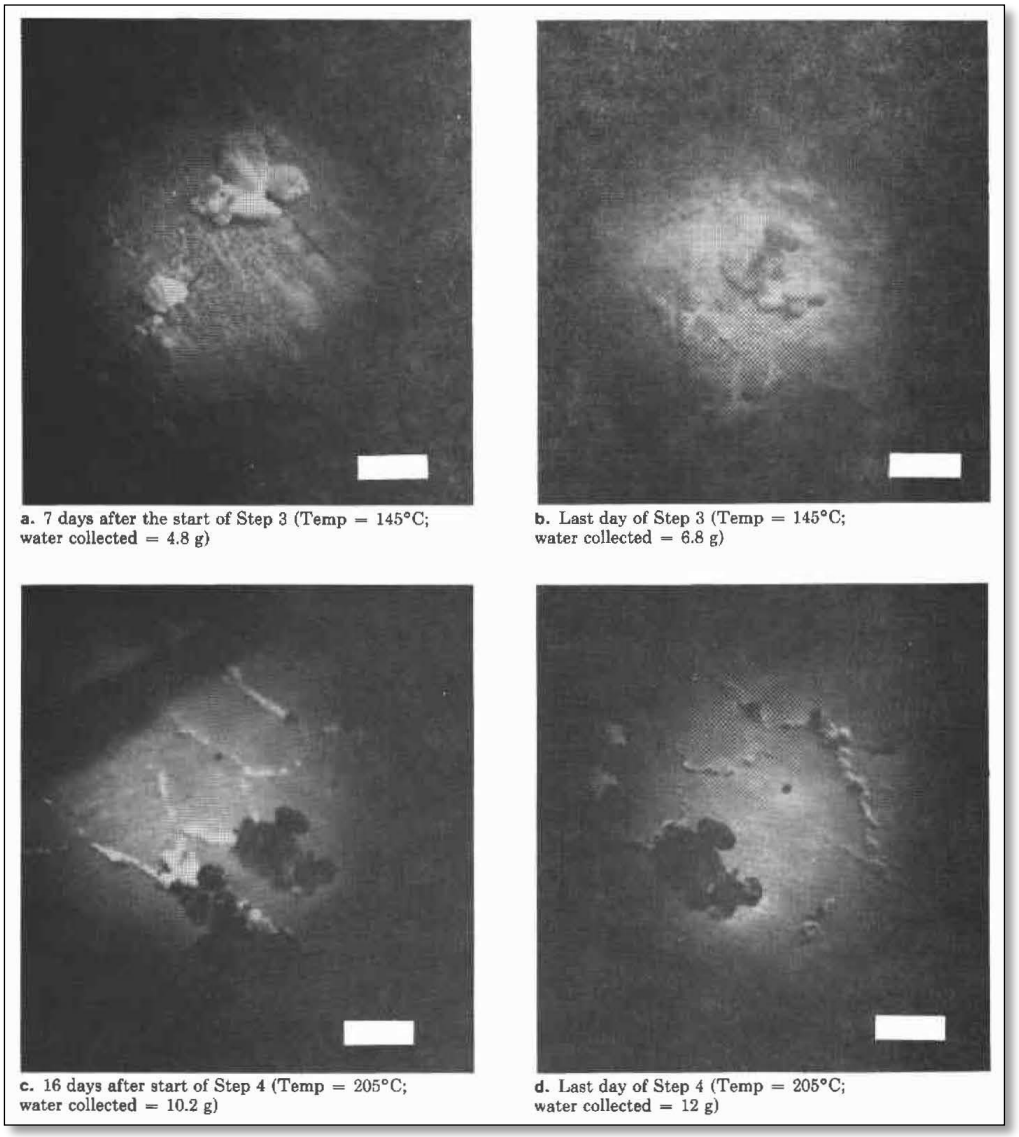

Figure 42. In situ growth of efflorescence in MCC three-heater experiment. Scale bar is ~0.5 cm (Figure 29 of Shefelbine 1982).

A-7.4 Brine Migration Test at Multiple Temperatures

The three-heater test at MCC included running the heaters in the boreholes at four different temperatures. Of the three boreholes (located 1 m apart), two were heated the whole time (boreholes A & C), while borehole B wasn't heated until the final step. Brine was collected in borehole B through the entire test (Figure 44). This shows the amount of brine inflow increases with temperature, but the steps chosen (90 °C, 110 °C, 145 °C, and 205 °C) do not correspond directly to the minerals discussed in Table 1.

The Salt Block II large-scale laboratory experiment (Hohlfelder 1979) also produced brine at multiple borehole heater temperatures (Appendix A-4). Data from these tests and the Salt Block II experiment are plotted in Figure 3 and listed in Appendix A-10.

A-7.5 Brine Collection in Unheated Boreholes

Figure 43 shows that the brine collected in borehole B did increase slightly when the temperature was increased to 145 °C in boreholes A & C. These boreholes might have been too far apart for a brine migration study, but too close to be unaffected by heating going on in adjoining boreholes.

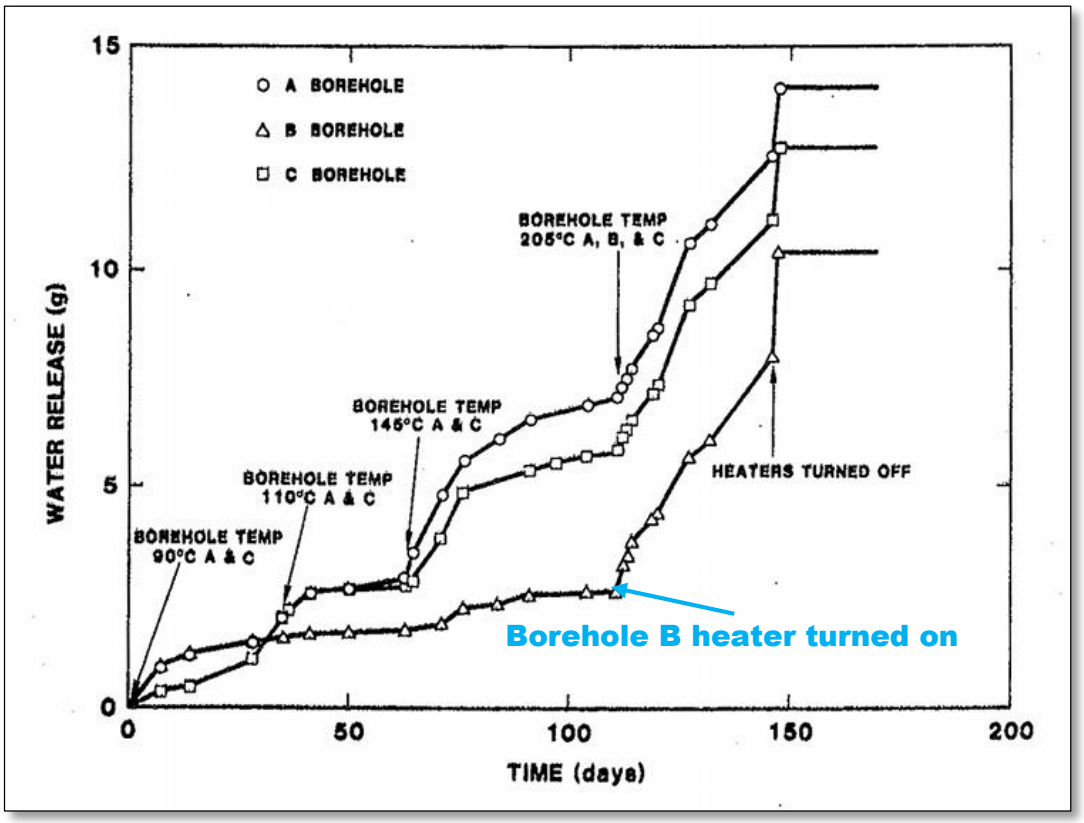

Figure 43. Water release for MCC three-heater experiment (Figure 28 of Shefelbine 1982).

A-8. Resistivity Measurements in Salt

Resistivity surveys or electrical resistivity tomography (ERT) can be used to estimate the brine content of the salt if a relationship between brine content and resistivity is available. Figure 44 shows some early data from WIPP (Skokan et al. 1989; Borns & Stormont 1988), while Figure 45 includes more recent references from an application in Germany at Asse (Jockwer & Wieczorek 2008).

If salt is dry (salt will still adsorb humidity from the air) resistivity of the salt will be high. WIPP salt tends to have low natural resistivity due to its brine content. Damaged salt also has higher resistivity than intact salt (Stormont 1997b, Figure 4). Resistivity of the brine itself is also a function of ionic strength and temperature (Figure 46); it is assumed any water in the salt will be a saturated brine.

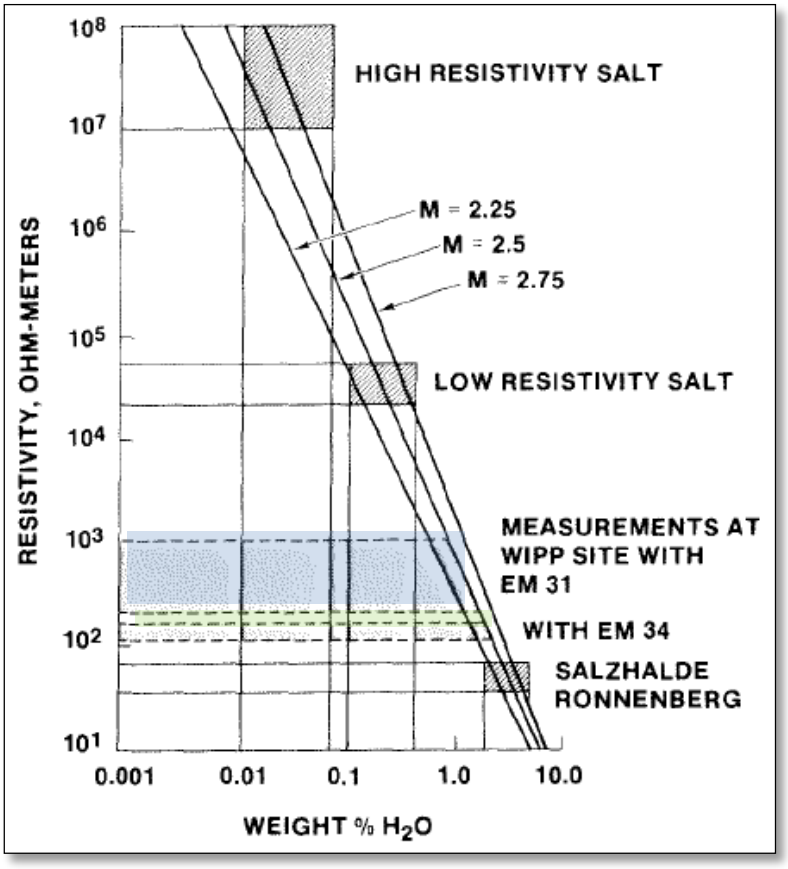

Figure 44. Resistivity of salt as a function of water content, showing range of resistivity observed at WIPP (Figure 7 of Skokan et al. 1989).

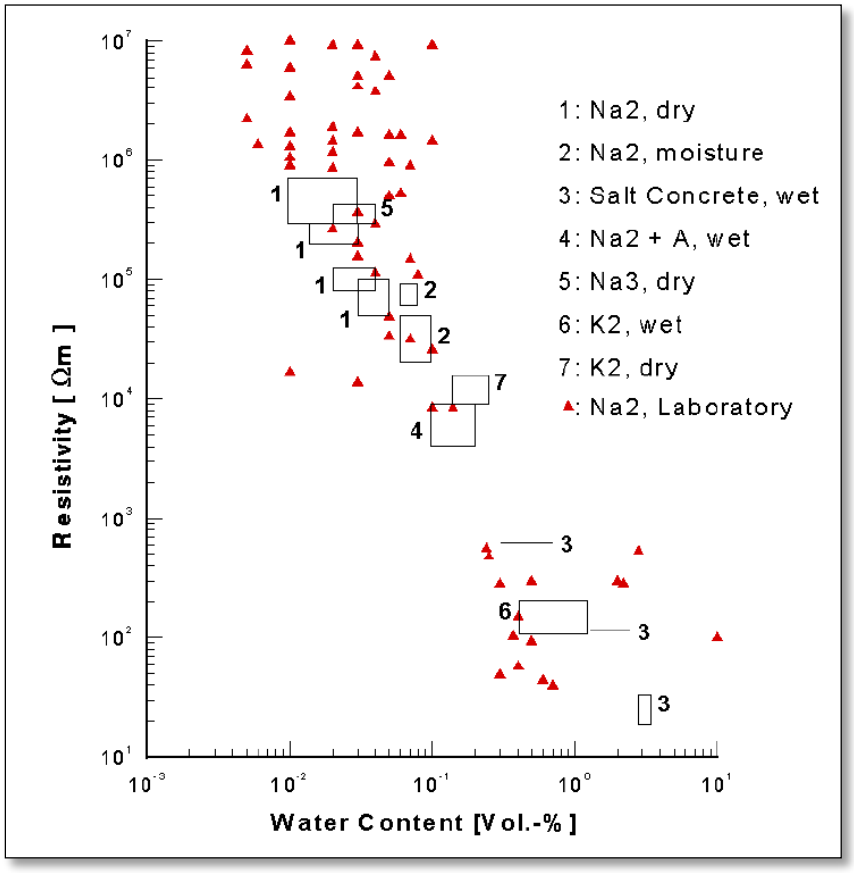

Figure 45. Relationship between water content and electrical resistivity for rock salt (Fig. 4-3 of Jockwer & Wieczorek 2008).

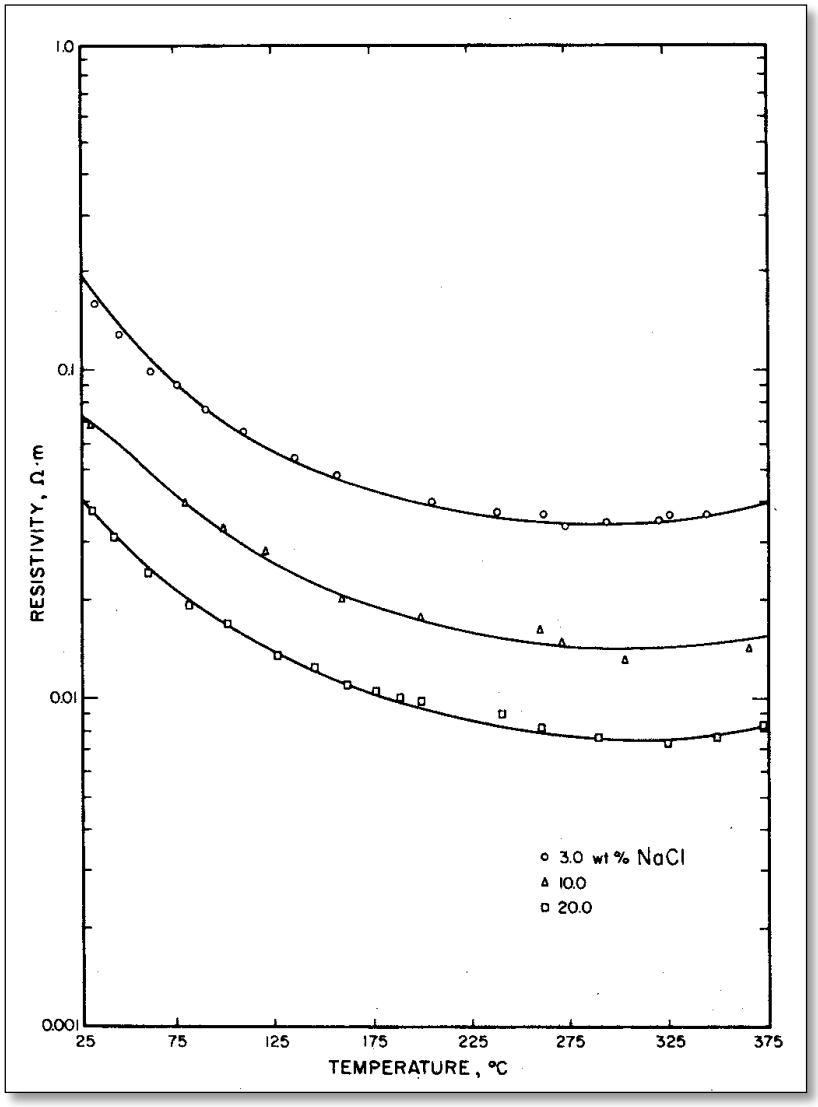

Figure 46. Brine resistivity as a function of ionic strength and temperature (Ucok et al. 1980).

A-9. Mapping the WIPP DRZ Extent with Gas Flow Tests

Gas permeability testing and gas tracer testing were conducted at WIPP to assess permeability and map the extent of the DRZ, and to assess transport pathways through the DRZ (Stormont 1997a). This series of tests is relevant because they conducted low-pressure constant-pressure and falling-pressure gas permeability tests of the types proposed in this report.

Figure 47 shows the results of a constant-head gas permeability borehole testing campaign at WIPP in the N1100 and N1420 drifts (North Experimental Area). This testing showed where high permeability exists, and is associated with the extent of the DRZ. Stormont (1988) published the test plan for these experiments, including a system drawing. Borns & Stormont (1988) discussed the testing results illustrated in Figure 47:

> "Beyond 1 m the flow rates are consistently small (< 1 SCCM [1 standard cubic centimeter per minute]) and within 1 m of the excavation, flow rates vary by many orders of magnitude (1 to 10^3 SCCM)."
>
> "In the 3.5 × 6 m N1100 drift an array of holes was drilled radially to a depth of about 10 m. Gas flow tests were conducted in numerous intervals along each hole. [Figure 48] presents the results as contours of the normalized flowrate magnitude surrounding the drift. These results clearly demonstrate increased flow rates in the immediate vicinity of WIPP facility excavations. The contours in the halite suggest a circular or elliptical pattern centered on the drift with flow rates decreasing radially outward from the excavation. Anomalous zones of high flow were measured in MB139."

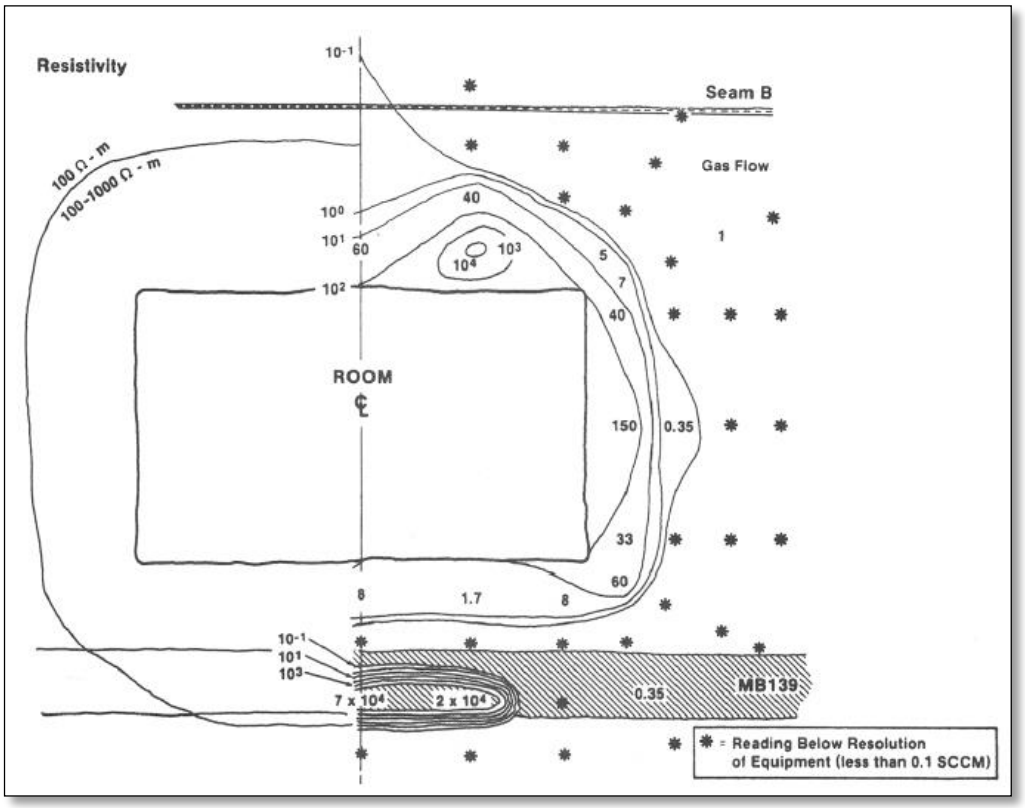

Figure 47. Results of gas flow tests and electrical geophysical surveys (Figure 5 of Stormont 1997a).

Beauheim & Roberts (2002) summarized extensive work to characterize the brine permeability of evaporites at WIPP. Brine permeability is more relevant to long-term flow and performance assessment, but gas permeability is much easier to measure. Gas has a much lower viscosity than brine, and it is largely unreactive with the salt. Gas flow through low-permeability rocks at low working pressures does have to take the Klinkenberg gas-slip mechanism into account, or absolute permeabilities will be overestimated.

A-10. Summary of Brine Production in Boreholes

Shefelbine (1982) summarized early heater tests in salt. Table 12 from his report is expanded here (Table 5) and modified to include additional tests, to separate Project Salt Vault test data, and to change the normalization of brine production (not dividing by wt-% H_2O in salt). Data from Table 5 are illustrated in Figure 3.

Table 5. Water released in bedded salt (expanded from Table 12 of Shefelbine 1982)

Experiment	wt-% H_2O	Heated Surface Area [m^2]	(V)ert. or (H)oriz.; Clay?	Max Temp [°C]	Test Duration [days]	H_2O Collected [g]	Steady Rate [g/day]	Norm. Rate [$g/d/m^2$]
Salt Vault Room 1£	0.25	12.3	V, No	200	572	≥1,710	≥3.0 <14	≥0.24 <1.1
Salt Vault Room 4£		12.3	V, No	175	572		≥1.5 <12	≥0.12 <0.98
Salt Vault Room 5£		12.3	V, Yes	142	580		>70 <650	>5.7 53
SB II – 1§	0.3	0.24	V, No	38	7	0.7	0.03	0.13
SB II – 2§				59	7	0.5	0.04	0.17
SB II – 3§				81	15	1.2	0.03	0.13
SB II – 4§				130	14	11	0.3	1.3
SB II – 5§				200	69	39	0.5	2.1
Thin Disk§	0.3	0.035	H, No	200	42	2.2	0.035	1.0
MCC single§	0.3	0.41	H, No	200	113	190	0.4	0.98
MCC3 – 1§	0.3	0.15	V, No	90	35	1.9	0.014	0.093
MCC3 – 2§				110	28	0.8	0.012	0.08
MCC3 – 3§				145	48	3.6	0.015	0.1
MCC3 – 4§				205	35	5.4	0.12	0.8
WIPP B041¥	0.22 to 0.75*	8.61	V, Yes	130	600	37,000	50	5.8
WIPP B042¥		7.17	V, Yes	130	600	35,000	50	7.0
WIPP A1041¥		7.17	V, Yes	50	425	4,200	8.5	1.2
WIPP A1042¥		7.17	V, Yes	52	425	4,300	9.5	1.3

* 0.22 wt-% water content reported for clean WIPP halite, while 0.75 wt-% water content reported for argillaceous WIPP halite (Finley et al. 1992; Appendix D)

§ data from Shefelbine (1982)

£ data from Bradshaw & McClain (1971)

¥ data from Nowak & McTigue (1987)

Appendix B Experimental Sequence

This appendix presents a high-level chronological summary of the testing

B-1. Borehole *in situ* Testing

1. Prior to drilling boreholes, map visible/accessible geology and stratigraphy in the access drift at the test location.
2. Core test borehole (samples to be preserved immediately to prevent dry-out, for use in laboratory measurements) and drill surrounding smaller-diameter observation boreholes.
3. Before heating:
    a. Visually characterize borehole surface (i.e. azimuthal borehole image log), observing presence and locations of unmapped clay stringers, spalling, open cracks, efflorescence, and liquid brine.
    b. Measure and record borehole dimensions (collar location and borehole diameter, length, orientation, and straightness).
    c. Perform gas flowrate packer tests at 30 cm [1'] intervals along the borehole to characterize damaged salt as a function of depth. In the test borehole, use dry N_2 for gas flow tests. In observation boreholes use mixtures of N_2 carrier gas with <10% Ar and Xe tracers.
    d. Mix and emplace cement sample to end of test borehole.
    e. Install electrical resistivity testing equipment in adjacent observation boreholes. Conduct an initial ERT survey before installing further metal components in observation and test boreholes.
    f. Install heater, packer, and sensor package into test borehole. This package should be initially assembled and tested in the laboratory to confirm correct wiring and plumbing.
    g. Add D_2O to interval in observation borehole, isolated with multiple plugs or packers.
    h. Begin continuously monitoring RH, barometric pressure, and air temperature in access drift.
    i. Install temperature sensors into observation boreholes.
    j. Install AE sensors by setting them at the end of observation boreholes via epoxy or grout. Install any active ultrasonic sources (other than piezoelectric AE sensors) in different intervals of the same boreholes.
4. During test (heating):
    a. Baseline monitoring will be conducted under isothermal conditions for two weeks before turning on the heater, to gather background data and to allow direct comparison of some results from the first two boreholes (i.e., assess heterogeneity and repeatability).
    b. External (access drift):
        1. Continuously monitor drift air conditions including temperature, barometric pressure, and RH.
    c. In test borehole:
        1. Monitor salt movement due to creep and borehole closure by collecting data from extensometers or BPCs in observation boreholes.
        2. Monitor borehole closure around heater block in test borehole via LVDT gauges.
        3. Monitor temperature in both radial and azimuthal profiles via RTDs.
        4. Collect 2-3 gas samples per week during test (starting with samples before heating).
        5. Collect 2-3 brine inflow samples per week during test (starting with samples before heating).
        6. Monitor flowrate, temperature, and pressure of circulating N_2 inflow.

7. Monitor flowrate, temperature, pressure, and RH of circulating N_2 outflow stream at CMH.
8. Passively monitor AE generated during heating and cooling.
9. Periodically conduct tomographic ultrasonic wave surveys using AE network.

d. In observation boreholes during test:
   1. Monitor radial profile of temperature via RTDs in two boreholes at different distances from the test borehole.
   2. Perform gas flowrate tests to characterize permeability of borehole as a function of depth during the test. Use gas with minor tracers.
   3. Perform electrical resistivity tomographic surveys between two observation boreholes (on either side of test borehole) to characterize changes in brine content with time.

5. Post-heating (for at least two weeks after the end of heating):
   a. In test borehole:
      1. Continue to monitor temperature in both radial and azimuthal profiles via RTDs.
      2. Continue to collect gas samples during cool-down part of test (possibly higher frequency).
      3. Continue to collect brine inflow samples during cool-down part of test.
      4. Continue to monitor flowrate, temperature, and pressure of circulating N_2 inflow.
      5. Continue to monitor flowrate, temperature, pressure, and RH of circulating N_2 outflow stream with CMH. There will likely be a pulse of increased brine inflow after turning off the heater, so the N_2 rate may need to be adjusted, or higher-frequency CMH readings may needed.
   b. In observation boreholes:
      1. Continue to monitor radial profile of temperature via RTDs in two boreholes at different distances from the test borehole.
      2. Continue to perform gas flowrate tests to characterize permeability as a function of depth during cooling.
      3. Perform electrical resistivity tomographic surveys between two observation boreholes (on either side of test borehole) to characterize changes in brine content with time.
6. Post-test (after heating and cool-down testing periods):
   a. Remove packers, plugs, and heater/sampling equipment from test borehole. Remove non-destructively if possible.
   b. Visually characterize borehole surface (i.e. azimuthal borehole image log), observing heating-induced damage, spalling, and open cracks, efflorescence, and liquid brine.
   c. Measure and record post-test borehole dimensions (diameter, length, and orientation).
   d. Perform gas flow tests at 30 cm [1’] intervals along the borehole to characterize damaged salt as a function of depth.
   e. Perform post-test ERT survey, once metal components have been removed from test borehole (for comparison with pre-test survey before metal components were installed).
   f. Collect efflorescence and precipitated salts deposited in borehole, preserving them for quantitative analysis of D_2O content and mineral composition (preserve to prevent dry-out).
   g. Sample cement plug by coring.
   h. Collect salt cores from around borehole and perform laboratory analysis.
      1. Some samples should be near the heater borehole, to observe high-temperature effects of fluid inclusions, dihedral angle, and any dissolution due to migration of steam through the salt (preserve samples to prevent dry-out).

2. Samples should be collected between the heater and observation boreholes to observe the distribution of D_2O in the intact salt porosity (preserve to prevent dry-out, including additional fractionation of water in samples).
3. Collect one core that intersects test borehole at an angle to test interval borehole, to observe how any changes to salt from heating vary moving away from the heater.

B-2. Laboratory Core Sample Testing

Laboratory testing on solid salt is summarized. Tests do not necessarily follow a strict sequence. Some laboratory tests could be conducted much later, if samples are properly preserved. Most of the core or solid salt analyses will be performed on sets of samples collected both during drilling the test hole (pre-test) and from the test interval after heating (post-test). Analyses will include the following tasks:

- Determine mineral distribution in core from both before and after testing by thin-section and X-ray diffraction.
- Determine elemental composition of solid samples from X-ray fluorescence and SEM/EDS.
- Determine fluid inclusion features such as size, frequency, brine chemistry.
- Characterize flow properties in core including porosity and pore size distribution (Hg-injection porosimetry).
- Characterize three-dimensional pore morphology, pore connectivity, micro-mechanical defects, and pore-grain dihedral angles using serial imaging methods, including: micro-CT, FIB-SEM, multi-beam SEM, STEM, the Robo-Met.3D optical imaging/polishing tool, and SANS.
- TGA will be used to analyze volatile content of salt samples, and may be used in conjunction with a gas chromatograph to quantify the composition of gases evolved during heating.
- Precipitated salt (i.e., efflorescence) samples scraped or cored from the borehole wall will be analyzed using similar methods used on intact salt.
- Gas chromatography will be used to analyze head space that develops after dissolving salt in de-aerated water inside a vacuum container.

B-3. Laboratory Liquid/Gas Sample Testing

Laboratory tests on fluid (i.e., liquid and gas) samples are summarized. Tests do not necessarily follow a strict sequence. Some laboratory tests could be conducted much later, if samples are properly preserved.

From the liquid brine samples collected during testing, perform the following tasks:

- Analysis of major and minor ions by ion chromatography and inductively coupled plasma mass spectrometry.
- Analysis of stable water isotopes using CRDS.
- Brine electrical conductivity, pH, alkalinity, total dissolved solids, fluid density, and equilibrium RH will be estimated using appropriate laboratory methods.

From the gas samples collected during testing, including both the borehole gas collection system and any samples of the drift air collected, perform the following tasks:

- Analysis of major gas components using gas chromatography (will be mostly N_2 and H_2O).
- Analysis of stable water isotopes using CRDS.
- Quantification of naturally present noble gases (e.g., He and Ar) that may have started off dissolved in brine or contained in salt grains, and were released from the salt during heating. These gases should be identifiable via gas chromatography.
- Consideration should be made for condensable components in the gas stream that might have entered the sample container, but may not remain in gas form in the laboratory during testing (e.g., H_2O and HCl).

Appendix C Nitrogen Tank Lifetime Estimate

This appendix presents a preliminary estimate of the required flowrate of dry N_2 gas in the moisture collection system.

The contents of a large N_2 gas tank at STP has a volume of $300\ [\mathrm{ft}^3] = 8{,}495\ [\mathrm{L}]$. The gas is dry at first, but for isothermal conditions (30 °C) and atmospheric pressure

$$P_{sat} = 0.0419\ [\mathrm{atm}] \times 0.75\ [\text{salt RH}] = 0.0314\ [\mathrm{atm}] = X_{H_20}$$

which is equivalent to the mole fraction of water vapor in equilibrium with salt. After circulating through the borehole, we assume the dry gas will be 75% RH and the same volume. At STP, water vapor has the density $0.804\ \mathrm{g/L}$.

$$8{,}495\ \left[\frac{\mathrm{L\ N_2}}{\text{cylinder}}\right] \times 0.023475\ \left[\frac{\mathrm{L\ H_2O\ vapor}}{\mathrm{L\ N_2}}\right] \times 0.804\ \left[\frac{\mathrm{g\ H_2O}}{\mathrm{L\ H_2O\ vapor}}\right] = 215\ \mathrm{g\ H_2O}$$

Appendix A-1.1 indicates between 3 and 5 g/day brine flowed into boreholes in room L4 under isothermal conditions. Assuming a density of 1.16 g/cm^3, this results in 2.6 to 4.3 g/day of H_2O flowing into a borehole of similar size in MU-0.

At a rate of 4 g/day brine production, and the lower limit of N_2 usage (assuming the gas becomes completely saturated as it passes through the borehole), it would be expected at 300 ft^3 tank of N_2 would last at most 53 days.